Aus der Klinik für Orthopädie und Unfallchirurgie
Muskuloskelettales Universitätszentrum München
Klinik der Universität München
Direktoren:
Prof. Dr. med. Wolfgang Böcker
Prof. Dr. med. Boris Holzapfel

Evaluation of BMP2-loaded hybrid 3D collagen scaffolds: Proliferation and osteogenic differentiation capacity of human mesenchymal stem cells

Dissertation
zum Erwerb des Doktorgrades der Medizin
an der Medizinischen Fakultät
der Ludwig-Maximilians-Universität zu München

vorgelegt von
Timo Tucholski
aus München
2023

Mit Genehmigung der Medizinischen Fakultät
der Universität München

Berichterstatter:	Prof. Dr. Wolf Christian Prall
Mitberichterstatter:	Prof. Dr. Florian Haasters
	Prof. Dr. Mohammad-Mehdi Shakibaei
Mitbetreuung durch den promovierten Mitarbeiter:	Dr. rer. nat. Maximilian Saller
Dekan:	Prof. Dr. med. Thomas Gudermann
Tag der mündlichen Prüfung:	25.05.2023

Abstract

In tissue engineering, collagen hydro-gels and 3D matrix grafts both feature distinct advantages and limitations as single scaffolds. Hydro-gels are a feasible carrier for human mesenchymal stem cells (hMSCs) and osteoinductive cytokines can easily be added while they rapidly degrade and lack structural stability. 3D matrix grafts are more difficult being seeded and coated but provide structural stability. Combining the advantages of both may be a promising approach to tissue engineering. Potential advancements should then be transferred to investigations on osteoporotic hMSCs, as especially BMP2 holds the promise of being an enhancer of osteogenic differentiation.

HMSCs were isolated from healthy donors and patients with osteoporosis. The cell survival on the collagen hydro-gel and the 3D matrix grafts was assessed utilizing fluorescein diacetate- and propidium iodide-based Life-Dead Assays. The cell distribution was evaluated using DAPI-Phalloidin staining. The release kinetics of the added BMP2 were measured by BMP2 ELISA. The biodegradability of the collagen hydro-gel was assessed by ImageJ time lapse analyses. Osteogenic differentiation was carried out according to standard protocols and Alizarin Red staining was quantified in a conventional 2D setup or using the introduced 3D hybrid scaffold. RNA sequencing of healthy and osteoporotic hMSCs was conducted prior to and after stimulation with BMP2.

The introduced 3D hybrid scaffold ensures homogeneous cell distribution and allows for sufficient cell survival. Furthermore, it can easily be loaded with BMP2 and features a steady release kinetic over time. The 3D hybrid scaffold allows for reliable quantification of osteogenic differentiation. The osteoinductive effects of BMP2 on healthy and osteoporotic hMSCs were analyzed in a conventional 2D as well as the introduced 3D setup. In both groups, hMSCs feature an improved osteogenic differentiation by tendency in the 2D setup due to the additional stimulation with BMP2 over 21 days. In the 3D hybrid scaffolds, no positive osteoinductive effect of additional BMP2 stimulation can be detected. While there is no effect of additional BMP2 stimulation on healthy hMSCs, BMP2 notably inhibits the osteogenic differentiation of hMSCs derived from osteoporotic patients. RNA sequencing reveals significant differences in single gene expression between both groups prior to BMP2 stimulation. Differential gene expression

encompasses structural bone matrix proteins (IBSP), ECM cell attachment proteins (CD34), ligands of the TGF-beta family (GDF15) and other proteins involved in osteogenic differentiation (PRG4, TRH, STMN2). In both groups, BMP2 stimulation leads to a significant up-regulation of a receptor for the TGF-beta family (BAMBI), a protein specific to BMP-mediated cell signaling (SMAD9) and an inhibitor of BMPs (NOG). Interestingly, there is a significant up-regulation of a bone development specific transcription factor (DLX) in healthy hMSCs that cannot be detected in osteoporotic hMSCs.

The introduced hybrid scaffold represents a reliable tool for osteogenic differentiation in a 3D set up and opens new opportunities in tissue engineering. Despite the steady release kinetic the additionally loaded BMP2 failes to enhance osteogenic differentiation of healthy hMSCs and even inhibits osteogenic differentiation of osteoporotic hMSCs. RNA sequencing reveals differently expressed genes across both groups and significant up-regulations of single genes in response to BMP2. The RNA sequencing provides further insights into osteoporosis but features limitations in explaining the observed inhibition of osteogenic differentiation due to BMP2.

Zusammenfassung

Im Bereich der Gewebezucht (engl. tissue engineering) weisen kollagenbasierte Hydrogele und 3D Matrix-Gerüste (Träger) jeweils spezifische Vor- und Nachteile auf. Hydrogele bilden eine geeignete Grundlage für menschliche mesenchymale Stammzellen (hMSCs) und können leicht mit osteoinduktiven Zytokinen beladen werden, während ihre Schwäche in der strukturellen Stabilität liegt. 3D Träger hingegen zeigen eine deutlich höhere Stabilität, jedoch ist die Applikation von Botenstoffen problematisch. Ein vielversprechender Ansatz in der Gewebezucht ist die Kombination beider Materialien und somit ihrer Vorteile. Weitere Nachforschungen und Fragestellungen sollten den Fokus auf die Verwendung hMSCs osteoporotischer Spender legen. Hier zeigt vor allem BMP2 vielversprechende Ergebnisse, um eine osteogene Differenzierung zu unterstützen.

Aus gesunden und osteoporotischen Spendern wurden hMSCs isoliert. Das Zellüberleben auf dem Kollagengel und den 3D Trägern wurde durch eine Färbung mit floureszieren Farbstoffen analysiert, welche tote und lebende Zellen verschieden anfärben. Die Zellverteilung wurde durch eine Färbung mit DAPI und Phalloidin untersucht. Eine ELISA Analyse für BMP2 wurde zur Darstellung der Freisetzung des Proteins aus den Trägern benutzt. Der Abbau des Kollagengels wurde mithilfe von ImageJ anhand einer Zeitreihe objektiviert. Die osteogene Differenzierung wurde gemäß Standardprotokollen durchgeführt und die Anfärbung der Differenzierung mittels Alizarin Red für einen 2D und einen 3D Versuchsaufbau durchgeführt. Eine RNA-Sequenzierung wurde sowohl mit als auch ohne BMP2-Einfluss realisiert.

Auf dem in der Studie neu etablierten 3D-Träger zeigt sich eine homogene Zellverteilung sowie ein gutes Zellüberleben. Durch die Kombination der Träger ist die Zuführung von BMP2 ebenfalls einfach und es zeigt sich eine konstante Freisetzung innerhalb des gesamten untersuchten Zeitraums. Des Weiteren ist die Analyse der osteogenen Differenzierung auf diesem Träger durchführbar. Diese wurde jeweils für hMSCs gesunder und osteoporotischer Spender in einem 2D und 3D Ansatz untersucht. Für beide Spendergruppen zeigt sich eine Tendenz zur erhöhten osteogenen Differenzierung im 2D Ansatz, während in der 3D Versuchsreihe kein positiver Effekt von BMP2 auf die Zellen nachgewiesen werden kann. Während sich hier keine Veränderung in der osteogenen Differenzierung bei gesunden Spendern zeigt, ist bei osteoporotis-

chen Spendern sogar eine hemmende Wirkung von BMP2 auf die osteogene Differenzierung festzustellen. Die RNA-Sequenzierung zeigt signifikante Unterschiede hinsichtlich der Expression einzelner Gene zwischen gesunden und osteoporotischen Spendern ohne BMP2-Einfluss. Hierzu zählen Gene, welche die Knochenmatrix (IBSP), die Extrazellulärmatrix (CD34) und Liganden der TGF-beta Familie (GDF15) beeinflussen sowie in die osteogene Differenzierung eingreifen (PRG4, TRH, STMN2). Nach BMP2-Gabe zeigt sich in beiden Spendergruppen eine signifikante Erhöhung der Expression eines Rezeptors der TGF-beta Familie (BAMBI) sowie eines Proteins, welches spezifisch die Signalkaskade von BMP2 beeinflusst (SMAD9). Ausserdem zeigt sich hier ein Hemmer von BMP (NOG) erhöht. Interessanterweise ist bei gesunden, jedoch nicht bei osteoprotischen Spendern nach BMP2-Gabe eine Erhöhung eines für die Knochenentwicklung spezifischen Transkriptionsfaktors (DLX) festzustellen.
Der hier eingeführte Hybrid-Träger zeigt sich zuverlässig für die osteogene Differenzierung in einem 3D Versuchsansatz und eröffnet somit neue Möglichkeiten zur Gewebezucht. Trotz der konstanten BMP2 Freisetzung zeigt sich keine verstärkte osteogene Differenzierung bei gesunden Spendern und sogar eine gehemmte Differenzierung bei osteoporotischen Spendern. Die Sequenzierungsanalyse zeigt verschiedene Veränderungen und Unterschiede in den Spendergruppen als Antwort auf die BMP2 Gabe und gewährt somit tiefere Einblicke in die Krankheit Osteoporose. Die gehemmte osteogene Differenzierung bei osteoporotischen Spendern kann hierdurch jedoch nicht erklärt werden.

Contents

List of Figures

List of Tables

Chapter 1

Introduction

1.1 Bone biology

The human body is composed of 223 bones (Aumüller et al., 2010). Beside the supporting function, the skeleton also has a protective function for the central nervous system, as well as for internal organs, which are located in the pelvic and thoracic skeleton. Furthermore, within the human skeleton hematopoesis takes place and it also serves as the largest storage of bound calcium (Aumüller et al., 2010).

1.1.1 Molecular mechanisms of bone formation in appendicular skeleton during development

Lateral plate mesoderm cells form skeletal tissues in the limbs in a proximal to distal manner (Cohn and Tickle, 1996; Olsen et al., 2000). These mesenchymal stem cells (MSCs) condensate and some of them differentiate into osteoblasts to directly built bone. This process is called intramembranous ossification (Berendsen and Olsen, 2015). Most of the mesenchymal stem cells differentiate into chondrocytes and start endochondral ossification, which can be divided into two major steps (Provot and Schipani, 2005). During the first step, chondrocytes start to proliferate and deposit an extracellular framework, which is used by osteoblasts in the second step to mineralize the chondrocyte-derived extracellular matrix (Kronenberg, 2003). Within this process, indian hedgehog and fibroblast growth factors, as well as parathyroid hormone-like hormone (PTHLH) play a key role in regulating chondrocyte proliferation, differentiation and activity (Provot and Schipani, 2005).
Furthermore, bone morphogenic proteins (BMPs) play an important role in bone development. BMPs appear to affect the condensation of mesenchymal cells, since inhibition of BMPs by NOGGIN leads to a suppressed condensation and thus to a decreased ossification (Pizette and Niswander, 2000). Furthermore, NOGGIN inhibits chondrogenesis of chondrocyte progenitor

cells by binding BMPs (Pizette and Niswander, 2000). This finding is supported by the discovery that *Noggin*$^{-/-}$ mice produce a much bigger cartilage frame for the subsequent ossification, leading to the conclusion that BMPs are, among other factors, responsible for chondrogenesis and osteogenesis (Brunet et al., 1998). This data is supported by studies, which showed that BMP2 and BMP4 deficient mice have a dysfunctional chondrogenesis and ossification in the limbs during development and severe defects (Bandyopadhyay et al., 2006).

1.1.2 Anatomy of mature bone

Mature bone is composed of an inner trabecular system and a surrounding cortical mass (Fig.1.1, A). The ratio between cortical and trabecular bone varies between the different bones (Clarke, 2008). Trabecular, as well as cortical bone, consists of osteons, which form lamellar, concentric structures. The central canal or Havers canal runs through the center of these structures and contains an artery, a vein and a nerve. Osteocytes are located in between these layers. The osteons are called Haversian systems in cortical bone and bone packets in trabecular bone, respectively. In this lamellar structure of bone, collagen fibrils are orientated in opposed directions contrary to the adjacent lamellae (Clarke, 2008) (Fig.1.1, B).
Contrary to the high strength of lamellar bone, woven bone is much weaker. Here, the collagen fibrils appear highly disorganized. Woven bone usually occurs during formation of primary bone or conditions of high bone turnover (e.g. Paget's disease or postmenopausal osteoporosis) (Clarke, 2008; Eriksen, 1986).
During aging, adult bone formation normally outreaches bone resorption on the outer periosteal surface, which leads to an increased diameter over time. On the other hand, bone formation succumbs to bone resorption on the endosteal surface, which leads to a growing marrow space with aging (Clarke, 2008).

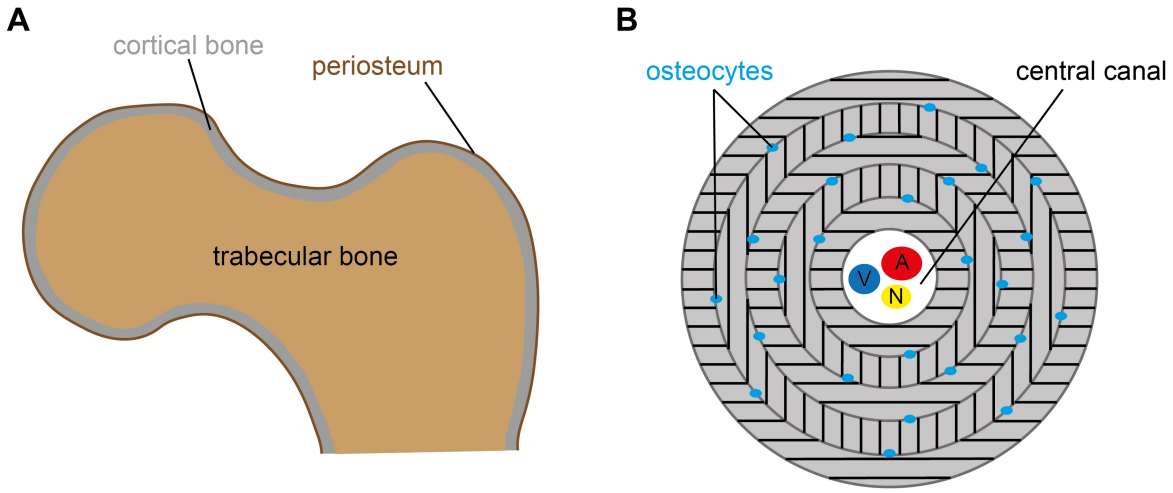

Figure 1.1: Anatomy of mature bone.

Outline of the anatomy of mature bone. The distribution of cortical and trabecular bone is shown in **A**. The ratio varies between the different bones. The basic setup of an osteon is shown in **B**. The collagen fibrils run in opposed directions in neighboring lamellars. Osteocytes are located in between the lamellars. The central canal contains the supplying blood vessels and nerve.

1.2 Physiology of bone remodeling

According to Wolff's Law, bone follows the concept of "form follows function", which means that bone re-adjusts its shape and structure due to the mechanical stress it is exposed to (Frost, 1994). In order to face this assignment, bone has a remodeling function by replacing older bone by new one and thus maintaining the functionality of bone during aging and physical strain (Parfitt, 2002).

Bone development has to be demarcated from bone remodeling. Frost defined bone modeling and development as a resorptive and formative mechanism, which is linked to growth and thus mainly takes place in the infantile skeleton. It mainly determines the size and architecture of bone (Frost, 1969). Disturbance of physiological bone development causes diseases like osteogenesis imperfecta for example. Contrary to this, bone remodeling is characterized by a bone turn-over, renewing the mature bone. It takes place throughout life and impaired remodeling leads to different diseases, such as osteoporosis or osteomalacia (Frost, 1969).

As mentioned above, the remodeling process endures the entire life time, with some higher and some lower peaks. It increases in perimenopausal and early postmenopausal women, to decrease again afterwards. At this point, bone remodeling stays at a higher level than in premenopausal women (Clarke, 2008; Hotchkiss and Karl, 2003).

The process of bone remodeling can be segmented into different episodes: activation, resorption, reversal and formation phase (Clarke, 2008; Frost, 1969). Activation is reflected by re-

cruitment and activation of osteoclast precursors, followed by bone resorption through mature osteoclasts. Subsequently, in the reversal phase osteoblast precursors are recruited to finally build new bone in the formation phase (Clarke, 2008). Frost named the sum of individual cells, responsible for bone remodeling, basic multicellular unit. The main components of these units are osteoblasts and osteoclasts (Frost, 1969).

1.2.1 Osteoblasts

Osteoblasts derive from mesenchymal stem cells, which can differentiate into various cell lines, such as adipogenic, chondrogenic or osteogenic cells (Pittenger et al., 1999). One of the most crucial factors for osteogenic differentiation is the wingless-type MMTV integration site family member (WNT) (Bennett et al., 2005). The maturation of osteoblasts starts with precursor cells, which become proliferating osteoblasts, then matrix producing osteoblasts and end up in osteocytes or bone lining cells (Fig.1.2) (Eriksen, 2010). Thereby, they are influenced by several growth factors and proteins, e.g. WNT/β-catenin, BMPs, transforming growth factor-beta (TGF-β), vitamin D and parathyroid hormone (PTH) (Chen et al., 2012; Eriksen, 2010; Florencio-Silva et al., 2015).

Pre-osteoblasts normally produce alkaline phosphatase (ALP), whilst mature osteoblasts also secrete collagen I and other matrix proteins, like osteocalcin, osteopontin, osteonectin, tumor necrosis factor superfamily member 11 (TNFSF11; also known as Receptor Activator of NF-$\varkappa$B Ligand (RANKL)) and receptor for PTH (PTHR1) (Clarke, 2008; Eriksen, 2010; Murshed et al., 2005). These proteins are in part essential for the mineralization of the bone matrix. In the following TNFSF11 is referred to as RANKL.

Mature osteoblasts secrete their proteins around themselves and thus they become embedded into mineralized matrix. They turn into osteocytes, when located within the bone or they cover the bone surface and transform into bone lining cells (Eriksen, 2010).

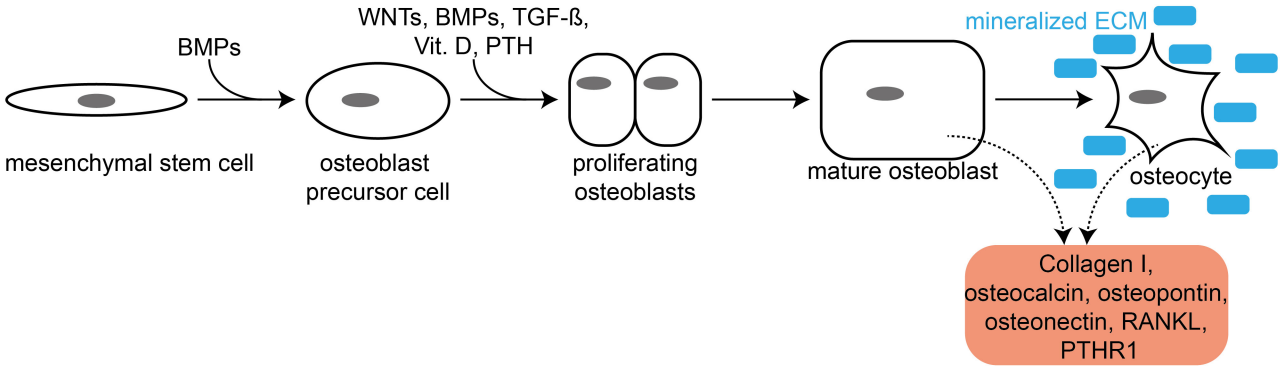

Figure 1.2: Maturation of osteoblasts.

Delineation of the osteoblast maturation and its important influencing factors. Mature osteoblasts and osteocytes secrete various proteins to regulate bone mineralization around themselves, becoming embedded into mineralized extracellular matrix (ECM, blue).

1.2.2 Osteoclasts

Osteoclasts have a hematopoietic origin and arise from the monocyte-macrophage lineage (Roodman, 1999). For maturation into osteoclasts, the precursor cells merge and need two important factors: RANKL and colony-stimulating factor-1 (CSF-1, or M-CSF), which belongs to the family of cytokines (Boyle et al., 2003) (Fig.1.3).

Osteoclasts are the main cellular source of bone resorption, which takes about two to four weeks (Clarke, 2008). They secrete several proteases and acid to demineralize the calcified extracellular matrix (ECM). The secreted proteases are mainly cathepsin K and tartrate-resistant acid phosphatase (TRAP), which help to digest the underlying bone in the resorption pits, named Howship's lacunae (Boyle et al., 2003) (Fig.1.3). In order to lower the pH in these Howship's lacunae, osteoclasts use an adenosine triphosphate (ATP)-dependent proton pump located in their membranes (Blair et al., 1989).

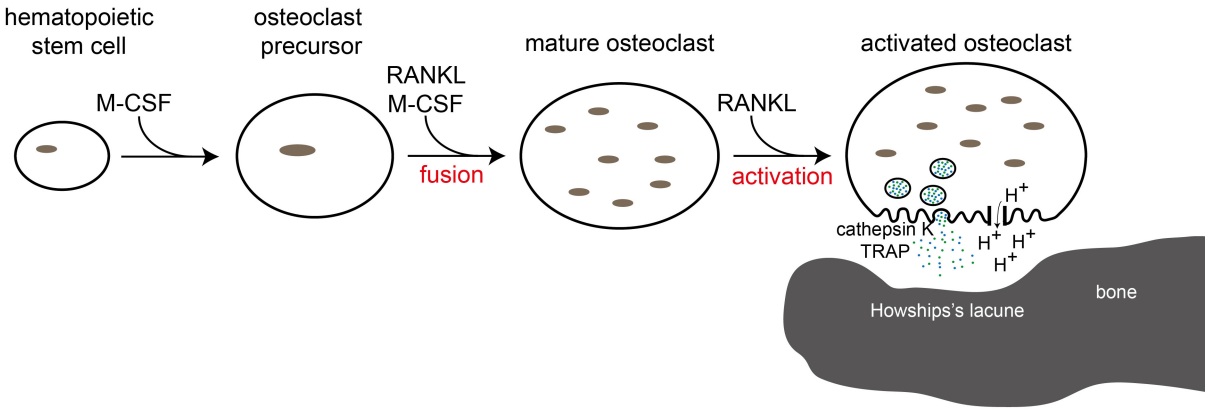

Figure 1.3: Maturation of osteoclasts.

Illustration of osteoclast maturation. Osteoclast precursors merge during maturation, so that mature osteoclasts have several nuclei. After activation, osteoclasts secrete proteases and protons to dissolve the underlying mineralized bone. The resorption zone is called Howship's lacune.

1.2.3 Osteocytes

Osteocytes represent the majority of cells in mature bone. It is assumed that osteocytes can sense mechanical stress with their cell processes, which are spread in the bone canaliculi and connect the osteocytes among each other in a complex 3D-network (Schaffler et al., 2014). They use soluble mediators, as well as cell-cell interactions to communicate (Goldring, 2015). One important task is regulating bone remodeling depending on mechanical stress the bone is exposed to. Xiong et al. discovered the importance of osteocytes for regulation of bone remodeling and osteoclast activation. They used *RANKL*$^{floxed/floxed}$*;Dmp1-Cre* mice, a mineralization-specific RANKL knockout, and showed that bone mineral density (BMD) in these knockout mice was significantly higher compared to control littermates (Xiong et al., 2011). Their experiments underline the importance of locally produced RANKL, giving convincing arguments, that RANKL is mainly responsible for osteoclast differentiation leading to bone remodeling. These RANKL knockout mice were protected from bone loss due to unloading, while control mice experienced bone loss (Xiong et al., 2011). Additionally, osteocytes also express tumor necrosis factor receptor superfamily member 11b (TNFRSF11B; aka. Osteoprotegerin, OPG), a strong inhibitor of RANKL, which regulates osteoclast bone resorption (Kramer et al., 2010). In the following TNFRSF11B is referred to as OPG.

Whilst unloading is followed by a loss of bone, mechanical loading results in increased bone formation. This may be caused by decreased expression of dickkopf WNT signaling pathway inhibitor 1 (DKK1) and sclerostin (SOST), which are both potent inhibitors of the WNT/β-catenin pathway, needed for osteoblast mediated bone formation (Robling et al., 2008). Furthermore, it is supposed that osteocytes also play an important role in preserving the functionality of mature osteoblasts (Tatsumi et al., 2007).

1.3 Underlying molecular mechanisms of bone remodeling

1.3.1 BMP-BMPR signaling

Bone morphogenic proteins (BMPs) are growth factors belonging to the TGF-β superfamily (Wozney et al., 1988). BMPs have multiple functions, i.a. osteoinduction and osteoclast stimulation (Termaat et al., 2005; Tasca et al., 2015). BMP2 is, for example, expressed by osteoblasts in a PTH-dependent matter, by MSCs, as well as vascular smooth muscle and endothelial cells and is partially stored in the extracellular matrix (Matsubara et al., 2012; Wozney et al., 1988; Zhang et al., 2011). Two known antagonists for BMPs are NOGGIN and CHORDIN (Groppe et al., 2002; Wagner and Mullins, 2002).
Like visualized in Fig.1.4, BMPs bind to BMP-receptors (BMPR), which are transmembrane serine-threonine kinases. Type 1A receptor (BMPR1A) can be found in embryonic mesenchyme, whilst type 1B receptor (BMPR1B) is mainly expressed in cartilage (Kronenberg, 2003). In order to generate a downstream signal, BMPR1 and BMPR2 have to form a heterodimer. The activated BMPR1 phorsphorylates the receptor-activated SMAD1 (protein similar to the gene products of the Drosophila gene 'mothers against decapentaplegic') (R-SMAD), whose activated form builds a complex with the R-SMADs 5 and 8. The activated R-SMADs, in turn, form a complex with its co-SMAD SMAD4 (Morikawa et al., 2013). This final complex translocates into the nucleus, directly binding to the DNA and activating or deactivating target genes, which i.a. regulate bone remodeling (Morikawa et al., 2013; Termaat et al., 2005; Tasca et al., 2015). In this way, BMP2 leads, for example, to an up-regulation of cathepsin K expression in osteoclasts (Tasca et al., 2015). It does not only directly interact with target genes, but also promotes the up-regulation of runt-related transcription factor 2 (RUNX2) and sequence-specific transcription factor 7(SP7, also known as Osterix or OSX), which are crucial for osteoblast differentiation and thus bone development and remodeling (Chen et al., 2012; Fakhry et al., 2013; Florencio-Silva et al., 2015; Franceschi and Xiao, 2003; Nakashima et al., 2011). RUNX2 and OSX promote several target genes in osteoblasts, like osteocalcin, bone sialoprotein, osteopontin, ALP and

Collagen I (Chen et al., 2012; Florencio-Silva et al., 2015; Franceschi and Xiao, 2003; Lee et al., 2000; Phimphilai et al., 2006). RUNX2 also leads to an enhanced responsiveness of cells for BMP2 (Phimphilai et al., 2006).

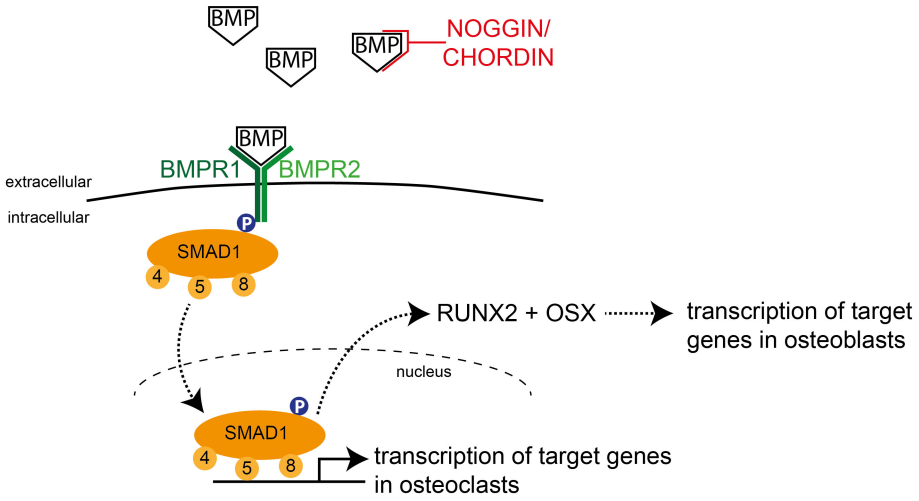

Figure 1.4: BMP-BMPR signaling pathway.

Visualization of the BMP pathway. NOGGIN and CHORDIN both can bind to BMP and thus inhibit it. After BMP activated the BMP-Receptor, the R-SMADs 1, 5 and 8 are phosphorylated and linked to SMAD4. This complex translocates into the nucleus, where it activates the transcription of target genes.

1.3.2 WNT/β-catenin signaling

Also the WNT/β-catenin pathway has a significant influence on bone homeostasis, osteoblast and osteoclast differentiation, as well as their activation (Bennett et al., 2005; Boyce and Xing, 2007).

WNT ligands are, for instance, produced by osteoblasts and have an autocrine function concerning maturation and bone mineralization. The WNT receptor with its co-receptors, like LDL receptor related protein 5/6 (LRP5/6) and FRIZZLED (MacDonald et al., 2009), activates an intracellular cascade including β-catenin and transcription factor 7 like 2 (TCF), leading to the transcription of target genes, for example osteoprotegerin (OPG) (Glass et al., 2005) (Fig.1.5). Knocking out sclerostin, a WNT-antagonist, leads to bone overgrowth comparable to diseases like sclerosteosis (van Buchem disease). Sclerostin inhibits the binding of WNT to LRP5/6 and is secreted by osteocytes. WNT3a, as well as WNT16, for example, induce the expression of OPG, which negatively influences osteoclastogenesis and thus leads to a higher bone mass. WNT16 also inhibits RANKL, leading to reduced nuclear factor kappa B sub-unit 1 (NF-κB) and nuclear factor of activated T-cells 1 (NFATC1) levels, causing reduced osteoclast formation and activity. NFATC1 acts directly on osteoclast precursors, by a WNT/β-catenin-independent man-

ner (Kobayashi et al., 2015b).

Osteoblasts express WNT5a and WNT16, which have different effects. For one thing, WNT5a promotes RANKL expression in osteoclast precursors and thus supports osteoclast formation, then again WNT16 also gives rise to osteoblast differentiation by enhanced expression of LRP5/6. Furthermore, WNT5a can partially abolish the effects of WNT16 on RANKL-depending osteoclast maturation (Kobayashi et al., 2015a). These findings underline that the WNT/β-catenin pathway has a significant influence on bone formation and resorption (Kobayashi et al., 2015b).

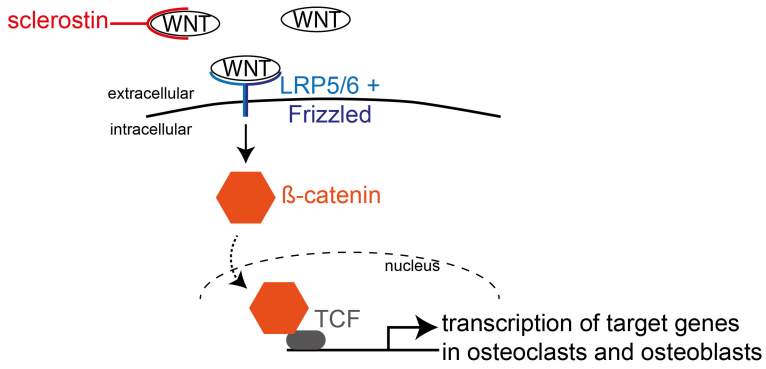

Figure 1.5: WNT/β-catenin pathway.

Simplified visualization of the WNT/β-catenin pathway. After binding to its receptors and co-receptors, the important downstream transcription factor β-catenin is translocated into the nucleus and leads to the transcription of target genes. Sclerostin can inhibit the pathway by binding comparatively to WNTs.

1.3.3 RANKL/OPG-RANK signaling pathway

As mentioned above, the RANKL/OPG-RANK signaling pathway is needed to regulate osteoclast differentiation and activity. RANKL is a secreted, as well as membrane-bound protein, expressed in several tissues like bone, dendritic, mammary or cancer cells (Boyce and Xing, 2007). But the main source of RANKL, concerning bone mass and osteoclast differentiation, are osteocytes (Xiong et al., 2015). RANKL may also be involved in osteoclast progenitor recruitment (Boyce and Xing, 2007). Its receptor is the tumor necrosis factor receptor superfamily member 11a (TNFRSF11A; aka RANK, in the following referred to as RANK). OPG is also found being expressed in several tissues apart from osteoblasts and osteocytes, like liver, spleen, kidney, heart, thymus, prostate, ovary, testis or adrenal glands for instance (Wada et al., 2006). It works as a decoy receptor for RANKL and inhibits its molecular effects, thus leading to an increased bone mass due to decreased bone resorption. OPG is regulated by several factors also regulating RANKL, as well as the WNT/β-catenin pathway (Boyce and Xing, 2007).

RANK is a widely expressed transmembrane protein, but mainly found on osteoclasts and its precursors. RANK is positively affecting osteoclast formation and activity, leading to an in-

creased osteolysis (Hughes et al., 2000).

As previously mentioned, RANKL is expressed and secreted by osteoblasts and osteocytes to later bind to RANK, expressed by osteoclast precursors. Hereupon, RANK binds to tumor necrosis factor (TNF) receptor associated factors (TRAFs), especially TRAF 6 and its co-factor growth factor receptor bound protein 2 (GRB 2) to activate an intercellular signaling cascade, leading to expression of NF-κB, followed by the leucine zipper protein FBJ murine osteosarcoma viral oncogene homolog (C-FOS) and finally NFATc1 (Fig.1.6). NFATc1 is described as the main regulator of osteoclastogenesis (Boyce and Xing, 2007; Wada et al., 2006). It enhances the expression of osteoclast specific genes like calcitonin, cathepsin K, TRAP, calcitonin receptor and β3-integrin (Boyle et al., 2003; Wada et al., 2006).

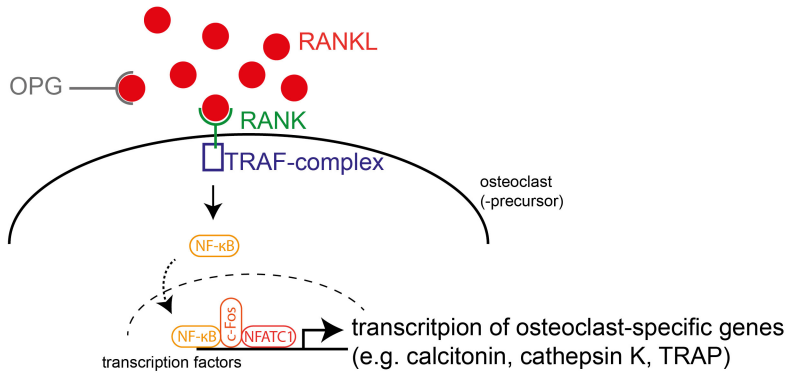

Figure 1.6: RANKL/OPG-RANK pathway.

Simplified visualization of the RANKL/OPG-RANK pathway. When binding to RANK, an intracellular cascade starts, leading to the transcription of osteoclast-specific genes like calcitonin, cathepsin K, TRAP, calcitonin receptor and β3-integrin. RANKL can be bound and inactivated by OPG.

1.3.4 Molecular cascade of fracture healing

Fracture healing can be divided into four stages. The initial inflammatory phase involves lymphocytes, macrophages, eosinophils and neutrophils (Hankenson et al., 2015). These inflammatory cells resolve the hematoma and cellular debris, stimulate the recruitment of new blood vessels and fibroblasts and release various cytokines, as well as pro- and anti-inflammatory mediators (Hankenson et al., 2015). Some of these released mediators have positive effects on bone healing and formation, such as prostaglandins, monocyte chemoattractant proteins and interleukins (IL), particularly IL 3, -6 and -10, and some have negative effects like TNF-α (Einhorn, 1998; Hankenson et al., 2015).

Following this initial phase, angiogenesis determines the second stage. New blood vessels do not only transport oxygen to the fracture site, but also provide osteoprogenitor cells. Endothelial cells are thought to express members of the BMP family, which promote bone formation and

osteogenetic differentiation (Einhorn, 1998; Jacobsen et al., 2008).
Callus is built over the fracture site. This callus contains a hard part, where intramembranous ossification takes place and a soft part built of endochondral ossification. Calcification of cartilage parts of the callus is very similar to calcification in the growth plate during development (Einhorn, 1998). Human MSCs (hMSCs) migrate to the fracture site and start to differentiate directly into osteoblasts or chondrocytes, which form a proteoglycan-rich ECM. The osteoblasts are responsible for intramembranous ossification, whilst chondrocytes start endochondral ossification. Factors promoting intramembranous ossification are for example various WNTs, BMPs, Notch ligand and integrin binding, whereas for instance BMP2, -4, -7, TGF-β and PTHLH are increasing endochondral ossification (Hankenson et al., 2014, 2015). This stage of initial bone formation and cell differentiation leads to an increase of callus and to a higher stability in the early state of healing.
In the final phase, newly built bone and callus are remodeled. It is, like physiologic bone remodeling, represented by osteoclastic bone resorption and osteoblastic bone formation. This phase takes the longest time of the healing process and is marked by intramembranous bone formation to recondition mechanical and biological function (Hankenson et al., 2014). Osteoclast bone remodeling is mainly regulated by the OPG/RANKL/RANK signaling system, the WNT/ß-catenin system, as well as PTH exposure (Hankenson et al., 2015).

1.4 Osteoporosis

1.4.1 The diagnosis Osteoporosis

Dual-energy X-ray absorptiometry (DXA or DEXA) is used to determine whether a patients' bone is osteoporotic. DXA measures the bone mineral density (BMD) and can be used at different sites, i.e. the femoral head, lower spine or total hip. The World Health Organization (WHO) defined the measurement of the femoral head as reference standard, setting a DXA T-score of -2.5 standard deviation (SD) or lower as the definition of osteoporosis (Bonjour et al., 2004). The T-score compares the measured BMD of the patient to a healthy 30-years old adult and is stated in standard deviations (National Osteoporosis foundation, 2021).

1.4.2 Prevalence of osteoporosis and its consequences for the health care system

Osteoporosis is a disease mainly affecting people aged 50 years and higher (Hernlund et al., 2013). This fact and the demographic change make osteoporosis a disease with an increasing

prevalence and importance, assuming an increase of osteoporosis cases of 23 % comparing 2010 to 2025 (Hernlund et al., 2013).
In Germany, the estimated prevalence of osteoporosis in 2017 was 4.4 % for women and 1.9 % for men between the ages of 45 and 64. In the age cohort of over 65 a prevalence of 24.0 % for women and 5.6 % for men is calculated (RKI, 2017).
This high number of cases is followed by an enormous burden for the health care system including costs of treatment of initial fractures (66 % of the total costs), long-term care (29 %) and pharmacological prevention (5 %), which all in all are estimated about 37 billion Euro in the EU in 2010 (Hernlund et al., 2013). Hip fractures represent the biggest part, taking 54 % of the costs. These vast costs underline the significance of osteoporosis in our society.

1.4.3 Pathogenesis of postmenopausal osteoporosis

Bone loss in elderly women is closely linked to a rapid decline of estrogen in the menopausal transition (Hotchkiss and Karl, 2003). During the menopausal changeover, serum estradiol declines by 80 % to 85 %, whilst serum estrone declines by 60 % to 65 % compared to premenopausal levels (Khosla et al., 1997). The reason for decreasing bone mass is the strongly enhanced bone resorption, increased by 79 % to 97 %, whilst bone formation increases less by only 37 % to 52 % (Garnero et al., 1996). As mentioned above, bone resorption is mainly mediated by the RANKL/OPG-RANK signaling pathway. Estrogen has various possibilities to affect this pathway, mostly by inhibiting RANKL expression (Fig.1.7). Estrogen decreases RANKL-levels produced by marrow stromal cells, as well as B- and T-cells (Eghbali-Fatourechi et al., 2003) and promotes gene expression of OPG (Hofbauer et al., 1999). Furthermore, estrogen induces apoptosis of osteoclasts mediated by TGF-β, which was shown by treating ovariectomized mice with 17β-estradiol for one, respectively three weeks (Hughes et al., 1996). Estrogen also appears to regulate osteoclasts in a direct way, since the osteoclastic bone resorption activity is significantly lower under 17β-estradiol administration (Oursler et al., 1994). Additionally, estrogen significantly increases bone formation markers expressed by osteoblasts, like serum N-terminal propeptide of type 1 collagen and osteocalcin. By decreasing serum levels of sclerostin, estrogen is also leading to a higher activity of WNT (Mödder et al., 2011) (Fig.1.7).

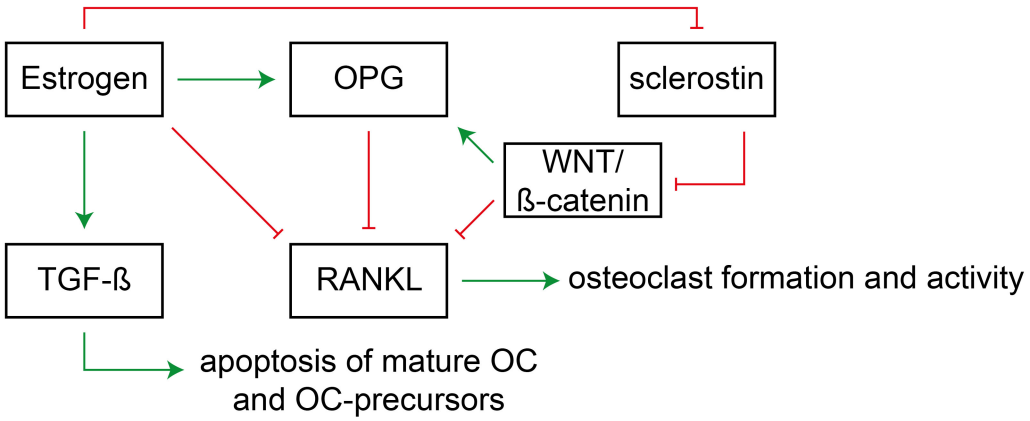

Figure 1.7: The influence of estrogen on bone metabolism.

Estrogen inhibits osteoclast (OC) maturation and promotes their apoptosis. Due to the decreased estrogen levels during the postmenopause, bone resorption is strongly enhanced and thus leading to osteoporosis.
Green arrows represent promotion, red arrows represent inhibition.

These findings point out the importance of estrogen for the regulation of the RANKL/OPG-RANK signaling pathway and osteoclast activity. Losing the majority of the female sex hormones during the menopause, osteoclasts get less inhibited, thus leading to an increased bone resorption, a decreased bone formation and a significant bone loss in perimenopausal women. This also has a big impact on fracture healing, since it requires a high bone formation activity.

1.4.4 Current treatment options for osteoporosis

Before pharmacological intervention, a non-pharmacological treatment is recommended. A large share comes to nutrition habits, periodical exercises to maintain body weight and muscle strength and fall prevention to prevent fractures. Diet should contain approximately 1200 mg of calcium per day and 800 IU (international units) of vitamin D_3 per day for osteoporotic women (Tella and Gallagher, 2014; Rizzoli et al., 2014; Dachverband Osteologie e.V., 2019).
There are several pharmacological treatment options against osteoporosis, which can be mainly separated into two categories: firstly drugs, which inhibit bone resorption, including selective estrogen receptor modulators (SERMs), bisphosphonates, Denusomab (Fig.1.8) and secondly drugs promoting bone formation, including recombinant human parathyroid hormones (rhPTH) like Teriparatide.
Since treatment of postmenopausal women with pure estrogen has severe side-effects, like increased rates of breast cancer (Rossouw et al., 2002), the administration rates of estrogen are very low. Raloxifene belongs to the SERM-family and is a partial estrogen agonist (Fig.1.8), which has similar effects on the bone like estrogen itself, but does not have the negative side-

effects of estrogen outside the bone (Chan et al., 2016). Actually, Raloxifene additively decreases the risk of invasive breast cancer by 76 % (Cummings et al., 1999), so it is indicated for treatment of osteoporotic women with a higher risk of breast cancer. Concurrently, Raloxifene lowers the risk for vertebral fractures by 30 - 50 % (Ettinger et al., 1999).

Bisphosphonates are inorganic pyrophosphate analogues, which have a high affinity for hydroxyapatite and consequently also for the bone (Hotchkiss and Karl, 2003). They slow down bone resorption by inhibiting osteoclast activity and leading them to apoptosis (Fig.1.8) (Carano et al., 1990; Chan et al., 2016; Tella and Gallagher, 2014). With bisphosphonates, a risk reduction from 40 to 70 % for vertebral fractures in postmenopausal women can be achieved (Black et al., 1996; Harris et al., 1999; Black et al., 2007).

Denusomab is a human monoclonal antibody. It specifically binds to RANKL and thus mimics the effect of OPG, leading to a lower degradation of the bone by osteoclasts (Tella and Gallagher, 2014) (Fig.1.8). With a long-term Denusomab treatment of six years, vertebral fracture rate can be lowered by about 50 % compared to a treatment with placebo (Bone et al., 2013).

There are some novel therapies, which are still in clinical trials. One of them are cathepsin-K inhibitors, e.g. Odanacatib. As mentioned above, cathepsin-K is expressed by osteoclasts and is important for bone resorption. By inhibiting this protease, bone resorption is decelerated and the BMD improves (Bone et al., 2010, 2015). Other novel drugs are sclerostin inhibitors, e.g. Romosozumab. Secreted by osteocytes, sclerostin is an antagonist of the WNT pathway. The effect of inhibiting sclerostin is as a consequence an increased bone formation by osteoblasts (Tella and Gallagher, 2014; Chan et al., 2016; Gupta and March, 2016). In a phase 2 trial this lead to an increase of BMD up to 11.3 % (McClung et al., 2014).

In the category of drugs, which promote bone formation, only Teriparatide is widely used and approved of. Teriparatide is a recombinant parathyroid hormone and has the same effects as endogenous PTH. The calcium level is elevated by a higher re-absorption of calcium in the kidneys, as well as by a higher intestinal calcium absorption (Chan et al., 2016). In addition, it activates several pathways in osteoblasts, leading to their recruitment to the remodeling site and thus to formation of new bone (Tella and Gallagher, 2014) (Fig.1.2). The rate of vertebral fractures can be reduced by about 65 % with a treatment with Teriparatide (Neer et al., 2001).

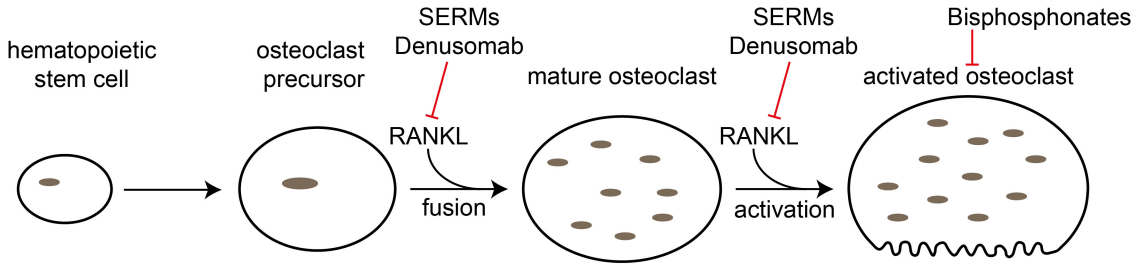

Figure 1.8: Schematic overview of the most common treatment options

Red arrows represent the inhibitory effect of the drugs. Most of these drugs affect the maturation and activation of osteoclasts. Inhibiting RANKL, SERMs and Denusomab act on the maturation and activation of osteoclasts, whilst bisphosphonates act on activated osteoclasts.

1.4.5 Current surgical treatment options

Concerning vertebral fractures, there are also surgical treatment options beside conservative treatment: vertebroplasty and kyphoplasty. The percutaneous injection of liquid cement (polymethylmethacrylate, PMMA) into a vertebral bone defect is called vertebroplasty. For kyphoplasty, a balloon is injected into the defect vertebral body and inflated to restore the vertebrate bodys' height and pattern. After removing the balloon the cavity left behind is filled with PMMA (Garfin et al., 2001).

Whilst some studies recommend percutaneous vertebral augmentation (Anderson et al., 2013; Lee et al., 2012; Boonen et al., 2011), other authors, like the American Academy of Orthopaedic Surgeons, strongly advise against these methods (Esses et al., 2011; McCarthy and Davis, 2016). In two randomized controlled studies no evidence could be found for an improvement of pain or functionality by vertebroplasty compared to a placebo group (Buchbinder et al., 2009; Kallmes et al., 2009). This missing effect and potentially severe complications like leakage of cement, neurologic injuries and associated vertebral fractures show that percutaneous vertebral augmentation has to be rated critically (McCarthy and Davis, 2016).

These controversial positions indicate the need for a clearly recommendable surgical treatment option. The idea of integrating tissue engineering into surgical treatment of osteoporotic fractures may provide an approach to directly affect the bone itself.

1.5 Tissue engineering

1.5.1 Tissue engineering principles

Basically there are five forms of cell based tissue engineering. Connective tissue progenitors can be targeted *in situ* by promoting the activation, migration, proliferation or differentiation at

the implantation site. This method was used in the present study. The implanted scaffolds supply a surface on which cells can adhere and proliferate. Additionally, it can be coated with growth factors, such as BMP2 for example, to support osteoinduction at the spot of application (Muschler et al., 2004). With the help of the scaffold, cells can be immobilized at the targeted area and protein concentrations can be upheld (Wozney and Seeherman, 2004).
Another strategy for tissue engineering is transplantation of autogenous tissue progenitors. It is performed to improve deficient number or function of local connective tissue progenitors (Muschler et al., 2004). Giving the opportunity of culturing a huge number of cells, *in vitro* expanded cells can also be transplanted. Thereby muscle, fat and bone tissue can be targeted by this method (Pittenger et al., 1999). A further application form of tissue engineering is transplanting genetically modified cells using viral or non-viral vectors changing the genetic expression pattern (Hannallah et al., 2003). Furthermore, tissue can be generated *ex vivo* and be transplanted like for example done with skin grafts. But there are still difficulties to realize this method, like generating a functional tissue at all, the functional transplantation and the fixation into normal tissue (Muschler et al., 2004).

1.5.2 Important features of scaffolds

Essential for targeted tissue engineering is the selection of the right scaffold. Scaffolds act as a carrier of proteins and provide a surface for cell attachment and activity (Muschler et al., 2004). In order to choose the best scaffold, various characteristics have to be considered. First of all, it has to be bio-compatible (Wozney and Seeherman, 2004). Further important factors are the bulk material (for example collagen or hydroxyapatite), the architecture and permeability of the matrix, the chemistry of the surface (for instance coated with BMP2), as well as the initial (pH, osmolarity) and late (characteristics after degradation) scaffold environment (Muschler et al., 2004). Cells have to be able to migrate within the scaffold and should be able to build ECM (Wozney and Seeherman, 2004).

1.5.3 Hybrid scaffolds in tissue engineering

Various scaffolds and materials have various advantages and disadvantages. One big disadvantage of collagen I based scaffolds is their biodegradability, whilst they have a good biocompatibility. In order to combine advantages of scaffolds and cut out their disadvantages as far as possible, hybrid scaffolds are becoming more and more common and successful. They can, for example, combine the biocompatibility of collagen I and the mechanical stability of other components (Roether et al., 2018; Liu et al., 2018b; Irawan et al., 2018). This has led to the idea, to use a mechanically stable product, which is also collagen based.

Chapter 2

Aims of the study

2.1 Establishment and evaluation of a hMSC seeded and BMP2 loaded three-dimensional hybrid collagen scaffold

The first objective was to establish and evaluate a three-dimensional (3D) scaffold meeting the following requirements:

- The actual structural matrix grafts should already have been clinically approved of in order to allow later translation into clinical applications.
- The scaffold construct should easily be seeded with hMSCs and allow sufficient cell survival.
- The 3D scaffold should allow reliable quantification of osteogenic differentiation.
- The scaffold should allow loading with additional osteoinductive cytokines such as BMP2 and should ensure appropriate release kinetics.

Collagen hydro-gels and 3D structural matrix grafts both feature distinct advantages and limitations as single scaffolds. Hydro-gels are feasible carriers for hMSCs and additional osteoinductive cytokines can easily be added, but they rapidly degrade and lack a primary structural stability. 3D matrix grafts are more difficult being seeded with hMSC and coated with additional cytokines, but provide a longer lasting structural support and a higher primary stability. The hypothesis was that the establishment of a hybrid 3D collagen scaffold would combine the advantages of both scaffolds.

2.2 Evaluating the influence of BMP2 on osteogenic differentiation of hMSCs in the 3D hybrid collagen scaffold

The second objective of this study was to examine the influence of BMP2 on osteogenic differentiation of hMSCs in the newly introduced 3D hybrid collagen scaffold in comparison to a two-dimensional (2D) setup. It was hypothesised that BMP2 shows comparable effects on osteogenic differentiation of hMSCs in 2D and 3D setups. Furthermore, the influence of BMP2 on osteogenic differentiation was evaluated stimulating hMSCs of donors with osteoporosis and healthy controls in order to reveal potential disease-specific differences.

2.3 Analysis of important BMP2-mediated gene expression during osteogenic differentiation of hMSCs derived from osteoporotic patients and healthy controls

The third objective was to evaluate the up- and down-regulation of genes in response to BMP2 stimulation. Again, these investigations were conducted stimulating hMSCs derived from osteoporotic patients and healthy controls in order to identify potential disease-specific differences. Such finding could contribute to a deeper understanding of the molecular biological alterations associated with osteoporosis and could allow new therapeutic approaches in the treatment of the disease.

Chapter 3

Material & Methods

3.1 Cell culture

3.1.1 Primary cells and donors

Human mesenchymal stem cells were isolated from femoral heads from patients, who underwent total hip arthroplasty. Samples were collected according to the assignment of the medical faculty ethics commission (project number 238-15). Inclusion criteria for both groups were female sex, a negative serology for HIV- and Hepatitis-C- and -B-infection and a signed informed consent. For osteoporotic patients further criteria were beeing older than 65 and a low velocity trauma. When both criteria were matching, a DXA-measurement was performed. The inclusion criteria was a T-value of $\leq$ -2.5, according to the definition of osteoporosis by the WHO (Bonjour et al., 2004). For healthy patients the inclusion criteria were beeing older than 50, a high velocity trauma and no signs of osteopenia or osteoporosis in the conventional x-ray. Therefore, the femoral cortical index (FCI) was measured in the pelvis ap view x-ray. A significant correlation between BMD and FCI is reported in a number of publications (Nguyen et al., 2018; Feola et al., 2015). According to Nguyen et al., a FCI cut-off value of $\geq$ 0.62 was used (Nguyen et al., 2018). Performing a DXA examination just for the study would not be justifiable because of the higher radiation exposure.
Like shown in table 3.1, grouping was carried out according to the above stated criteria, separating the patients into two groups: osteoporotic donors and healthy donors.

Table 3.1: List of donors.

group	donor	age	DXA
osteoporotic donors	#6	70 years	T: -2,6
	#9	78 years	T: -4,8
	#10	85 years	T: -3,9
healthy donors	#12	60 years	-
	#18	66 years	-
	#48	52 years	-

Overview of donors age and DXA values referred to their serial number of recruiting. DXA measurements were only available for patients in the osteoporosis-group.

3.1.2 Cell isolation and culture condition

In order to isolate hMSCs from the bone marrow of femoral heads, the bone marrow was scraped out with a sharp Volkmann spoon (Ustomed Instrumente, Germany). The bone marrow was transferred into a falcon and washed three times in 15 ml PBS (phosphate-buffered saline, Merck, Germany) and vortexed. The supernatant was strained through a 100 μm cell strainer (Fisherbrand, USA). Subsequently a collagenase I solution (50 mg Collagenase Type 2 CLS 1 with 260 u/mg, (Worthington Biochemical, USA) diluted in 50 ml DMEM (1x) + GlutaMAX-I (life technologies, USA)) was added, agitated on a nutating shaker (GyroMini nutating shaker, Sigma-Aldrich, USA) at 37 °C for 10 minutes and afterwards again strained through a cell strainer. This was repeated three times. The strained supernatant was then centrifuged for five minutes at 500 g (Heraeus Megafuge 1.0 R, ThermoFisher Schientific, USA) in order to pellet the cells. The supernatant was discarded and total cells were seeded in T75 cell culture flasks (NUNC ThermoScientific, USA) with 10 ml standard α-MEM (MEM alpha Medium (1x) + GlutaMAX-I + FBS, (life technologies, USA)). In order to prevent fungal infestation, 100 μl Patricin (Patricin (fungicid), Merck, Germany) were added. Cells were incubated in a cell culture incubator at 37 °C with 5 % CO_2.

The hMSCs were cultured in standard α-MEM, which contains α-MEM enriched with 10 % FBS (fetal bovine serum, life technologies, USA) and 1 % Penicillin/Streptomycin (Merck, Germany). Media was changed at regular intervals of three to four days.

3.1.3 Cell harvesting and counting

Initially, the cell monolayer was washed with PBS and then detached with 1x concentrated Trypsin/EDTA (Trypsin/ ethylene diamine tetraacetic acid, Merck, Germany) for five minutes at

37 °C. When cells were still attached, 3x Trypsin was used. Trypsin was then neutralized with double the volume of fresh standard α-MEM. The cell suspension was mixed and 10 µl were inserted into a Neubauer chamber (Brand, Germany). Cells were counted in the four quadrants and the total number of cells per ml was calculated using the following formula:

$$Cells/ml = total\,counted\,cells * 0.25 * 10^4 \tag{3.1}$$

Finally, a certain amount of cells could be used for experiments or cryopreserved. In order to go on with the cells, they were centrifuged at 500 g for five minutes and suspended in fresh standard α-MEM.

3.1.4 Cryopreservation and thawing of cells

After counting and centrifuging (see 3.1.3), the cells were resuspended in freezing media composed of 70 % of standard α-MEM, 20 % of FBS and 10 % of DMSO (Dimethyl sulfoxide, Serva, Germany). Afterwards, this cell suspension was aliquoted, each 1 ml into cryovials (Thermofischer Scientific, USA), then placed on dry ice and, when frozen, stored in liquid nitrogen.
To thaw the cells, cryovials were taken out of the liquid nitrogen and placed in a water bath at 37 °C to liquefy the cell suspension. Cells were added to standard α-MEM and incubated at 37 °C with 5 % CO_2. After 24 hours, the media was changed in order to remove dead or non-attached cells.

3.1.5 Osteogenic differentiation

Osteogenic differentiation was performed for 21 days in triplets, each starting with 100'000 cells being seeded. In order to induce osteogenic differentiation, osteogenic differentiation media (ODM) was used. It is composed of 98.8 % DMEM, which is enriched with 10 % FBS and 1 % P/S (together in the following referred to as culture DMEM), 0.2 % Dexamethasone (Sigma-Aldrich, USA), 0.6 % β-Glycerophosphat (β-Glycerophosphate disodium salt hydrate, Sigma-Aldrich, USA) and 0.4 % L-Ascorbic Acid (L-Ascorbic Acid-2-phosphate, Sigma-Aldrich, USA). Culture DMEM was used for the control group. The media was changed every three to four days.

3.1.6 Osteogenic differentiation with BMP2

The osteogenic differentiation with BMP2 was performed the same way as described in 3.1.5. In this study rhBMP2 (R and D Systems, USA) was used. In the 2D-trial the BMP2 was added to the media and the BMP2-concentration was set to 100 ng/ml. In the 3D-trial BMP2 was added

in the manufacturing-step of the hydro-gel in a concentration of 100 ng per 75 μl gel. Osteogenic differentiation was again run for 21-days and the media was changed every three to four days.

3.2 Scaffolds

3.2.1 Potential scaffolds

Three different scaffolds were taken into consideration. Firstly, Orthoss Collagen (Geistlich Surgery, Suisse), a natural, deproteinized bone combined with native collagen. Collagen is added to have a flexible and moldable scaffold with nano and macro pores.
Secondly, KOLLAGEN resorb (Resorba, Germany, in the following considered as Resorba), a sponge consisting of equine collagen. It has osteoinductive properties, is pH-stable and permeable for cells and liquids, which is a good basis for a wide distribution within the 3D-scaffold (RESORBA GmbH, 2017).
Thirdly, a collagen I gel was fabricated. For the gel preparation 1 part of chilled 10x α-MEM (ThermoFisher Scientific, USA) was added to 8 parts of chilled collagen I (Collagen type 1 rat tail, Merck, Germany) solution through pipetting. Subsequently, the pH-value of the mixture had to be adjusted to 7.2 - 7.6 by adding sterile 0.1 M NaOH (Sodium hydroxide solution, Sigma-Aldrich, USA) and monitored by pH paper (Macherey-Nagel, Germany). Additionally, water, cells or proteins could be added to get a final volume of 10 parts. In order to prevent gelation of the mixture, the working temperature was arranged at 2 - 10 °C by working on ice. When the mixture was finished, gelation was started by incubating gels at 37 °C with 5 % CO_2 for 120 minutes.

3.2.2 3D hybrid collagen scaffold

In order to generate equal parts of Resorba, 3.0 mm biopsy punches with plunger (kai industries co., ltd., Japan) were used. The hybrid scaffold was created by putting one punched Resorba part into a not yet polymerized, prepared collagen gel, which included 300,000 hMSCs and, if needed, BMP2. After polymerization, the construct was put into 24 well plates, prepared with 1 % Agarose (Biozym LE Agarose, Biozym Scientific GmbH, Germany) at the bottom to prevent cell attachment to the plates. The cell culture media was added like described in 3.1.6.

3.3 Methods for quantification

3.3.1 Measurement of gel shrinking

In order to quantify the shrinkage of the collagen gel around the Resorba-core, pictures were taken on day 0, 3, 4, 9, 22 and 30. Therefore, the outline of the scaffolds was taken and the area was computed with ImageJ (Wayne Rasband, National Institutes of Health, USA). The size of the scaffold on day one was set at 100 %. Six scaffolds were measured and each compared to its baseline value.

3.3.2 BMP2 ELISA

The BMP2 enzyme-linked immunosorbent assay (ELISA) was performed out of the supernatant surrounding the scaffolds after 2, 24, 48, 96, 120 and 144 hours to quantify the release kinetics of BMP2. A hBMP2 DuoSet ELISA (R and D Systems, USA) was used and the assay was carried out according to standard protocol. This experiment was performed three times in triplicates.

3.3.3 Life-Dead Assay

For preparation of the Life-Dead-Assay (LDA), 10 mg Fluorescein diacetate (FDA, Sigma-Aldrich, USA) was dissolved in 2 ml Acetone (Sigma-Aldrich, USA) and vortexed. This stock solution was diluted 1:500 in PBS (PBS, Sigma-Aldrich, USA). Dead cells were counterstained with undiluted propidium iodide (PI, Sigma-Aldrich, USA). Samples were stained by dyeing them for 30 seconds in FDA and for four seconds in PI. Subsequently, samples were washed four times in PBS and pictures were taken with AxioObserver Zeiss (Zeiss, Germany).

3.3.4 Alizarin Red staining and microscopy

In order to prepare an Alizarin Red (AR) staining solution of 25 ml, 0.34 g Alizarin Red S (Sigma-Aldrich, USA) were diluted in 20 ml double distilled water (ddH_2O). When completely dissolved, the pH-value was set at 4.1 – 4.3 by adding 0.5 % ammonium hydroxide (Sigma-Aldrich, USA) and afterwards, the solution was filled up to 25 ml with ddH_2O.
After 21 days, 2D-cultured cells were rinsed twice with PBS and fixed with 4 % paraformaldehyde (PFA, Merck, Germany) in PBS for 15 minutes under continuous agitation. Finally, each well was again washed twice with ddH_2O and air dried.
3D scaffolds were washed twice with PBS, then covered with 1 ml 4 % PFA for 30 minutes and placed on a shaker. The washing step with PBS was realized three times. To store the samples until quantification, 1 ml PBS was given to each sample and then kept at 4 °C.

Staining of the 2D-differentiation was started by carefully adding 1 ml of AR staining solution to each well. After incubation for 20 minutes on a shaker, each well was washed three times with ddH_2O for five minutes and then dried.
The 3D scaffold was stained by adding 1 ml of AR staining solution, then incubated on a shaker for 30 minutes at RT and washed four times with 10 % Tween (Tween 20, Sigma-Aldrich, USA) on a 3D-shaker for ten minutes.
The stained hybrid 3D scaffold was frozen in Tissue Tek (Tissue Tek O.C.T Compound, Sakura Finetek, Japan) and cut at a gauge of 12 μm with CryoStar NX50 (Thermo Fischer Scientific, USA). Pictures were taken with Axiovert CFL 40 Zeiss (Zeiss, Germany).

3.3.5 Quantification of Alizarin Red Staining

To quantify the 2D-staining results, firstly 1 ml of freshly made 10 % acetic acid (Sigma-Aldrich, USA) was put onto each well and then incubated for 30 minutes on a shaker at room temperature (RT). Subsequently, the cell layer was scraped off with a cell scraper and transferred into a LoBind Eppi Tube (Eppendorf, Germany) together with the acetic acid. After being vortexed for 30 seconds, it was heated to 85 °C for 10 minutes. After cooling down on ice for five minutes, it was centrifuged at 14,000 g for 15 minutes. Following this, 375 μl of the supernatant were transferred into a new tube and pH was then neutralized by adding 150 μl 10 % ammonium hydroxide. Afterwards, it was put into a 96-well plate and measured at 405 nm in Multiskan FC Microplate Photometer (Thermo Fisher Scientific, USA).
To prepare AR standards, buffer had to be established. Therefore ammoniumacetat was used, produced by adding 7.5 ml of 100 % ammonium hydroxide to 80 ml dH_2O in a glass bottle, placing this solution on ice and slowly adding 7.5 ml of 100 % acetic acid. Standards were prepared by serial dilution starting with 40 μl AR (2mM) diluted in 760 μl of buffer.
Quantifying the 3D-staining results was done the same way, but skipping the scraping step.

3.3.6 Visual quantification of Alizarin Red in 3D scaffolds

For visual quantification of the Alizarin Red staining, ImageJ and pictures from 3.3.4 were used. Firstly, the level of red color in a control scaffold, which did not run osteogenic differentiation, was measured. This level was subtracted from all pictures in order to measure the gain of red color due to the Alizarin Red staining.
The area and the color-intensity of the stained spots of the scaffold was scaled and set relative to the area of the whole scaffold.

3.3.7 DAPI/Phalloidin staining

In order to visualize cells within the 3D scaffold, cell-seeded scaffolds were fixed after 1, 3 and 8 days in 4 % PFA at RT for 15 - 30 minutes and washed three times in PBS for five minutes. Afterwards, cells were incubated with 0.2 % Triton X-100, dissolved in PBS at RT for five minutes to ensure the permeability of the cell membrane. This step was again followed by a ternary washing step for five minutes with PBS.
Cells were stained with Alexa Flour 546 Phalloidin (Thermo Fisher Scientific, USA) diluted 1:15 in PBS for 30 - 40 minutes in a dark chamber at RT. For the nuclear contrastaining with 4,6-Diamidin-2-phenylindol (DAPI, Thermo Fisher Scientific, USA), the concentrated DAPI-solution was diluted 1:10,000 in ddH_2O and applied to the slides. After five minutes of incubation at RT, they were washed three times with PBS for five minutes. Finally, the stained scaffolds were mounted on the glass slides with Mowiol (Mowiol, Sigma-Aldrich, USA).

3.4 RNA sequencing

HMSCs from three osteoporotic and three healthy donors were cultured in osteogenic differentiation media (see 3.1.5) for 3 days in a T-25 flask with and without BMP2 and directly lysed using Tryzol (Invitrogen, USA). For the RNA isolation, a standard protocol was performed and its quality was measured with with a BioAnalyzer (Agilent, USA). The cDNA library was prepared with hexamer primers using a Lexogen mRNA kit (SENSE mRNA-Seq Library Prep Kit V2, Lexogen, Austria). Subsequently, the cDNA library was sequenced with approximately 15 million reads on an Illumina HiSeq1500 (Illumina, USA) using a read length of 50 bp. Obtained raw data was mapped to the human reference genome (GRCH38.92) with STAR. DESeq2 was used to analyze the differential gene expression. The level of significance for changed genes was defined with a p value of less than 0.05. REVIGO or STRING were used to visualize functional protein association networks as well as gene ontology.

3.5 Statistics

Graph Pad Prism 8 (USA) was used to perform statistical analyses. At least triplicates were used for all experiments. In the present trial, a p-value of 0.05 or lower was defined as significant. For statistical analyses, a Gaussian distribution was determined and one-way ANOVA tests or t-tests with appropriate post-hoc tests were performed (GraphPad Prism, USA). Data is represented as the mean and the standard deviation.

Chapter 4

Results

4.1 Establishment of the 3D scaffold

4.1.1 Cells show a good survival in collagen I gels and on Resorba

Two commercially available 3D structural matrix grafts were identified being clinically approved of: a collagen I based sponge-like scaffold (Resorba) and a decellularized cancellous bone matrix (Orthoss). Those two scaffolds were investigated according to the above stated aims of the present study. Intending to establish a 3D collagen I hybrid scaffold, a self-fabricated collagen I hydro-gel was investigated in addition.

At first, the survival of hMSCs on the different scaffolds was evaluated. So, LDAs of each scaffold at different time-points were performed (Fig.4.1 and Fig.4.2). In all LDAs living cells are stained green, whilst dead cells are stained red or orange. In the self-fabricated collagen I gel, the cells are distributed homogeneously from day one (Fig.4.1, A). In the first three days, the cells spread out their appendixes and show a good survival in the gel (Fig.4.1, B and C).

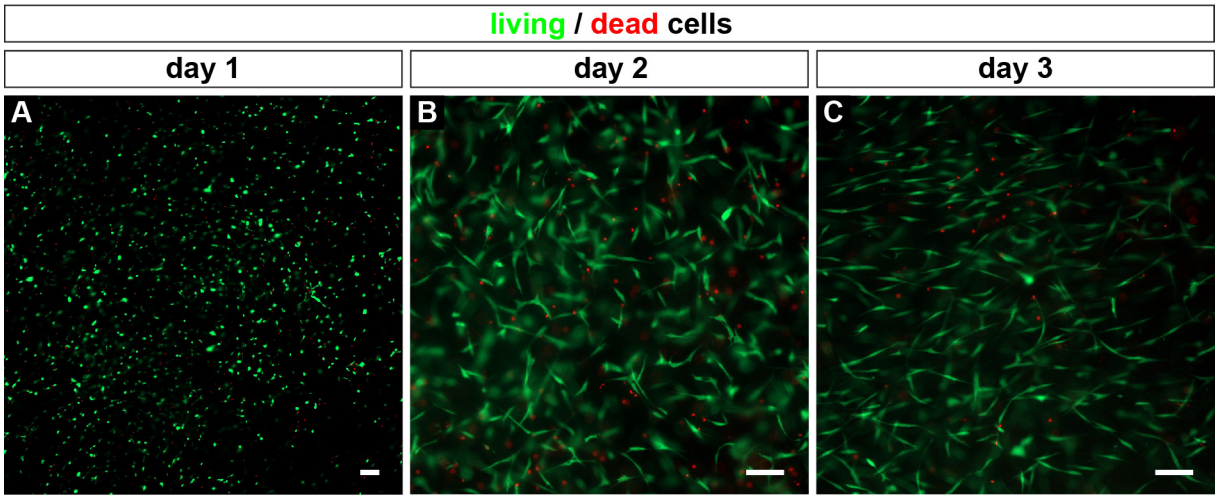

Figure 4.1: Life-Dead Assay of hMSCs in the self-fabricated collagen I gel.

The hMSCs are homogeneously distributed within the gel and show a good survival at all time-points investigated (**A** to **C**, green cells) with only a few dead cells (red cells). After the first day, the cells start to spread, indicating an appropriate extracellular environment for the adhesion of the cells to the collagen I fibrils (**B**, **C**). The proportion of living (green) and dead (red) cells is very similar at all points of time. Scale bar: 100 µm.

Since the sole collagen I gel contracts within a few days (see Fig.4.6 and Fig. 4.7) and later completely dissolves, a more stable solution had to be found. On Orthoss, fewer cells adhere compared to Resorba, although both scaffolds were seeded with the same amounts of cells (Fig.4.2). On day 10 (Fig.4.2, A' and B'), a better survival can be observed in the Resorba scaffold compared to the Orthoss scaffold.

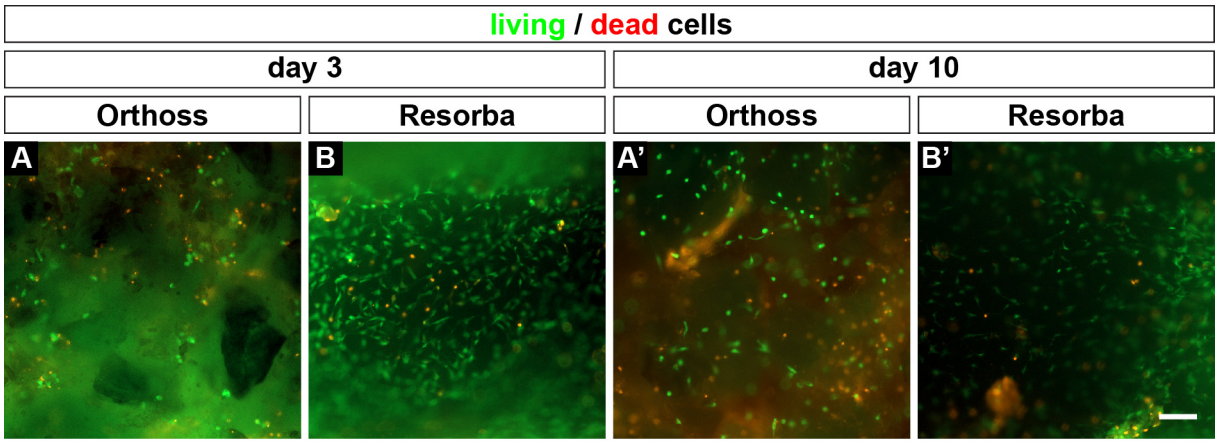

Figure 4.2: Life-Dead Assay of hMSCs seeded on Orthoss and Resorba scaffolds.

After three days, a homogeneous cell distribution over the scaffolds is only observed in Resorba (**B**), but not in Orthoss (**A**). At this time, the living/dead cell ratio is better in Resorba than in Orthoss. After ten days, the same findings can be observed (**A'**, **B'**). This indicates that Resorba embodies a better setting for 3D *in vitro* culture of hMSCs. Scale bar: 100 µm.

These findings indicate that the collagen I gel provides the best and Resorba still a better environment for cell survival than Orthoss.

4.1.2 Only Resorba and the collagen I hydro-gel are suitable to quantify osteogenic differentiation

In order to allow for specific detection and quantification of the newly synthesized extracellular matrix, the native scaffolds must not assimilate the Alizarin Red dye.
Native Orthoss gets stained with Alizarin Red and keeps the dye, even after repeated washing (Fig.4.3, A). In contrast, native Resorba is not stained after repeated washing steps (Fig.4.3, B).

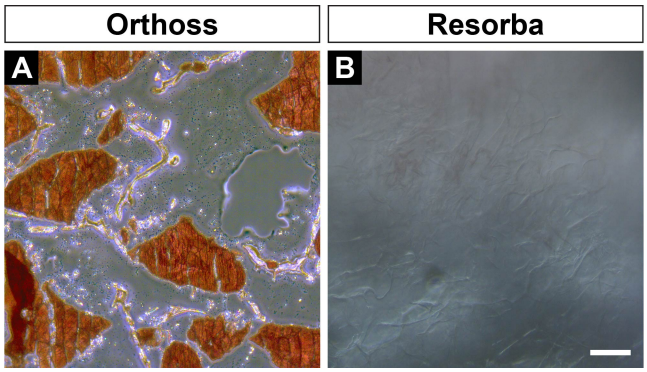

Figure 4.3: Alizarin Red staining of native Orthoss and Resorba.

Native Orthoss scaffold features a high affinity for Alizarin Red (**A**, red), whereas Resorba does not assimilate the staining (**B**). Scale bar: 100 µm.

The poor cell survival as well as the high affinity of native Orthoss with Alizarin Red lead to the exclusion of Orthoss.

4.1.3 The collagen I hydro-gel shows an appropriate release kinetic of BMP2

In order to qualify the release kinetics of BMP2 out of the collagen I gel, a BMP2 ELISA out of the culturing media surrounding the gel was performed at different points of time within the first six days (Fig.4.4).

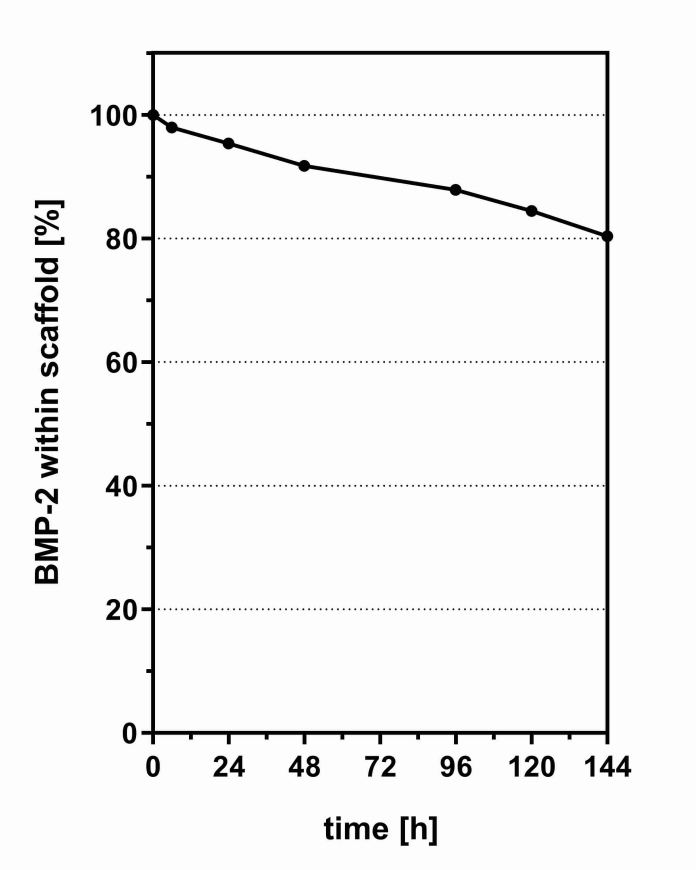

Figure 4.4: BMP2 release kinetic of the collagen I gel during the first 6 days.

The self-fabricated BMP2-loaded collagen I hydro-gel shows an almost linear release of BMP2 over the whole time of investigation. After six days 80 % of the initially added BMP2 is still within the gel.

After six days approximately 20 % of the BMP2 was released into the media. Consequently, the gel contains enough BMP2 for the 21-days differentiation.

4.1.4 The 3D hybrid scaffold combines the advantages

The advantages of the self-fabricated collagen I hydro-gel are the easy production (see 3.2.1) and the possibility to add any biologically active factors during production. The disadvantage is the contraction of the scaffold, when cells are added (Fig.4.6) and the lack of a primary structural stability. As a consequence, the gel alone is not utilizable for a differentiation of over at least 21 days. In order to maintain the stability of Resorba and the advantages of the gel, the two scaffolds were combined. The result is a 3D collagen I based hybrid scaffold.
LDAs were performed at three points of time in order to examine the survival in this 3D scaffold: on day 1, 9 and 30 (Fig.4.5). Analogous to the LDA of the sole scaffolds (see 4.1.1), the living cells show a homogeneous distribution across the whole structure, as well as a very good survival at every time-point investigated. This is the basic prerequisite for an osteogenic

differentiation lasting 21 days as well as further experiments.

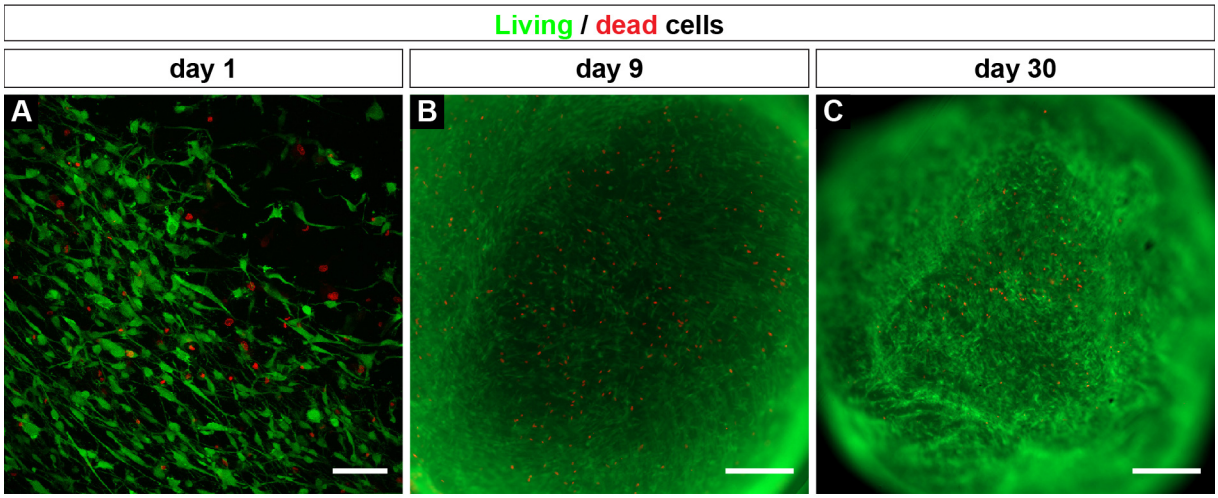

Figure 4.5: Life-Dead Assay of hMSCs in the three dimensional hybrid scaffold.

Throughout all points of time investigated, cells show a very good survival (green)/death (red) ratio. The survival and the homogeneous distribution indicate that the hybrid scaffold supplies a very good environment for hMSCs. Scale bar: 100 µm (A), 1mm (B and C).

The fusion of the two scaffolds also improves the stability. Figures 4.6 and 4.7 show the development of the hybrid scaffolds' size over 30 days. Though it also contracts in the first few days, contraction slows down after approximately three weeks.

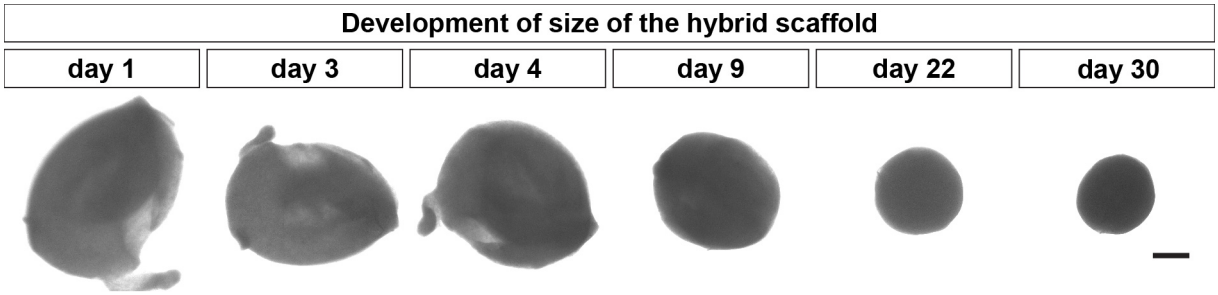

Figure 4.6: Development of the hybrid scaffolds size over 30 days.

Overview images of the hybrid scaffold. The collagen I gel around the Resorba core contracts until the scaffold reaches its final size. Scale bar: 2 mm.

Within ten days, the scaffold shrinks to half of its size, but then the speed of shrinking slows down. After 22 days, it still has 28.6 % and after 30 days 24.0 % of its original size left (Fig.4.7). This proves a higher stability for the hybrid scaffold, than for the collagen I hydro-gel alone.

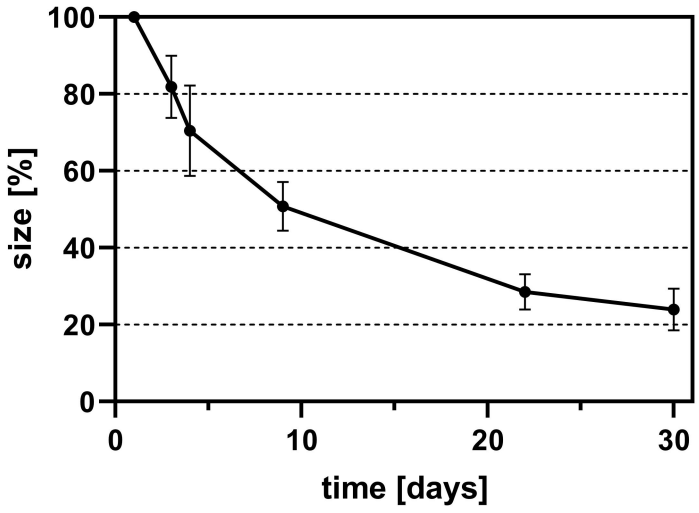

Figure 4.7: Illustration of the alterations in size of the hybrid scaffold over 30 days.

The size of the scaffold decreases to 24.0 % of its original size within 30 days. All six scaffolds were pooled in this graphic for each point of time.

The difference to the sole collagen I hydro-gel, which completely dissolves, is most probably referable to the Resorba core. The main part of the collagen I hydro-gel around the 3D matrix shrinks and the sponge itself remains as the lasting scaffold. Hereby, the disadvantage of the collagen I gel concerning the contraction is counterbalanced. The Resorba itself is not directly loaded with cells, but the surrounding collagen I hydro-gel is. Since the main part of the hydro-gel contracts, it is important to examine, if the cells migrate into the Resorba core. Therefore, images of the hybrid scaffold were taken on day 1, 3 and 8 with a confocal microscope to investigate the three dimensional distribution of the cells in the two components (Fig.4.8). A and B show the distribution on day 1 with a Life-Dead Assay (Fig.4.8, A) and a Phalloidin-DAPI staining (Fig.4.8, B). On days 3 (Fig.4.8, C) and 8 (Fig.4.8, D) a Phalloidin-DAPI staining was carried out, highlighting the actin cytoskeletons with green (Fig.4.8, B) and purple (Fig.4.8, C and D) colour. In A, B and C the dotted lines indicate the transition between collagen I gel to the right of the line and Resorba to the left. Picture D represents a cut-out in the Resorba-area. On day 1, the majority of the cells are still evenly spread in the collagen I hydro-gel. Two days later, more cells have migrated into the Resorba scaffold, forming filopodia among themselves (Fig.4.8, C). After eight days, a homogeneous cell distribution in Resorba can be observed (Fig.4.8, D).

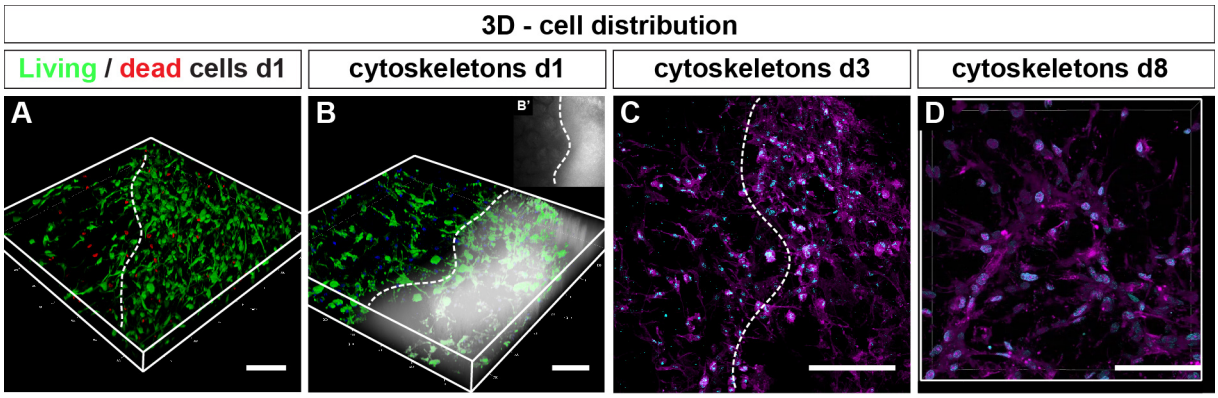

Figure 4.8: Cell distribution in the hybrid scaffold.

Cells are spread over the whole scaffold. The dotted lines in **A**, **B** and **C** indicate the transition zone between the collagen I hydro-gel on its right and Resorba scaffold on its left. In **A** a Life-Dead Assay was performed, living cells are stained green, dead cells red. A Phalloidin-DAPI staining was carried out on days 1 (**B**), 3 (**C**) and 8 (**D**), visualizing actin cytoskeletons (green in **B**, purple in **C** and **D**). Counterstaining was realized with DAPI, colouring nucleuses blue (**B**) and cyan (**C** and **D**). **B'** highlights the transition zone between collagen gel and Resorba in 2D. **D** shows a cut-out in Resorba. Scale bar: 100 µm.

Consequently, this 3D hybrid scaffold combines the advantages of the sole scaffolds and allows the cells to survive and migrate.

4.2 BMP2 enhances osteogenic differentiation in a 2D cell culture

In order to later perform osteogenic differentiation within the 3D hybrid scaffold, osteogenic differentiation was first carried out in a 2D setting. The experiments were carried out utilizing hMSCs derived from patients suffering from a manifest osteoporosis and healthy controls (Tab.3.1).
In each group osteogenic differentiation was carried out for 21 days. The first group did not receive any BMP2-treatment, a second group was treated with BMP2 for the first four days and the third group for 21 days. After 21 days of differentiation, an Alizarin Red staining was performed to detect newly formed mineralizations (Fig.4.9).
A similar cell density can be observed in every group. Osteogenic differentiation succeeded in every group, indicated by Alizarin Red. When comparing the Alizarin Red levels visually, there is no apparent difference between the four-day-BMP2 group and the no-BMP2 group for healthy and osteoporotic donors (Fig.4.9, compare A with A' and B with B'). The third group, with a 21-day-treatment, has larger areas stained by Alizarin Red than the first two groups (compare A" and B" with A/A' and B/B'). This indicates a higher rate of osteogenic differentiation in healthy and osteoporotic donors after a treatment of 21 days.

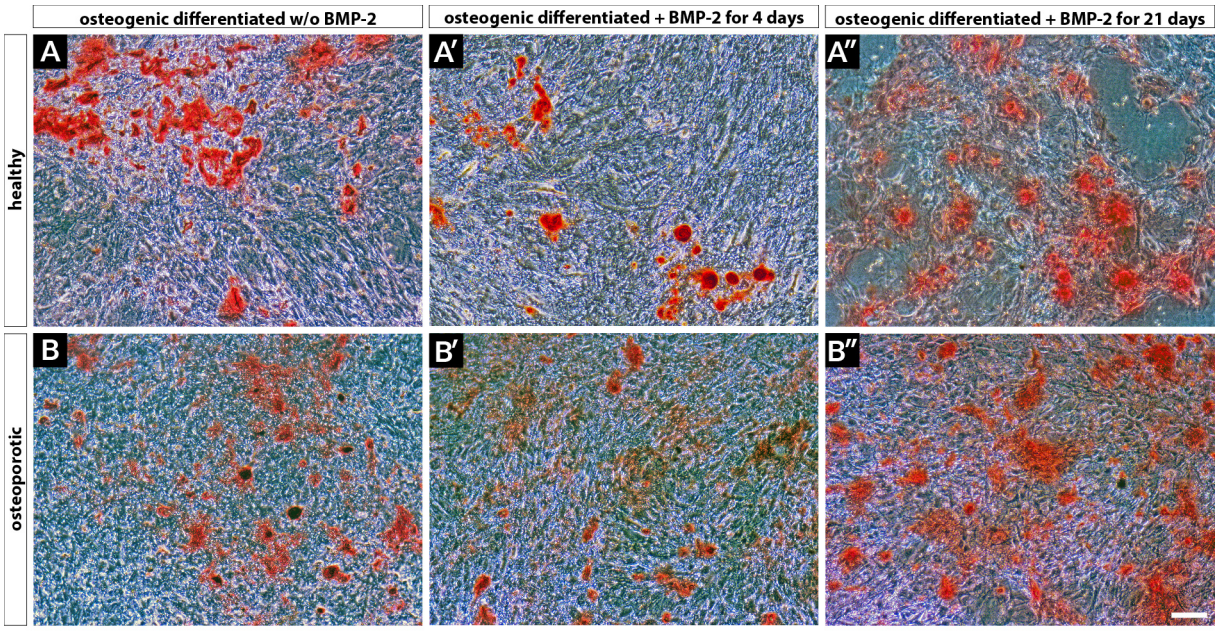

Figure 4.9: Alizarin Red staining of the osteogenic differentiation in 2D cell culture conditions.

A to **A"** show healthy donors, **B** to **B"** show osteoporotic donors. The visual assessment reveals similar Alizarin Red levels in the osteogenic differentiation without BMP2 and with four days of BMP2-treatment in healthy and osteoporotic donors. For both groups, the 21-days treatment shows the highest rate of Alizarin Red. Scale bar: 100 µm.

Figure 4.10 shows the results of the Alizarin Red quantification. In accordance to the visual evaluation of the staining, there is no significant difference between the no-BMP2 group and the four-day-treatment group (Fig.4.10). Here, no difference can be observed between healthy and osteoporotic donors. In both groups, the 21-day-treatment leads to higher levels of Alizarin Red staining compared to none or four-day-treatment. This difference is by tendency and statistically not significant.

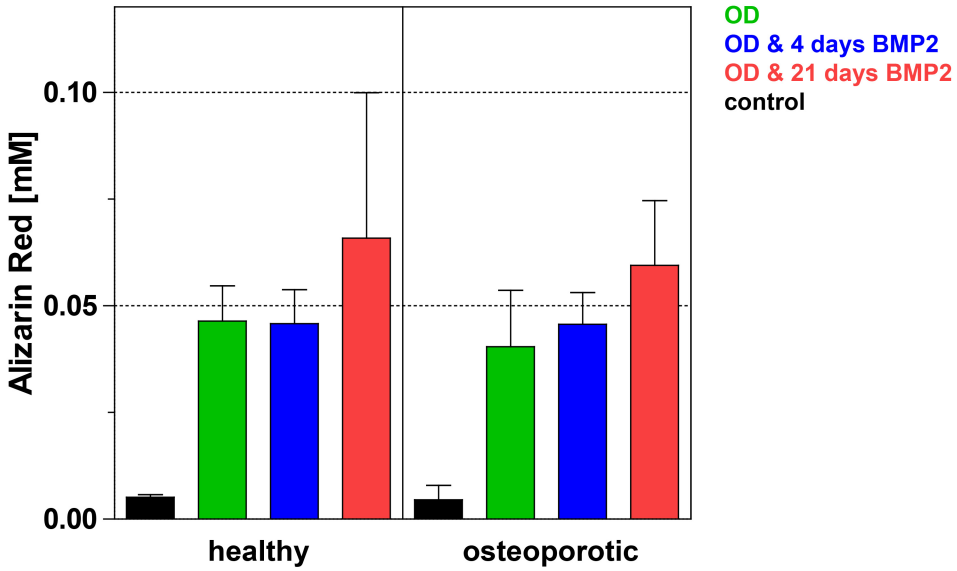

Figure 4.10: Quantification of 2D Alizarin Red staining.

Quantifying the Alizarin Red staining of the two dimensional osteogenic differentiation does not show a significant difference between osteoporotic and healthy donors concerning the intensity of staining. In both cohorts, the 21-day-treatment shows the highest rates of staining. But the results are not significant. The control group, treated with culture DMEM, did not get stained in either group.

These results suggest that the 21-day-BMP2 treatment has a slight, but not significant benefit on osteogenic differentiation, when compared to a four-day-treatment with BMP2.

4.3 HMSCs of healthy donors show a slightly higher response to a BMP2 induced osteogenic differentiation in the 3D setting compared to osteoporotic donors

The hybrid scaffold was proved to be a sufficient scaffold for 3D tissue engineering. Next, it was to examine, if there was a difference between healthy and osteoporotic donors in osteogenic differentiation depending on BMP2 in the 3D setting. Healthy and osteoporotic donors were incubated on the hybrid scaffold and each separated into two groups, respectively: one group without BMP2 influence and one group with 21 days of BMP2 treatment (Fig.4.11).

In osteoporotic donors, BMP2 does only lead to an enhanced osteogenic differentiation in donor #6 (Fig.4.11, A to A”). In contrast, healthy donors show a slightly higher level of staining under BMP2 treatment (Fig.4.11, C to C”). Within the two groups of healthy donors, the intensity of staining is similar.

The transition zone between the collagen I gel and the Resorba can be observed pretty well

(illustrative enlargement in B') by analyzing the structure of the scaffold. The surrounding collagen I gel has a homogeneous surface, whereas Resorba presents itself with a rougher and ragged surface (indicated by dotted lines).

For osteoporotic donors treated with BMP2, only donor #6 shows a staining with AR, whilst donors #9 and #10 do not show a significant coloring (Fig.4.11, A to A"). In the non-BMP2 group by contrast, all donors show a coloring with AR (B to B"). Again donor #6 shows the most intensive coloring (B), whilst donor #9 and #10 show a lighter staining (B' and B").

In all samples of the donors (excluded A' and A"), the area of Resorba is slightly more colored red than the surrounding collagen I gel area. In group A, only donor #6 can be used as a comparison, because of the non-staining of the other samples. The whole scaffold is colored in a similar level and structure. It is conspicuous, that the highest saturation of red color can be found in transition zones and frames of the scaffold (illustrative enlargements in B' and B"). The frames show a thin coating with red color. The collagen I gel itself is not as much stained as the frame and the transition zone between the two components.

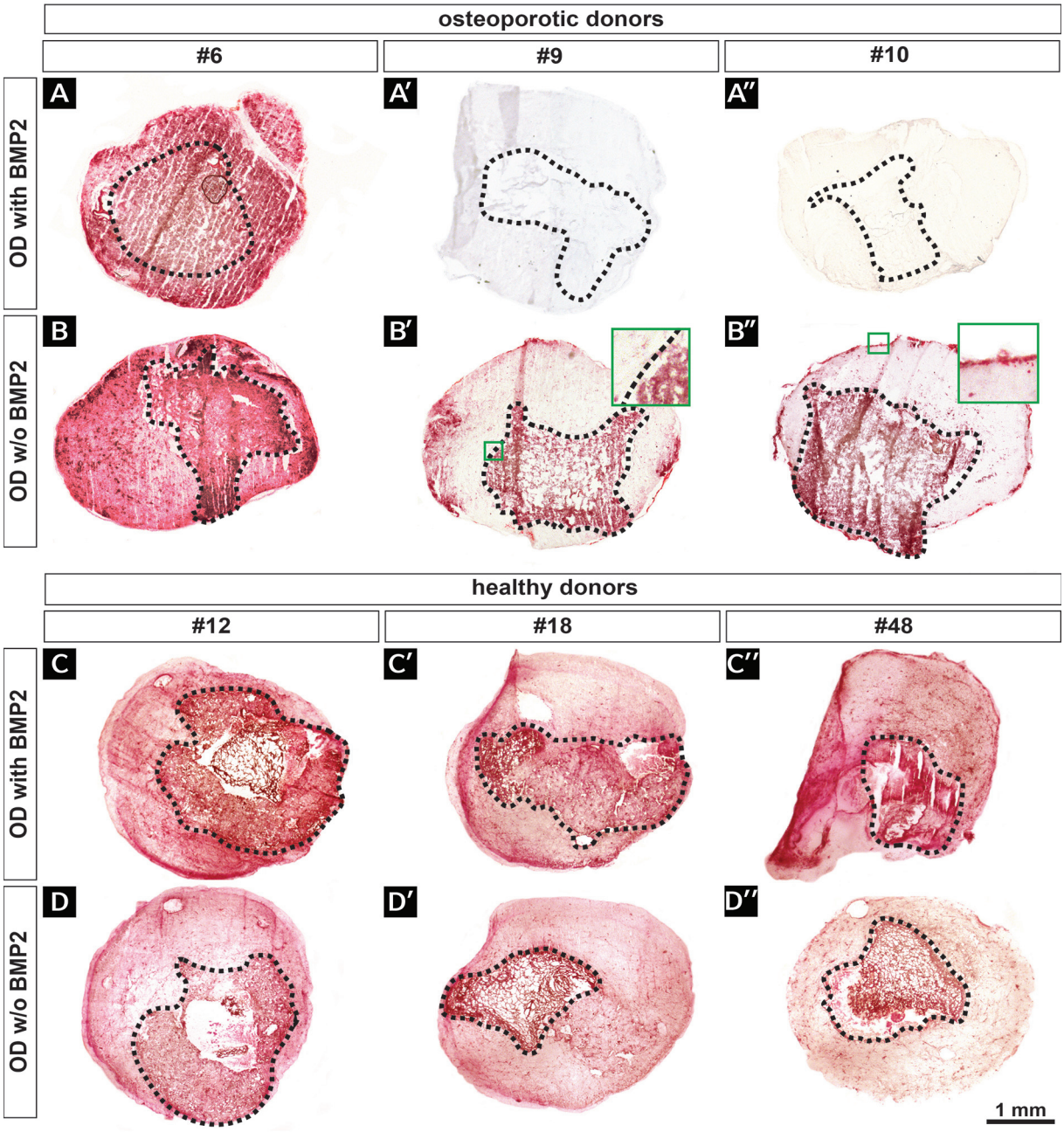

Figure 4.11: Alizarin Red staining of BMP2 dependent osteogenic differentiation of osteoporotic and healthy donors.

Osteoporotic donors (**A** and **B**) compared to healthy donors (**C** and **D**) after osteogenic differentiation and Alizarin Red staining. The dotted lines indicate the transition zone between the two components of the hybrid scaffold. In **A** the transition zone cannot be identified for certain. An addition of BMP2 does not lead to an improved osteogenic differentiation in osteoporotic donors, whilst it slightly does in healthy donors. The dark circle in the middle of picture A most likely correlates to an air bubble, which was trapped during staining.

Looking at these results, the main difference between osteoporotic and healthy donors seems to be the improvement of osteogenic differentiation under BMP2 influence in healthy

donors, whilst BMP2 does not necessarily lead to a higher differentiation in osteoporotic donors. In order to objectify these results, a visual quantification of the staining was made after 21 days (Fig.4.12). There cannot be found any significant difference within the two groups of donors. Even if not significant, the healthy donors show a slightly better osteogenic differentiation without BMP2. This contradicts the findings in Fig. 4.11. In the osteoporotic donor groups, BMP2 does not show any influence in osteogenic differentiation after 21 days.

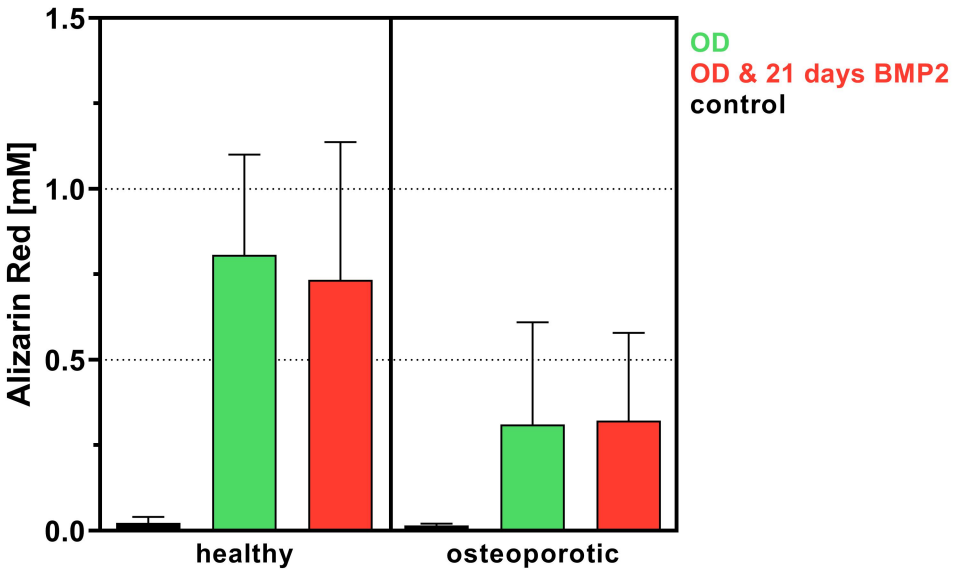

Figure 4.12: Visual quantification of Alizarin Red staining in the 3D setting comparing healthy and osteoporotic donors.

Each differentiation was performed for 21 days, one group with BMP2 addition (red) and one without (green). The control group (black) was run without differentiation media.

To differentiate if the Resorba or the hydro-gel provides a better scaffold for osteogenic differentiation for healthy and osteoporotic donors a further quantification was performed. The proportional area stained with Alizarin Red was calculated for the two different sections of the scaffold by visual quantification (Fig.4.13). For all groups, except for osteoporotic donors with BMP2 treatment, a higher differentiation rate was found in Resorba than in the hydro-gel. But again, no significant difference can be found comparing the use of BMP2 to the non-use of it within the different groups of donors (compare green and red bars in Fig.4.13).

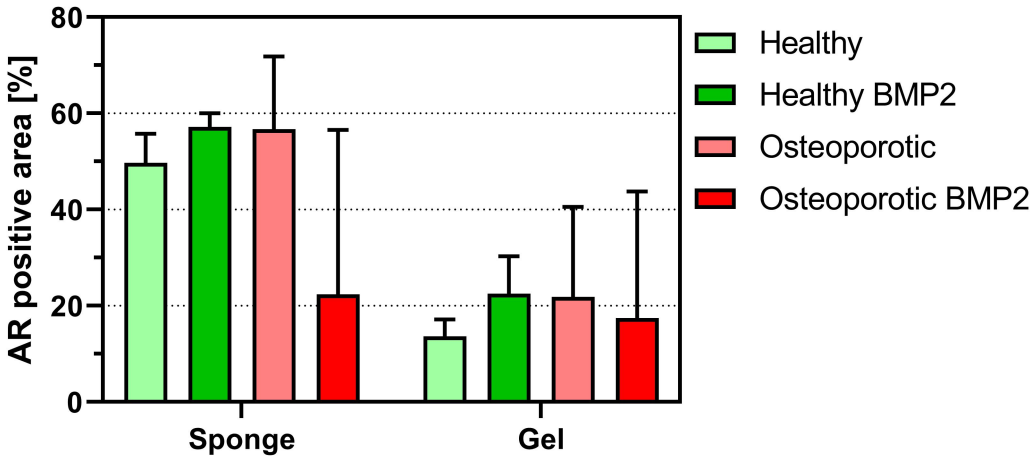

Figure 4.13: Visual quantification of Alizarin Red staining in the 3D setting comparing the Resorba (sponge) and the hydro-gel.

The donors were pooled in groups and the area proportion stained with AR was calculated for the Resorba and for the hydro-gel.

The osteogenic differentiation in this 3D setting does not seem to be improved by BMP2 in healthy as well as in osteoporotic donors. Since some donors even show an impaired differentiation under BMP2, it is of strong interest to find out, if BMP2 leads to an adjusted gene expression as regards genes being involved in osteogenic differentiation.

4.4 RNA sequencing could not identify specifically activated genes after BMP2 treatment

4.4.1 Sample heat maps show big differences between donors' reactions to BMP2

In order to examine the influence of BMP2 treatment to hMSCs of healthy and osteoporotic patients on levels of gene expression, a RNA sequencing of four sample groups was carried out. The donors were, like in the prior experiments, separated into healthy donors with (HBMP) and without (HNM) BMP2 treatment and osteoporotic donors with (OBMP) and without (ONM) BMP2 treatment. Figure 4.14 shows the relative differences in a comparing heat map.
When comparing the donor-related HNM and HBMP groups, a slight to medium difference can be seen in gene expression (Fig.4.14, A). Donor 48 shows the biggest adjustment of gene expression after BMP2 treatment. The main differences in picture A are related to the donors amongst each others and not to the BMP2 treatment.
For osteoporotic donors, the same results can be observed (Fig.4.14, B). Again, the main differences can not be traced back to the BMP2 treatment, although the osteoporotic donors show a

slightly higher variation of gene expression after BMP2 treatment than healthy donors do.
The next groups to be compared are HNM and ONM (Fig.4.14, C). This analysis was made to see the general differences between all donors and to set a basic value for the comparison under BMP2 influence. Like in A and B, donors 10 and 48 show the biggest differences overall. It is to notice that the gene expression of osteoporotic and healthy donors are way more different than they are within the single groups. None the less the slightest differences in this analysis can be found within osteoporotic donors.
The final setting is to compare BMP2 affected groups (Fig.4.14, D). Analyzing the heat map leads to the conclusion that the differences between the single donors in gene expression grow after the BMP2 treatment. Donor 10 can be taken as an example. The difference between donor 10 and donors 6 and 9 is approximately equal in ONM (picture C, second row, third and fourth box). In the BMP2 treated group (OBMP) the differences grow between the compared donors, but not at the same rate (D, first row, fifth and sixth box). The smallest change can be observed between donors 12 and 18.

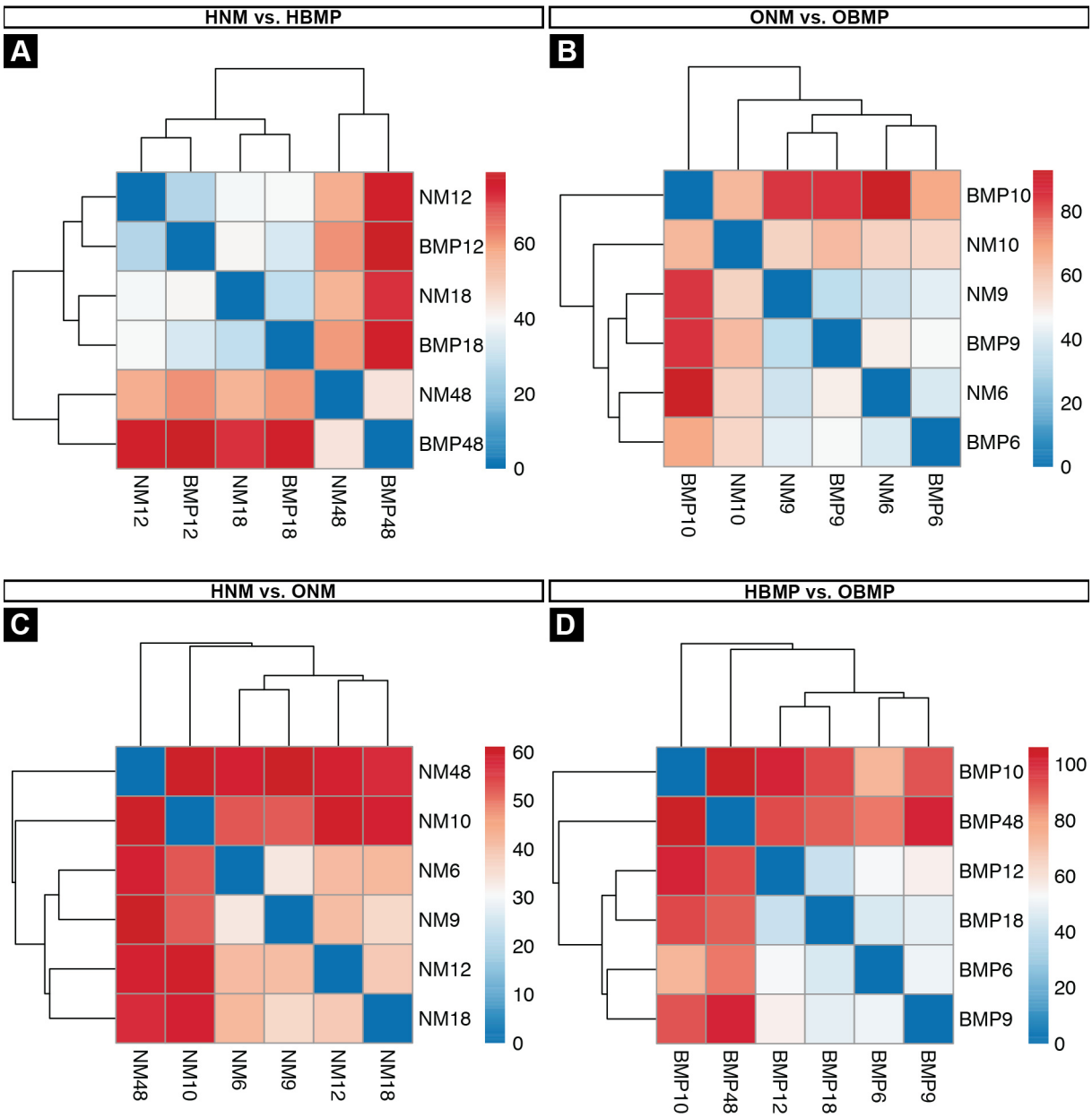

Figure 4.14: Sample heat maps show the relation between the different groups.

Relative difference is indicated by range of colour. NM stands for "normal differentiation" (without BMP2) and BMP stands for the BMP influenced groups. In picture **A** healthy donors, in picture **B** osteoporotic donors are compared to their correlating BMP2 groups. Picture **C** represents the comparison between healthy and osteoporotic donors, both without BMP2 influence, whilst in picture **D** both have been treated with BMP2.

Summing up, BMP2 has an apparent influence on the gene expression of the investigated hMSCs. But, considering these results, the different donors react to this treatment in a different way, or at least in a different intensity.

4.4.2 Genetic heat maps do not reveal uniform changes

The comparison of the most significant changes in gene expression can be visualized in heat maps. In every heat map sample genes, which have an impact on osteogenic differentiation, are highlighted. The analysis-program set the order of the donors in the heat maps depending on the statistic distance.

Figure 4.15 shows the comparison of the healthy donors with and without BMP2-influence. In general, donor 48 reacts most intensely to BMP2 treatment compared to donors 12 and 18. The gene *HSD11B1* encodes an enzyme, which catalyzes the reaction of cortisol to its inactive metabolite cortisone, as well as the opposite direction of this conversion. The BMP2-influenced group of each healthy donor has a higher level of transcription of this gene than the non-treated group. The biggest difference in expression can be seen in donor 48. A reduced expression of *IGFBP1* can be observed in the BMP2-groups of all three healthy donors. The encoded protein increases the life time of insulin-like growth factors (IGFs), which are important for bone development and growth. Another significant change in expression levels can be seen for *GDNF*. The encoded protein leads to recruitment of SMAD family members, which are important for osteogenic differentiation and the BMP2-pathway. But only in donor 48 a change can be observed. In donor 12 and 18 the expression levels of this gene stay consistent.

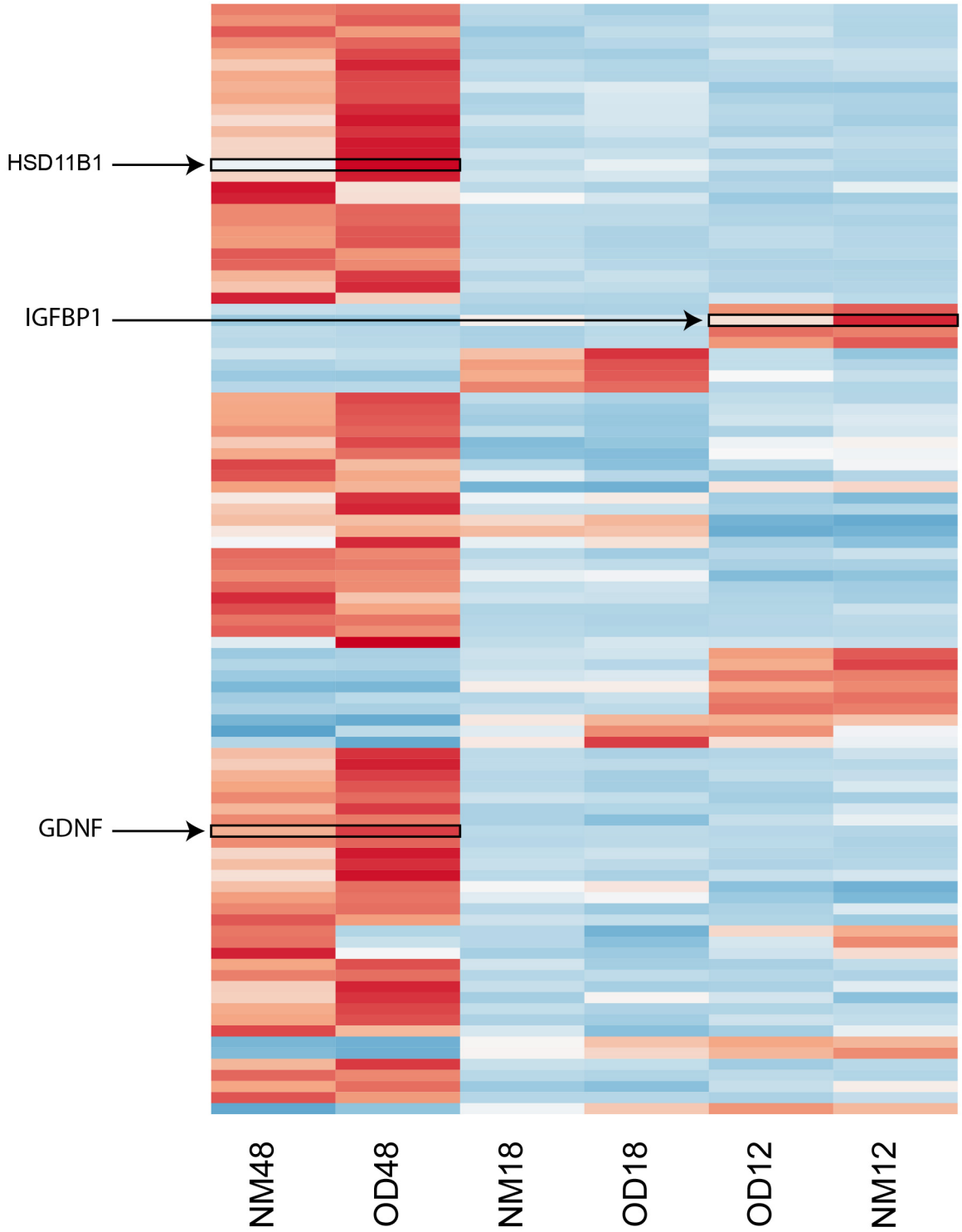

Figure 4.15: Heat map of significant changes in gene expression in healthy donors.

Significant differences in gene expression illustrated in a heat map. This figure shows the group of healthy donors with (OD) and without (NM) influence of BMP2. Exemplary genes are marked by boxes and explained in the text above.

Figure 4.16 shows the heat map for osteoporotic donors depending on BMP2-treatment. Exemplary changes in gene expression in osteoporotic donors are *STMN2* and the *POU5F1*-family (Fig.4.15). *STMN2* is expressed in higher levels in BMP2 treated cells in all osteoporotic donors. The encoded protein plays a role in signal transduction and most probably in osteogenesis. The proteins encoded by the gene-family of *POU5F1* are important for embryonic development and stem cell pluripotency. The biggest difference can be observed in donor 9.

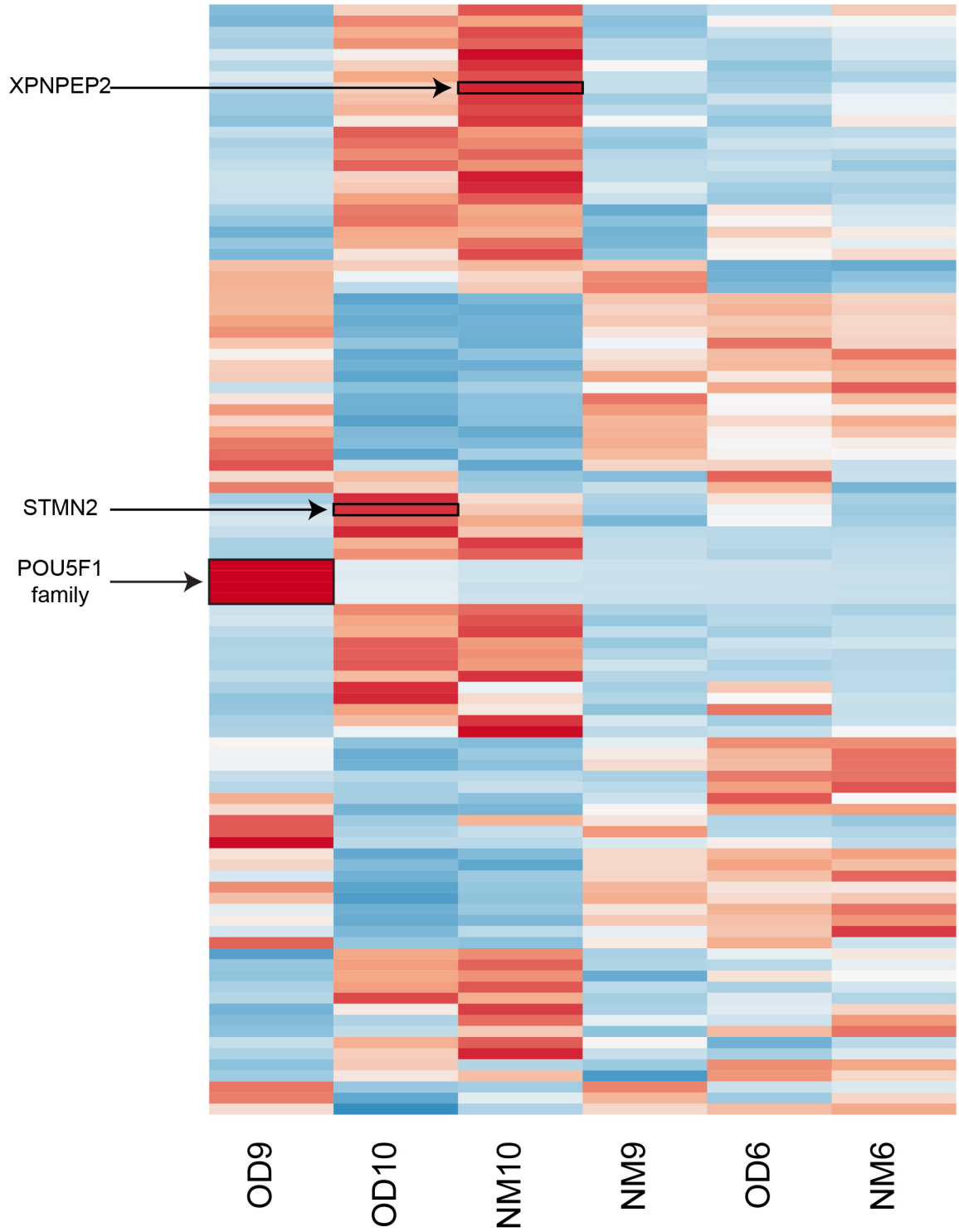

Figure 4.16: Heat map of significant changes in gene expression in osteoporotic donors.

Significant differences in gene expression illustrated in a heat map. This figure shows the group of osteoporotic donors with (OD) and without (NM) influence of BMP2. Exemplary genes are marked by boxes and explained in the text above.

Comparing the genetic landscape of osteogenic and healthy donors, no consistent changes can be found in the present trial (Fig.4.17). One gene, which is expressed in higher levels in healthy donors than in osteogenic donors is *GDF15*. Its encoded protein recruits and activates SMAD family proteins and plays a role in the stress response after cell injury. Other significant differences in expression are observed for *GPRC5B*, which plays a role in insulin secretion and development of diabetes type 2, as well as for *IBSP*. It shows a higher expression in two of the three osteoporotic donors than in healthy donors and its encoded protein is an important structural protein of the extracellular bone matrix.

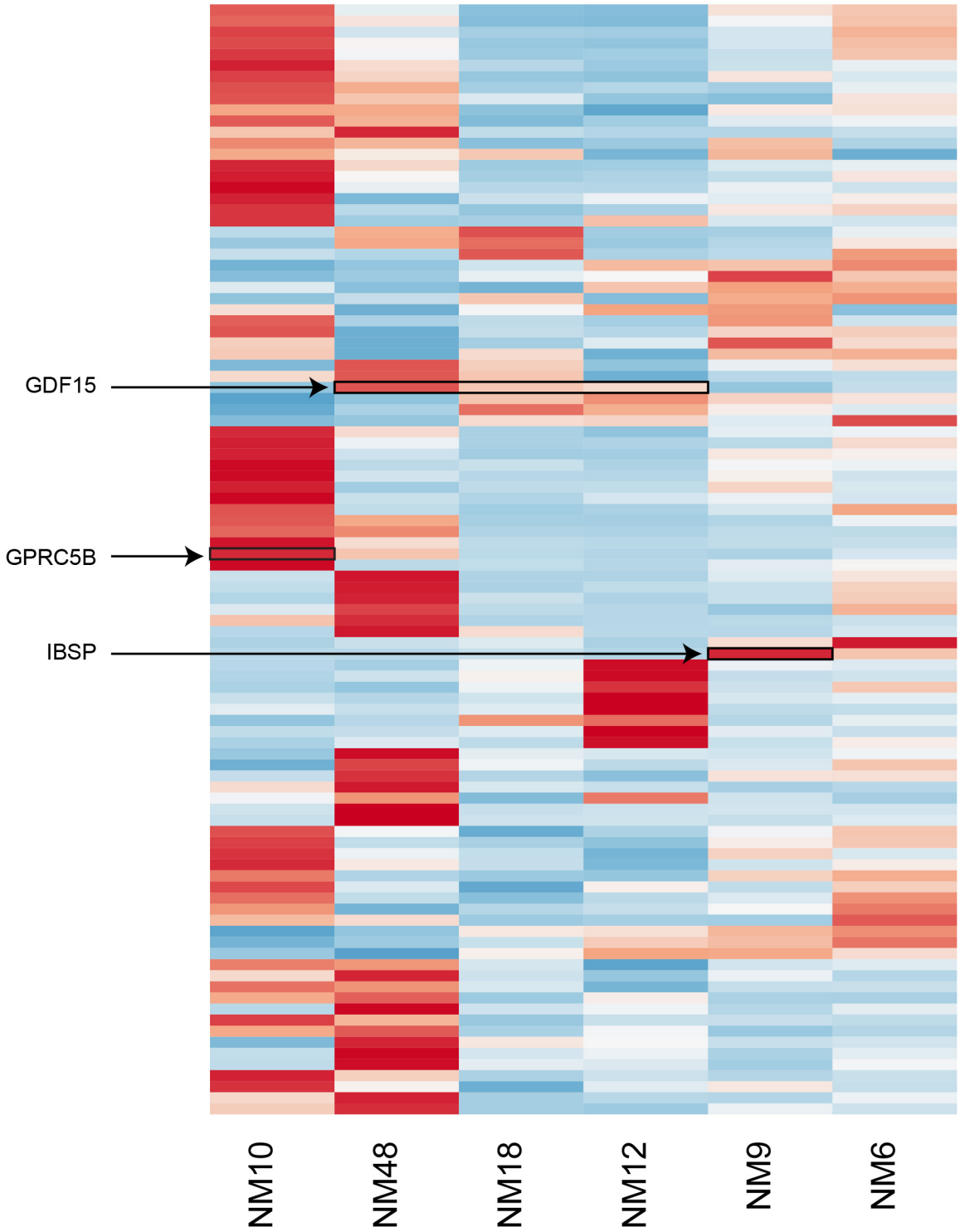

Figure 4.17: Heat map of significant differences in gene expression of healthy versus osteoporotic donors.

Significant differences in gene expression illustrated in a heat map. The figure shows the group of healthy donors and osteoporotic donors without the influence of BMP2. Exemplary genes are marked by boxes and explained in the text above.

The last heat map compares healthy and osteoporotic donors' gene expression under BMP2 influence (Fig.4.18). *FOSB, TFAP2A* and *PRG4* are three exemplary genes. *FOSB* is higher expressed in healthy donors than in osteoporotic donors. Its encoded protein is a leucine zipper protein and regulates cell proliferation and differentiation. *TFAP2A* also has a higher expression in the healthy group and encodes an unspecific transcription factor. In contrast, *PRG4* shows higher levels in osteoporotic donors. The related protein is an important proteoglycan, secreted by chondrocytes at the surface of articular cartilage.

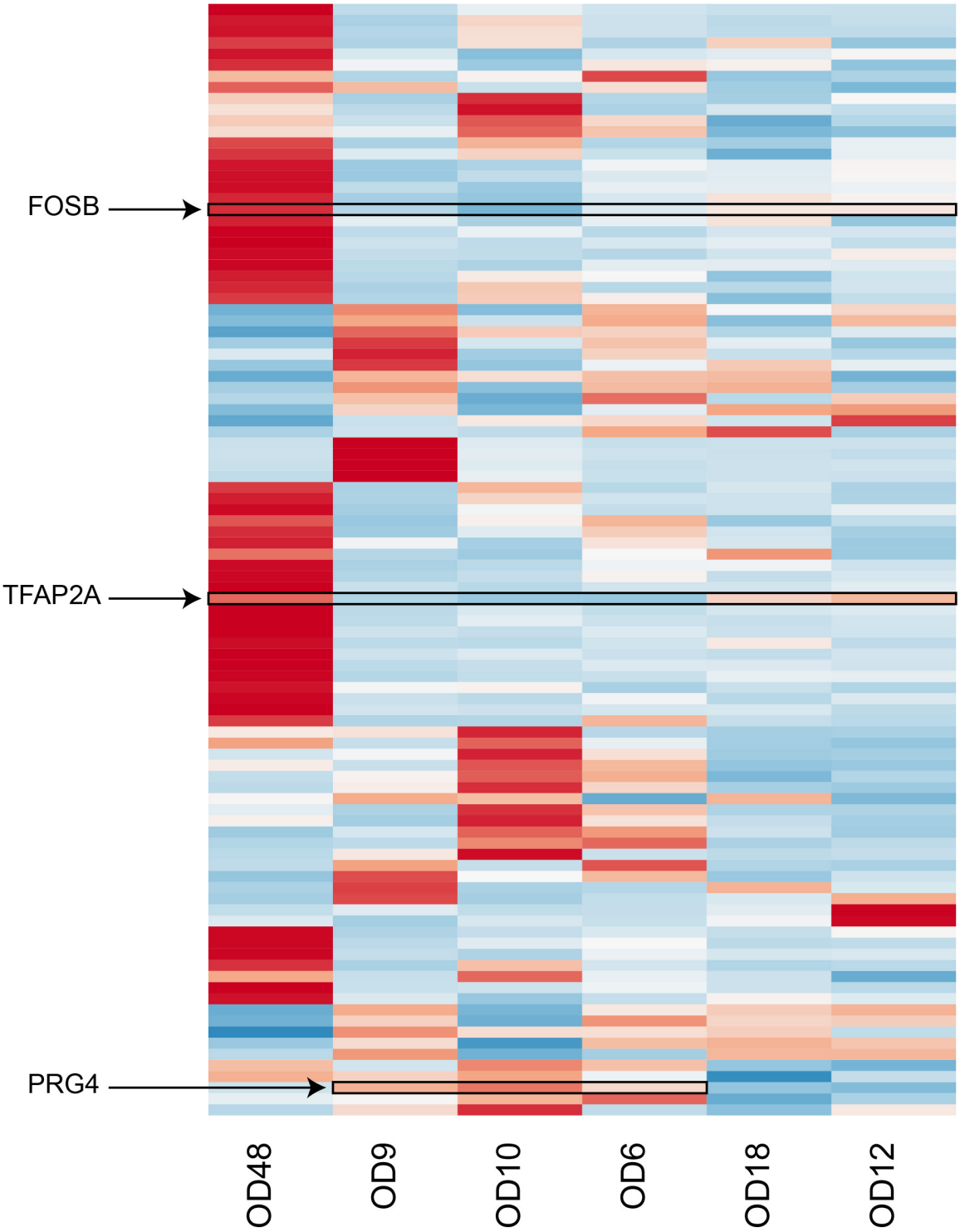

Figure 4.18: Heat map of significant differences in gene expression of healthy versus osteoporotic donors after BMP2 treatment.

Significant differences in gene expression illustrated in a heat map. The figure shows the group of healthy donors and osteoporotic donors with the influence of BMP2. Exemplary genes are marked by boxes and explained in the text above.

4.4.3 Significant changes in gene expression regarding single genes

Comparing the gene expressions of the different groups, the significant changes were filtered out. Subsequent tables show significant changes concerning genes, which play a documented role in osteogenic differentiation.

Again, the first comparison of gene expression was made between healthy donors with and healthy donors without the influence of BMP2 (Table 4.1). The smallest difference in level of expression is seen for *SMAD7*. It is followed by *FZD1* encoding a receptor protein for WNT signaling, *BAMBI* encoding a pseudoreceptor for the TGF-beta family, *NOG* encoding the protein NOGGIN and *DLX5* encoding a transcription factor which is involved in bone development. Furthermore a significant change is detected for *SMAD9* encoding a protein involved in the BMP pathway. All the named genes show a higher expression after BMP2 treatment.

Table 4.1: List of significant changes in gene expression comparing healthy donors with and without BMP2 treatment.

gene	log2foldchange	expression-ratio
SMAD7	1.624	OD>NM
FZD1	1.804	OD>NM
BAMBI	2.147	OD>NM
NOG	2.225	OD>NM
DLX5	2.269	OD>NM
SMAD9	2.496	OD>NM

Overview of genes arranged after the log2foldchange. OD represents donors treated with BMP2, NM represents donors without BMP2 treatment.

The second comparison was made between osteoporotic donors with and without BMP2 treatment (Table 4.2). A negative log2foldchange means a higher expression in cells without BMP2 treatment than in cells with BMP2 influence. *GDF5*, encoding a ligand of the TGF-beta family, is down-regulated under the influence of BMP2. No other gene is found, documented to be involved in osteogenic differentiation, that is down-regulated by BMP2 treatment. Up-regulated genes are *SMAD6* encoding an inhibiting protein regarding BMP signaling, *BAMBI, SMAD9* and *NOG*.

Table 4.2: List of significant changes in gene expression comparing osteoporotic donors with and without BMP2 treatment.

gene	log2foldchange	expression-ratio
GDF5	-3.388	NM>OD
SMAD6	1.994	OD>NM
BAMBI	2.245	OD>NM
SMAD9	2.265	OD>NM
NOG	3.041	OD>NM

Overview of genes arranged after the log2foldchange. OD represents donors treated with BMP2, NM represents donors without BMP2 treatment.

The next comparison was made between healthy donors and osteoporotic donors, each without BMP2 treatment (Table 4.3). There are a lot of significant differences in gene expression between those two groups, but only a few are documented to be involved in osteogenic differentiation. In this comparison, a negative log2foldchange means that genes are higher expressed in osteoporotic donors, a positive log2foldchange means a higher expression in healthy donors. Genes with a negative log2foldchange are for example *PRG4*, *TRH* encoding a thyrotropin-releasing hormone, *IBSP* encoding a structural protein in bone matrix, *STMN2* encoding a protein functioning in signal transduction and *CD34* encoding a protein for cell attachment in bone ECM. A positive log2foldchange can be seen for *GDF15* encoding a ligand of the TGF-beta family. Other detected significant differences with a positive log2foldchange are not documented to be important for osteogenic differentiation or bone growth.

Table 4.3: List of significant changes in gene expression comparing healthy and osteoporotic donors without BMP2 treatment.

gene	log2foldchange	expression-ratio
PRG4	-6.890	O>H
TRH	-5.808	O>H
IBSP	-5.061	O>H
STMN2	-4.885	O>H
CD34	-4.468	O>H
GDF15	3.512	H>O

Overview of genes arranged after the log2foldchange. O represents osteoporotic donors, H represents healthy donors.

The fourth comparison was made between healthy and osteoporotic donors with BMP2 treatment (Table 4.4). Again a lot of different gene expressions can be observed, but just a few significant differences are correlated to genes known to be involved in osteogenic differentiation. A negative log2foldchange means a higher expression in osteoporotic donors than in healthy ones. A negative value can be observed for *STMN2*, *COL10A1* encoding a part of collagen type X, *TRH, PRG4* and *IBSP*. A positive log2foldchange is found for *FOSB* encoding leucine zipper proteins involved in cell differentiation.

Table 4.4: List of significant changes in gene expression comparing healthy and osteoporotic donors with BMP2 treatment.

gene	log2foldchange	expression-ratio
STMN2	-5.569	O>H
COL10A1	-5.344	O>H
TRH	-4.950	O>H
PRG4	-3.942	O>H
IBSP	-3.771	O>H
FOSB	3.753	H>O

Overview of genes arranged after the log2foldchange. O represents osteoporotic donors, H represents healthy donors.

The findings of the analyzation of the particular genes are consistent in the heat maps shown above. The treatment with BMP2 shows adjustments in gene expression, also for genes being involved in osteogenic differentiation. But summing up, no particular genes can be identified to cause the differences between osteoporotic and healthy donors.

Chapter 5

Discussion

Osteoporosis is an important disease of the elderly and due to the demographic change its prevalence will increase in the future. The present surgical treatment options for osteoporotic vertebral fractures are vertebroplasty and kyphoplasty, which have to be seen critically because of their lack of efficiency and their possible complications (McCarthy and Davis, 2016). Another approach to develop further treatment options is tissue engineering. Different scaffolds have various advantages and limitations as single scaffolds. Therefore, the combination of different scaffolds is a promising possibility to rule out the limitations.
One aim of this study was to find a three dimensional, bio-compatible scaffold, which could be a link between the present surgical treatment and tissue engineering for the future. Furthermore it was investigated, if BMP2 enhances the osteogenic differentiation in hMSCs in the 3D setting and if there are specific differences in the BMP2-mediated gene expression in osteoporotic compared to healthy hMSCs.

5.1 The choice of the hybrid 3D scaffold

The first task was to find a bio-compatible 3D scaffold, that allows cells to adhere and differentiate on it and to which proteins or growth factors can be added to influence the cells. Therefore, three scaffolds were taken into consideration: Orthoss Collagen, a deproteinized material for bone replacement, Resorba, a collagen I based sponge and a self made collagen I hydro-gel.
In order to investigate the survival of hMSCs on the different scaffolds Life-Dead Assays were run at different points of time. Like shown in 4.1.1, the survival is worst on Orthoss, whilst the cells on Resorba and the collagen I gel appear to have a very good survival.
Since Alizarin Red stains calcium depositions and Orthoss is made out of bovine bone, it is not possible to differentiate between the scaffold and the new mineral deposition (see 4.1.2) (Puchtler et al., 1969).

Due to the worse survival of the cells and the coloring of native Orthoss, it was excluded.
The survival of hMSCs in Resorba and in the collagen I gel are similar. Also, they both do not get stained with Alizarin Red when native. A disadvantage of the collagen I gel is its shrinking (see 4.1.4). Within a few days, the gel contracts and eventually nearly dissolves. This effect of biodegradability was already observed in various other trials and is a well-known problem with hydro-gels (El-Fiqi et al., 2013; Takallu et al., 2018; Velegol and Lanni, 2001). On the other hand, the gel provides a good medium to easily add cells, proteins and/or growth factors during production.
The Resorba sponge does not shrink but stays in shape, even after 30 days in culture, which indicates a big advantage over the collagen I gel. Its disadvantage is the difficulty to colonize the scaffold with cells and to add proteins or growth factors in a reliable way.
In order to combine the advantages of both scaffolds, a new 3D hybrid scaffold was created. Hereby the collagen I gel coats the Resorba sponge. This is a common and effective way to avoid the scaffolds' shrinkage (Takallu et al., 2018). By this fusion, the disadvantages can be ruled out and the advantages are combined.
The survival and the dispersal of the cells in the hybrid scaffold as well as the changes in its size were examined. Like shown in Figure 4.5, the survival of the cells stays on an excellent level over the whole time of 30 days. This survival leads to the conclusion, that the hybrid scaffold allows enough soluble factors to reach the cells inside the scaffold. Within 30 days in culture, the new scaffold contracts to 24 % of its original size. Its trend of contraction (Fig.4.6 and Fig.4.7) suggests that it will not contract to a significant smaller size afterwards. This provides a higher stability for the hybrid scaffold, than the gel alone does.
From the results presented in Fig.4.8 it can be assumed that cells migrate from the surrounding collagen I gel into Resorba with time and contraction of the gel. Cell migration in the gel is possible due to the alignment of collagen fibrils, which are initially orientated randomly (Dickinson et al., 1994). This cell migration is very important for the functionality of the hybrid scaffold, since the osteogenic differentiation shall mainly take place in the sponge, after the gel has dissolved.
In summary, the created hybrid scaffold allows a good survival and migration of the cells. Also, BMP2 can easily be added and it allows for quantification. These are basic requirements to later perform osteogenic differentiation. A similar concept is described in another study, which confirms the advantages of the present hybrid scaffold (Wang et al., 2012).
Apart from organic scaffolds, like collagen based ones, there are more and more synthetic materials in use. The advantages of these synthetic materials are their exact reproducibility, the easier contamination with proteins and less problems with immune response from the host (Wozney and Seeherman, 2004). Using poly-l-lactic acid (PLLA) nanofiber scaffolds, good ossification results were achieved in combination with BMP2 (Schofer et al., 2011). It has been

proved that a collagen scaffold is an efficient and working way to enhance osteoinduction with BMP2 (Burkus et al., 2002). A combination of both kinds of scaffolds might link the advantages of them and needs to be investigated in future.

5.2 2D osteogenic differentiation

A 2D osteogenic differentiation was performed to investigate, whether BMP2 increases the rate of differentiation in non-osteoporotic ("healthy") and osteoporotic donors and to ensure that all donors' hMSCs are able to differentiate into the osteogenic lineage.
Both donor groups show a slightly, but not significantly higher differentiation rate after stimulation with BMP2. The differentiation rates in the two BMP2-dependent groups are similar between healthy and osteoporotic donors. Both donor groups do not change the differentiation rate significantly when adding BMP2 for four days, compared to groups without BMP2 addition (Fig.4.10). Compared to other publications, the differentiation rates in this study are lower. It was shown, that adding BMP2 to the osteogenic differentiation media leads to a significantly higher differentiation rate for healthy and osteoporotic donors (Prall et al., 2013). Another publication pointed out, that adding BMP2 for 21 days leads to an almost abrogated osteoinduction and thus nearly no osteogenic differentiation, whilst a four-day-treatment would lead to the highest rate of osteoinduction (Heggebö et al., 2014). These findings cannot be reproduced in the present study. Diverse results and effects of BMP2 on osteogenic differentiation are known and so there are also studies showing only a slight effect of BMP2 on hMSCs, which underlines the present results (Chou et al., 2011; Zuk et al., 2011; Waselau et al., 2012). A possible explanation for these varying results might be the different expression of BMP receptors on different cell lines or the origin of BMP2 used in the different trials (Vanhatupa et al., 2015). Another possible explanation could be the donors' ages and co-morbidities. In the present trial, different rates of osteogenic differentiation between osteoporotic and healthy donors cannot be shown in the two-dimensional setting. Unfortunately, it is not possible to compare co-morbidities, since the donors were anonymized. This could be a possible task for future investigations.
Based on the results of the two dimensional osteogenic differentiation, a 21-day-treatment with BMP2 was chosen for the three dimensional setup, since this leads to a higher rate of differentiation (Fig.4.10).

5.3 3D osteogenic differentiation

There are mainly two options to add growth factors in order to affect osteogenic differentiation in a 3D scaffold. Firstly, the growth factor can be added to the media surrounding the scaffold and

so the growth factor would be renewed with each change of the media. Secondly, the growth factor can be added to the scaffold itself and so it is "loaded" with the factors. When hydro-gels are loaded with growth factors, especially BMP2, higher osteogenic differentiation rates are observed, than in trials with dissolved BMP2 in the surrounding media (Samorezov et al., 2016). Another important parameter is the concentration of the growth factor added to the scaffold. The highest rate of released BMP2 and osteogenic differentiation is found with a concentration of BMP2 of 100 ng/ml (Pountos et al., 2010; Samorezov et al., 2016). In the present trial, scaffolds were loaded with BMP2 in a concentration of 100 ng/75 μl hydro-gel. This means a thirteen-fold higher concentration and in accordance with studies mentioned above, this could be an inhibiting factor for osteogenic differentiation, although it could not be finally validated that a higher concentration leads to an abrogated differentiation.

In the 2D setting, the addition of BMP2 leads to a higher differentiation rate. These results cannot be reproduced in the 3D setting for osteoporotic donors. Only donor #6 shows a higher osteogenic differentiation with BMP2 (Fig.4.11), whilst donors #9 and #10 do not show any osteogenic differentiation in the BMP2 treated group (see 4.3). Interestingly, osteogenic differentiation can be observed in the absence of BMP2 in donors #9 and #10, but still to a lesser extent compared to donor #6. Thus, BMP2 treatment leads to an abrogated differentiation in osteoporotic hMSCs, whilst no effect can be seen for healthy hMSCs.

In the present trial experiments were run at least in triplets, so human or material sources of error can be excluded. Another supposable reason for the missing osteogenic differentiation in donors #9 and #10 could have been a cell deficit. Since the cells for the BMP2 group and the non-BMP2 group were harvested from the same cell lines and flasks, a cell deficit is also very unlikely.

The different extent of osteogenic differentiation between the donors might also be traced back to the different types of response to BMP2. Basically, there are three groups of response concerning BMP2 induced osteogenic differentiation. The first group (about 52 %) is directly affected in a positive way, supporting the osteogenic differentiation (Ehnert et al., 2016). The second group (about 17 %) shows various responses to BMP2 and the third group (about 31 %) is not affected significantly by BMP2 (Ehnert et al., 2016). This might be an explanation for the various responses in the different donors in general.

Basically, other studies confirm that osteogenic differentiation in a 3D scaffold is possible and shows promising results (Lin et al., 2021; Schofer et al., 2011; Ryu et al., 2011). In the present trial, bio-compatible, collagen I based scaffolds were used. Hereby, no persisting foreign body would remain at the fracture site after fracture healing. This would probably be an advantage over metallic implants, like titanium implants, for example, used in other studies (Huang et al., 2016). The biocompatibility of collagen is higher than of titanium, most likely due to possible

failures in the titanium-coating process of scaffolds (He et al., 2018; van Hove et al., 2015).
Another approach to combine a 3D scaffold with BMP2 to enhance osteogenic differentiation was shown by Bayat et al. (Bayat et al., 2019). They showed a similar induction of osteogenic differentiation of stem cells for a BMP2-loaded Saghez-scaffold in DMEM-media with differentiation factors. But they could not prove a significant superiority compared to stem cells in media without differentiation factors.

Comparison of osteoporotic and healthy donors

When comparing osteoporotic and healthy donors (Fig.4.12), one big difference can be noticed. The baseline of osteogenic differentiation is lower in osteoporotic hMSCs. Beside this, no difference in differentiation rate can be seen between the groups.
Contrary to our findings, BMP2, connected with tissue engineering, leads to an increased bone formation in osteoporotic rats (Tang et al., 2008). In this trial, however, cells were not incubated with BMP2 and scaffolds were not loaded with it, but BMP2 expression was increased by gene transfection (Tang et al., 2008). This might be an explanation for the differences.
BMP2 levels are shown to be lower in osteoporotic patients than in control groups and higher levels of BMP2 and SMADs walk along with an improved osteoinduction (Liu et al., 2018a). Furthermore, an over-expression or wide availability of BMP2 impairs fracture healing in osteoporotic humans and rats (Liu et al., 2018a). This strengthens the importance of establishing a BMP2-loaded scaffold to promote fracture healing in osteoporotic fracture sites as a local treatment option.
The distribution pattern of the osteogenic differentiation between the hydro-gel and the Resorba (Fig.4.13) shows more Alizarin Red stained areas and thus osteogenic differentiation in Resorba. This might be due to the migration of the cells into the sponge, like mentioned above. It confirms the effectiveness of the present scaffold.

5.4 Transcriptional differences between healthy and osteoporotic donors after BMP2 treatment

In the last part of this trial, a RNA-sequencing was carried out to analyze how the different donor groups change their gene expression after BMP2 treatment. Summing up, there are some significant changes and differences in gene expression, but it is not possible to filter out uniform changes.

Healthy hMSCs with BMP2 treatment versus healthy hMSCs without BMP2 treatment
Comparing healthy donors with and without BMP2 treatment, the biggest differences can be seen between the various donors, regardless of BMP2 treatment. This was expected, since the donors within a group were not matched for any factors but the presence or absence of osteoporotic fractures. The age, previous illnesses, the diet, hormonal balance or other factors were not taken into consideration. This is a weakness of the present trial and matching more donors for these factors might show more significant results.
Comparing the single donors within the two groups shows a change in gene expression after BMP2 treatment. To evaluate which genes were up- or down-regulated table 4.1 visualizes the most significant changes. Donor #48 shows the most intense changes in gene expression. For example, *HSD11B1* and *GDNF* show a higher expression after BMP2 treatment. *HSD11B1* encodes a protease which catalyzes the conversion of cortisol to its inactive metabolite cortisone, but also the reverse reaction. A known adverse effect of a therapy with glucocorticoids is a drug-induced osteoporosis (Rahaman et al., 2018). *HSD11B1* is thought to be involved in trabecular bone loss in patients treated with glucocorticoids (Fenton et al., 2019). *GDNF*, in contrast, is involved in recruitment of SMAD-family members and thus has a positive effect on bone formation (Yi et al., 2020).
Another example regarding significant gene changes in healthy donors is *IGFBP1* in donor #12. Its expression decreases with BMP2 treatment. *IGFBP1* is associated with elevated bone resorption due to increased osteoclast formation and activity (Wang et al., 2015). This would, in turn, support the osteogenic potential of BMP2 treatment in healthy donors. But again, comparing the three healthy donors, the single genes only change in single donors. Again, a larger group of donors has to be analyzed.
Regarding the significant changes in the pooled analyzation (see table 4.1), a rise of supporting as well as inhibiting genes can be observed. The strongest increase of transcription is seen for *SMAD9*, which is known to be part of the BMP2 pathway and is found to negatively regulate this pathway (McDonald et al., 2021; Tsukamoto et al., 2014). Also *NOG* and *BAMBI* are involved in inhibiting BMP2 induced osteoinduction and bone formation. *BAMBI* and *BMPs* are

co-expressed, but *BAMBI* encodes for a pseudoreceptor which does not activate an intracellular cascade when binding to BMP (Onichtchouk et al., 1999). Thus, higher levels of expression of *BAMBI* means impaired osteogenic differentiation (Liu et al., 2021). NOGGIN is an extracellular ligand, competing for receptor binding with BMP and thus having inhibiting influence on the BMP-pathway (Ehnert et al., 2016). NOGGIN expression is also known to be enhanced by BMP2 itself, having a self-restricting role (Hsu et al., 2020). On the other hand side, *DLX5* is known to be involved in bone formation by being part of the BMP pathway, promoting bone formation (Holleville et al., 2007; Lin et al., 2021). Summing up, these inhibiting genes are up-regulated after BMP2 treatment, which could also explain the different results.

Osteoporotic hMSCs with BMP2 treatment versus osteoporotic hMSCs without BMP2 treatment

In this comparison (Table 4.2) an up-regulation of genes, inhibiting and supporting osteogenic differentiation can be seen after BMP2 treatment. This might be a marker for a higher osteogenic activity.

Osteoporotic hMSCs versus healthy hMSCs without BMP2-treatment

The analysis of gene expression levels between healthy and osteoporotic donors prior to BMP2 treatment shows a higher level of several genes, thought to be involved in osteogenesis in osteoporotic donors (Table 4.3). *PRG4* encodes a proteoglycan which is expressed in chondral cells and is discussed to be a marker for enhanced endochondral ossification (Abubacker et al., 2019; Novince et al., 2012; Zweifler et al., 2021). *IBSP* encodes an important structural protein of the bone matrix (Qin et al., 2021). Furthermore, *STMN2* encodes a marker for osteogenesis which is thought to be involved in regulation of osteoblasts and is higher expressed when bone formation takes place (Chiellini et al., 2008; Tuerlings et al., 2021). *CD34* is involved in the attachment of stem cells to bone ECM and has a supporting impact on bone formation (Hertweck et al., 2018). All these genes are found to be higher expressed in osteoporotic donors than in healthy donors.

Osteoporotic hMSCs versus healthy hMSCs with BMP2-treatment

After treatment with BMP2, this distribution mainly remains the same. Osteoporotic donors might have a higher baseline-activity of osteogenic genes compared to healthy donors. The cells used for this trial were harvested of fracture sites in osteoporotic patients. Because of the previous trauma, the local cells might already have begun with fracture healing and thus have a higher baseline of osteogenic genes. Furthermore osteoporotic donors have a higher bone turnover, another possible reason for a higher baseline-activity. After BMP2 treatment, similar genes are significantly higher expressed in both donor groups, which indicates that both groups

react similarly to BMP2 treatment.

Other authors have already questioned the differences in gene expression between healthy and osteoporotic donors. In a gene expression analysis, significant differences between postmenopausal osteoporotic donors and non-osteoporotic donors were found for 9 genes. *CD36* and *TWIST2* were higher expressed in osteoporotic donors, whilst *ALPL, COL1A1, MMP2, MMP9, MMP13, PDGFA* and *NFKB1* were higher expressed in non-osteoporotic donors (Balla et al., 2008). Comparing these results with the significant changes in the present trial, no accordance can be found. In both trials there was just a small number of donors, which could lead to this missing accordance (7 and 10 donors versus 3 and 3 donors). Another possible explanation might be the lack of changes in gene expression in osteoporotic patients due to the disease osteoporosis. Another trial compared osteoporotic donors and non-osteoporotic donors with different donor-sites. Taking cells from different sites also leads to a different gene expression (Jemtland et al., 2011). But again, the most significant genes do not correlate with the findings in the present study and the results can not be reproduced.

Pooled donors without BMP2-treatment versus BMP2-treatment

Comparing the gene expression of healthy and osteoporotic donors between the groups with and without BMP2, it is noticeable that in both donor-pools the inhibiting genes, like *NOG, SMAD9* and *BAMBI*, are higher expressed in groups treated with BMP2. This strongly suggests inhibiting effects of BMP2 on osteoinduction and has already been discussed by Heggebö et al., who postulated time-dependent inhibitory effects of BMP2 treatment (Heggebö et al., 2014). To further investigate this aspect, RNA sequencing at different points of time would be necessary in following trials.

Like mentioned above, Ehnert et al. described three types of reaction to BMP2 treatment (Ehnert et al., 2016). The first type (in their trial about 52 % of all donors) positively responds to BMP2 treatment with an enhanced osteogenic differentiation, whilst the second type (about 17 %) only reacts indirectly and in a reduced manner. The third group (about 1/3 of all donors) does not react to BMP2 treatment with an enhanced osteogenic differentiation. They found a high base-line expression of *BAMBI* in group two and three, which can also be found in the present trial. They also described a direct interaction between *BMP2, SOST* and *NOG*. Since the present trial just has 6 donors in total and *BAMBI* is highly expressed in several donors, they might belong to group two (slight reaction) or group three (no reaction). This might be the reason for the missing increase of osteogenic differentiation in these donors after BMP2 treatment.

In a similar trial, osteoblasts were also treated with 100 ng/ml BMP2 and an increased expression of *LGR4* has been observed (Pawaputanon Na Mahasarakham et al., 2016). *LGR4* is part of the WNT-pathway and thus involved in osteogenic differentiation. It also promotes bone for-

mation as a receptor for RANKL (Carrillo-López et al., 2021). *LGR4* is also found in the present sequencing but does not show a significant rise in expression after treatment with BMP2.

All in all, RNA sequencing shows significant differences in gene expression between osteoporotic and healthy patients prior to BMP2 treatment concerning bone formation. This includes structural bone matrix proteins (IBSP), ECM cell attachment proteins (CD34), ligands of the TGF-beta family (GDF15) and others (PRG4, TRH, STMN2). After BMP2 stimulation an up-regulation of several genes affecting bone formation can be observed in both groups. Though, healthy donors also show an up-regulation of a bone development specific transcription factor (DLX), which is not seen in osteoporotic donors. Thus healthy donors seem to have a more comprehensive response to BMP2 treatment.

Summing up, the current study situation provides hints that BMP2 treatment increases the osteogenic differentiation of hMSCs and thus can be supportive for fracture healing. But it also has to be mentioned that there are not enough studies investigating genetic changes in osteoporotic donors and at the moment no reliable statement can be made. The results of the present study show that the effect of this treatment depends on several factors. Before establishing a BMP2 treatment into the daily treatment of patients, these factors have to be identified and the therapy has to be optimized in order to reduce possible side effects and raise the efficiency. All in all, a treatment with BMP2 cannot be recommended for patients at the moment.
Molecular engineering could be a possible way to achieve more significant results and to further enhance osteogenic differentiation by BMP2 induction. BMP4 and BMP6 are found to be more effective in inducing osteogenic differentiation than BMP2 (Lissenberg-Thunnissen et al., 2011; Jane et al., 2002). This superiority is probably due to a higher resistance of these BMPs to NOGGIN. In BMP6, a lysine at a particular position is thought to be responsible for this resistance (Song et al., 2010). Song et al. also performed molecular engineering and inserted a lysine at this position in BMP2 and thus achieved a higher resistance to NOGGIN. These are promising approaches for future investigations.

Bibliography

Abubacker, S., Premnath, P., Shonak, A., Leonard, C., Shah, S., Zhu, Y., Jay, G. D., Schmidt, T. A., Boyd, S. and Krawetz, R. (2019). Absence of Proteoglycan 4 (Prg4) Leads to Increased Subchondral Bone Porosity Which Can Be Mitigated Through Intra-Articular Injection of PRG4. *Journal of orthopaedic research : official publication of the Orthopaedic Research Society* **37**, 2077–2088. ISSN 1554-527X.

Anderson, P. A., Froyshteter, A. B. and Tontz, W. L. (2013). Meta-analysis of vertebral augmentation compared with conservative treatment for osteoporotic spinal fractures. *Journal of bone and mineral research : the official journal of the American Society for Bone and Mineral Research* **28**, 372–82. ISSN 1523-4681.

Aumüller, G., Aust, G., Doll, A., Engele, J., Kirsch, J., Mense, S., Reißig, D., Salvetter, J., Schmidt, W., Schmitz, F., Schulte, E., Spanel-Borowski, K., Wolff, W., Wurzinger, L. J. and Zilch, H.-G. (2010). 4. Bewegungssystem – Grundlagen. In G. Aumüller, G. Aust, A. Doll, J. Engele, J. Kirsch, S. Mense, D. Reißig, J. Salvetter, W. Schmidt, F. Schmitz, E. Schulte, K. Spanel-Borowski, W. Wolff, L. J. Wurzinger and H.-G. Zilch, eds., *Anatomie*. Stuttgart: Georg Thieme Verlag.

Balla, B., Kósa, J. P., Kiss, J., Borsy, A., Podani, J., Takács, I., Lazáry, A., Nagy, Z., Bácsi, K., Speer, G., Orosz, L. and Lakatos, P. (2008). Different gene expression patterns in the bone tissue of aging postmenopausal osteoporotic and non-osteoporotic women. *Calcified tissue international* **82**, 12–26. ISSN 0171-967X.

Bandyopadhyay, A., Tsuji, K., Cox, K., Harfe, B. D., Rosen, V. and Tabin, C. J. (2006). Genetic analysis of the roles of BMP2, BMP4, and BMP7 in limb patterning and skeletogenesis. *PLoS Genetics* **2**, 2116–2130. ISSN 15537390.

Bayat, H., Shahabinejad, H., Bayat, M., Shirian, S., Mohamadnia, A., Alijani, M., Godarzi, A., Shojaei, P., Shojaei, S., Shevidi, A. and Bahrami, N. (2019). Osteogenic differentiation of follicular stem cells on nano-Saghez scaffold containing BMP2. *Journal of orthopaedic surgery and research* **14**, 442. ISSN 1749-799X.

Bennett, C. N., Longo, K. A., Wright, W. S., Suva, L. J., Lane, T. F., Hankenson, K. D. and MacDougald, O. A. (2005). Regulation of osteoblastogenesis and bone mass by Wnt10b. *Proceedings of the National Academy of Sciences of the United States of America* **102**, 3324–9. ISSN 0027-8424.

Berendsen, A. D. and Olsen, B. R. (2015). Bone development. *Bone* **80**, 14–18. ISSN 1873-2763.

Black, D. M., Cummings, S. R., Karpf, D. B., Cauley, J. A., Thompson, D. E., Nevitt, M. C., Bauer, D. C., Genant, H. K., Haskell, W. L., Marcus, R., Ott, S. M., Torner, J. C., Quandt, S. A., Reiss, T. F. and Ensrud, K. E. (1996). Randomised trial of effect of alendronate on risk of fracture in women with existing vertebral fractures. Fracture Intervention Trial Research Group. *Lancet (London, England)* **348**, 1535–41. ISSN 0140-6736.

Black, D. M., Delmas, P. D., Eastell, R., Reid, I. R., Boonen, S., Cauley, J. A., Cosman, F., Lakatos, P., Leung, P. C., Man, Z., Mautalen, C., Mesenbrink, P., Hu, H., Caminis, J., Tong, K., Rosario-Jansen, T., Krasnow, J., Hue, T. F., Sellmeyer, D., Eriksen, E. F., Cummings, S. R. and HORIZON Pivotal Fracture Trial (2007). Once-yearly zoledronic acid for treatment of postmenopausal osteoporosis. *The New England journal of medicine* **356**, 1809–22. ISSN 1533-4406.

Blair, H. C., Teitelbaum, S. L., Ghiselli, R. and Gluck, S. (1989). Osteoclastic bone resorption by a polarized vacuolar proton pump. *Science (New York, N.Y.)* **245**, 855–7. ISSN 0036-8075.

Bone, H. G., Chapurlat, R., Brandi, M.-L., Brown, J. P., Czerwinski, E., Krieg, M.-A., Mellström, D., Radominski, S. C., Reginster, J.-Y., Resch, H., Ivorra, J. A. R., Roux, C., Vittinghoff, E., Daizadeh, N. S., Wang, A., Bradley, M. N., Franchimont, N., Geller, M. L., Wagman, R. B., Cummings, S. R. and Papapoulos, S. (2013). The effect of three or six years of denosumab exposure in women with postmenopausal osteoporosis: results from the FREEDOM extension. *The Journal of clinical endocrinology and metabolism* **98**, 4483–92. ISSN 1945-7197.

Bone, H. G., Dempster, D. W., Eisman, J. A., Greenspan, S. L., McClung, M. R., Nakamura, T., Papapoulos, S., Shih, W. J., Rybak-Feiglin, A., Santora, A. C., Verbruggen, N., Leung, A. T. and Lombardi, A. (2015). Odanacatib for the treatment of postmenopausal osteoporosis: development history and design and participant characteristics of LOFT, the Long-Term Odanacatib Fracture Trial. *Osteoporosis international : a journal established as result of cooperation between the European Foundation for Osteoporosis and the National Osteoporosis Foundation of the USA* **26**, 699–712. ISSN 1433-2965.

Bone, H. G., McClung, M. R., Roux, C., Recker, R. R., Eisman, J. A., Verbruggen, N., Hustad, C. M., DaSilva, C., Santora, A. C. and Ince, B. A. (2010). Odanacatib, a cathepsin-K inhibitor for osteoporosis: a two-year study in postmenopausal women with low bone density. *Journal of bone and mineral research : the official journal of the American Society for Bone and Mineral Research* **25**, 937–47. ISSN 1523-4681.

Bonjour, P., Clark, P., Cooper, C., Dawson-Hughes, B., Laet, C. D., Delmas, P., Johansson, H., Johnel, O., Melton, J., Miller, P., Oden, A., Toroptsova, N., Khaltaev, N. and Pfleger, B. (2004). WHO SCIENTIFIC GROUP ON THE ASSESSMENT OF OSTEOPOROSIS AT PRIMARY HEALTH Care Level. In *World Health Organization*, volume May.

Boonen, S., Wahl, D. A., Nauroy, L., Brandi, M. L., Bouxsein, M. L., Goldhahn, J., Lewiecki, E. M., Lyritis, G. P., Marsh, D., Obrant, K., Silverman, S., Siris, E., Akesson, K. and CSA Fracture Working Group of International Osteoporosis Foundation (2011). Balloon kyphoplasty and vertebroplasty in the management of vertebral compression fractures. *Osteoporosis international : a journal established as result of cooperation between the European Foundation for Osteoporosis and the National Osteoporosis Foundation of the USA* **22**, 2915–34. ISSN 1433-2965.

Boyce, B. F. and Xing, L. (2007). Biology of RANK, RANKL, and osteoprotegerin. *Arthritis research & therapy* **9 Suppl 1**, S1. ISSN 14786354.

Boyle, W. J., Simonet, W. S. and Lacey, D. L. (2003). Osteoclast differentiation and activation. *Nature* **423**, 337–42. ISSN 0028-0836.

Brunet, L. J., McMahon, J. A., McMahon, a. P. and Harland, R. M. (1998). Noggin, cartilage morphogenesis, and joint formation in the mammalian skeleton. *Science (New York, N.Y.)* **280**, 1455–7. ISSN 0036-8075.

Buchbinder, R., Osborne, R. H., Ebeling, P. R., Wark, J. D., Mitchell, P., Wriedt, C., Graves, S., Staples, M. P. and Murphy, B. (2009). A randomized trial of vertebroplasty for painful osteoporotic vertebral fractures. *The New England journal of medicine* **361**, 557–68. ISSN 1533-4406.

Burkus, J. K., Gornet, M. F., Dickman, C. A. and Zdeblick, T. A. (2002). Anterior lumbar interbody fusion using rhBMP-2 with tapered interbody cages. *Journal of spinal disorders & techniques* **15**, 337–49. ISSN 1536-0652.

Carano, A., Teitelbaum, S. L., Konsek, J. D., Schlesinger, P. H. and Blair, H. C. (1990). Bisphosphonates directly inhibit the bone resorption activity of isolated avian osteoclasts in vitro. *The Journal of clinical investigation* **85**, 456–61. ISSN 0021-9738.

Carrillo-López, N., Martínez-Arias, L., Fernández-Villabrille, S., Ruiz-Torres, M. P., Dusso, A., Cannata-Andía, J. B., Naves-Díaz, M., Panizo, S. and European Renal Osteodystrophy (EUROD) Workgroup (2021). Role of the RANK/RANKL/OPG and Wnt/β-Catenin Systems in CKD Bone and Cardiovascular Disorders. *Calcified tissue international* **108**, 439–451. ISSN 1432-0827.

Chan, C. K. Y., Mason, A., Cooper, C. and Dennison, E. (2016). Novel advances in the treatment of osteoporosis. *British medical bulletin* **119**, 129–42. ISSN 1471-8391.

Chen, G., Deng, C. and Li, Y.-P. (2012). TGF-β and BMP signaling in osteoblast differentiation and bone formation. *International journal of biological sciences* **8**, 272–88. ISSN 1449-2288.

Chiellini, C., Grenningloh, G., Cochet, O., Scheideler, M., Trajanoski, Z., Ailhaud, G., Dani, C. and Amri, E.-Z. (2008). Stathmin-like 2, a developmentally-associated neuronal marker, is expressed and modulated during osteogenesis of human mesenchymal stem cells. *Biochemical and biophysical research communications* **374**, 64–8. ISSN 1090-2104.

Chou, Y.-F., Zuk, P. A., Chang, T.-L., Benhaim, P. and Wu, B. M. (2011). Adipose-derived stem cells and BMP2: part 1. BMP2-treated adipose-derived stem cells do not improve repair of segmental femoral defects. *Connective tissue research* **52**, 109–18. ISSN 1607-8438.

Clarke, B. (2008). Normal bone anatomy and physiology. *Clinical journal of the American Society of Nephrology : CJASN* **3 Suppl 3**, 131–139. ISSN 1555905X.

Cohn, M. J. and Tickle, C. (1996). Limbs: a model for pattern formation within the vertebrate body plan. *Trends in genetics : TIG* **12**, 253–7. ISSN 0168-9525.

Cummings, S. R., Eckert, S., Krueger, K. a., Grady, D., Powles, T. J., Cauley, J. a., Norton, L., Nickelsen, T., Bjarnason, N. H., Morrow, M., Lippman, M. E., Black, D., Glusman, J. E., Costa, A. and Jordan, V. C. (1999). The effect of raloxifene on risk of breast cancer in postmenopausal women: results from the MORE randomized trial. Multiple Outcomes of Raloxifene Evaluation. *JAMA* **281**, 2189–97. ISSN 0098-7484.

Dachverband Osteologie e.V. (2019). S3-Leitlinie Osteoporose .

Dickinson, R. B., Guido, S. and Tranquillo, R. T. (1994). Biased cell migration of fibroblasts exhibiting contact guidance in oriented collagen gels. *Annals of biomedical engineering* **22**, 342–56. ISSN 0090-6964.

Eghbali-Fatourechi, G., Khosla, S., Sanyal, A., Boyle, W. J., Lacey, D. L. and Riggs, B. L. (2003). Role of RANK ligand in mediating increased bone resorption in early postmenopausal women. *The Journal of clinical investigation* **111**, 1221–30. ISSN 0021-9738.

Ehnert, S., Aspera-Werz, R. H., Freude, T., Reumann, M. K., Ochs, B. G., Bahrs, C., Schröter, S., Wintermeyer, E., Nussler, A. K. and Pscherer, S. (2016). Distinct Gene Expression Patterns Defining Human Osteoblasts' Response to BMP2 Treatment: Is the Therapeutic Success All a Matter of Timing? *European surgical research. Europaische chirurgische Forschung. Recherches chirurgicales europeennes* **57**, 197–210. ISSN 1421-9921.

Einhorn, T. a. (1998). The cell and molecular biology of fracture healing. *Clinical orthopaedics and related research* , 7–21ISSN 0009-921X.

El-Fiqi, A., Lee, J. H., Lee, E.-J. and Kim, H.-W. (2013). Collagen hydrogels incorporated with surface-aminated mesoporous nanobioactive glass: Improvement of physicochemical stability and mechanical properties is effective for hard tissue engineering. *Acta biomaterialia* **9**, 9508–21. ISSN 1878-7568.

Eriksen, E. F. (1986). Normal and pathological remodeling of human trabecular bone: three dimensional reconstruction of the remodeling sequence in normals and in metabolic bone disease. *Endocrine Reviews* **7**, 379–408. ISSN 0163769X.

Eriksen, E. F. (2010). Cellular mechanisms of bone remodeling. *Reviews in endocrine & metabolic disorders* **11**, 219–227. ISSN 1573-2606.

Esses, S. I., McGuire, R., Jenkins, J., Finkelstein, J., Woodard, E., Watters, W. C., Goldberg, M. J., Keith, M., Turkelson, C. M., Wies, J. L., Sluka, P., Boyer, K. M. and Hitchcock, K. (2011). The treatment of symptomatic osteoporotic spinal compression fractures. *The Journal of the American Academy of Orthopaedic Surgeons* **19**, 176–82. ISSN 1067-151X.

Ettinger, B., Black, D. M., Mitlak, B. H., Knickerbocker, R. K., Nickelsen, T., Genant, H. K., Christiansen, C., Delmas, P. D., Zanchetta, J. R., Stakkestad, J., Glüer, C. C., Krueger, K., Cohen, F. J., Eckert, S., Ensrud, K. E., Avioli, L. V., Lips, P. and Cummings, S. R. (1999). Reduction of vertebral fracture risk in postmenopausal women with osteoporosis treated with raloxifene: results from a 3-year randomized clinical trial. Multiple Outcomes of Raloxifene Evaluation (MORE) Investigators. *JAMA* **282**, 637–45. ISSN 0098-7484.

Fakhry, M., Hamade, E., Badran, B., Buchet, R. and Magne, D. (2013). Molecular mechanisms of mesenchymal stem cell differentiation towards osteoblasts. *World journal of stem cells* **5**, 136–148. ISSN 1948-0210.

Fenton, C. G., Doig, C. L., Fareed, S., Naylor, A., Morrell, A. P., Addison, O., Wehmeyer, C., Buckley, C. D., Cooper, M. S., Lavery, G. G., Raza, K. and Hardy, R. S. (2019). 11β-HSD1 plays a critical role in trabecular bone loss associated with systemic glucocorticoid therapy. *Arthritis research & therapy* **21**, 188. ISSN 1478-6362.

Feola, M., Rao, C., Tempesta, V., Gasbarra, E. and Tarantino, U. (2015). Femoral cortical index: an indicator of poor bone quality in patient with hip fracture. *Aging clinical and experimental research* **27 Suppl 1**, 45–50. ISSN 1720-8319.

Florencio-Silva, R., Rodrigues, G., Sasso, S., Sasso-Cerri, E., Simões, M. J. and Cerri, P. S. (2015). Biology of Bone Tissue: Structure, Function, and Factors That Influence Bone Cells. *BioMed Research International* **2015**, 1–17. ISSN 2314-6141.

Franceschi, R. T. and Xiao, G. (2003). Regulation of the osteoblast-specific transcription factor, Runx2: Responsiveness to multiple signal transduction pathways. *Journal of Cellular Biochemistry* **88**, 446–454. ISSN 07302312.

Frost, H. M. (1969). Tetracycline-based histological analysis of bone remodeling. *Calcified tissue research* **3**, 211–237. ISSN 0008-0594.

Frost, H. M. (1994). Wolff's Law and bone's structural adaptations to mechanical usage: an overview for clinicians.

Garfin, S. R., Yuan, H. A. and Reiley, M. A. (2001). New technologies in spine: kyphoplasty and vertebroplasty for the treatment of painful osteoporotic compression fractures. *Spine* **26**, 1511–5. ISSN 0362-2436.

Garnero, P., Sornay-Rendu, E., Chapuy, M. C. and Delmas, P. D. (1996). Increased bone turnover in late postmenopausal women is a major determinant of osteoporosis. *Journal of bone and mineral research : the official journal of the American Society for Bone and Mineral Research* **11**, 337–49. ISSN 0884-0431.

Glass, D. A., Bialek, P., Ahn, J. D., Starbuck, M., Patel, M. S., Clevers, H., Taketo, M. M., Long, F., McMahon, A. P., Lang, R. A. and Karsenty, G. (2005). Canonical Wnt signaling in differentiated osteoblasts controls osteoclast differentiation. *Developmental cell* **8**, 751–64. ISSN 1534-5807.

Goldring, S. R. (2015). The osteocyte: key player in regulating bone turnover. *RMD open* **1**, e000049. ISSN 2056-5933.

Groppe, J., Greenwald, J., Wiater, E., Rodriguez-Leon, J., Economides, A. N., Kwiatkowski, W., Affolter, M., Vale, W. W., Izpisua Belmonte, J. C. and Choe, S. (2002). Structural basis of BMP signalling inhibition by the cystine knot protein Noggin. *Nature* **420**, 636–42. ISSN 0028-0836.

Gupta, A. and March, L. (2016). Treating osteoporosis. *Australian prescriber* **39**, 40–6. ISSN 0312-8008.

Hankenson, K. D., Gagne, K. and Shaughnessy, M. (2015). Extracellular signaling molecules to promote fracture healing and bone regeneration. *Advanced drug delivery reviews* **94**, 3–12. ISSN 1872-8294.

Hankenson, K. D., Zimmerman, G. and Marcucio, R. (2014). Biological perspectives of delayed fracture healing. *Injury* **45 Suppl 2**, S8–S15. ISSN 1879-0267.

Hannallah, D., Peterson, B., Lieberman, J. R., Fu, F. H. and Huard, J. (2003). Gene therapy in orthopaedic surgery. *Instructional course lectures* **52**, 753–68. ISSN 0065-6895.

Harris, S. T., Watts, N. B., Genant, H. K., McKeever, C. D., Hangartner, T., Keller, M., Chesnut, C. H., Brown, J., Eriksen, E. F., Hoseyni, M. S., Axelrod, D. W. and Miller, P. D. (1999). Effects of risedronate treatment on vertebral and nonvertebral fractures in women with postmenopausal osteoporosis: a randomized controlled trial. Vertebral Efficacy With Risedronate Therapy (VERT) Study Group. *JAMA* **282**, 1344–52. ISSN 0098-7484.

He, Y., Liu, W., Guan, L., Chen, J., Duan, L., Jia, Z., Huang, J., Li, W., Liu, J., Xiong, J., Liu, L. and Wang, D. (2018). A 3D-Printed PLCL Scaffold Coated with Collagen Type I and Its Biocompatibility. *BioMed research international* **2018**, 5147156. ISSN 2314-6141.

Heggebö, J., Haasters, F., Polzer, H., Schwarz, C., Saller, M. M., Mutschler, W., Schieker, M. and Prall, W. C. (2014). Aged human mesenchymal stem cells: the duration of bone morphogenetic protein-2 stimulation determines induction or inhibition of osteogenic differentiation. *Orthopedic reviews* **6**, 5242. ISSN 2035-8237.

Hernlund, E., Svedbom, A., Ivergård, M., Compston, J., Cooper, C., Stenmark, J., McCloskey, E. V., Jönsson, B. and Kanis, J. A. (2013). Osteoporosis in the European Union: medical management, epidemiology and economic burden. A report prepared in collaboration with the International Osteoporosis Foundation (IOF) and the European Federation of Pharmaceutical Industry Associations (EFPIA). *Archives of osteoporosis* **8**, 136. ISSN 1862-3514.

Hertweck, J., Ritz, U., Götz, H., Schottel, P. C., Rommens, P. M. and Hofmann, A. (2018). CD34+ cells seeded in collagen scaffolds promote bone formation in a mouse calvarial defect model. *Journal of biomedical materials research. Part B, Applied biomaterials* **106**, 1505–1516. ISSN 1552-4981.

Hofbauer, L. C., Khosla, S., Dunstan, C. R., Lacey, D. L., Spelsberg, T. C. and Riggs, B. L. (1999). Estrogen stimulates gene expression and protein production of osteoprotegerin in human osteoblastic cells. *Endocrinology* **140**, 4367–70. ISSN 0013-7227.

Holleville, N., Matéos, S., Bontoux, M., Bollerot, K. and Monsoro-Burq, A.-H. (2007). Dlx5 drives Runx2 expression and osteogenic differentiation in developing cranial suture mesenchyme. *Developmental biology* **304**, 860–74. ISSN 0012-1606.

Hotchkiss, R. S. and Karl, I. E. (2003). The pathophysiology and treatment of Osteoporosis. *The New England journal of medicine* **348**, 138–150. ISSN 0028-4793.

Hsu, M.-N., Yu, F.-J., Chang, Y.-H., Huang, K.-L., Pham, N. N., Truong, V. A., Lin, M.-W., Kieu Nguyen, N. T., Hwang, S.-M. and Hu, Y.-C. (2020). CRISPR interference-mediated noggin knockdown promotes BMP2-induced osteogenesis and calvarial bone healing. *Biomaterials* **252**, 120094. ISSN 1878-5905.

Huang, L., Luo, Z., Hu, Y., Shen, X., Li, M., Li, L., Zhang, Y., Yang, W., Liu, P. and Cai, K. (2016). Enhancement of local bone remodeling in osteoporotic rabbits by biomimic multilayered structures on Ti6Al4V implants. *Journal of biomedical materials research. Part A* **104**, 1437–51. ISSN 1552-4965.

Hughes, a. E., Ralston, S. H., Marken, J., Bell, C., MacPherson, H., Wallace, R. G., van Hul, W., Whyte, M. P., Nakatsuka, K., Hovy, L. and Anderson, D. M. (2000). Mutations in TNFRSF11A, affecting the signal peptide of RANK, cause familial expansile osteolysis. *Nature genetics* **24**, 45–8. ISSN 1061-4036.

Hughes, D. E., Dai, A., Tiffee, J. C., Li, H. H., Mundy, G. R. and Boyce, B. F. (1996). Estrogen promotes apoptosis of murine osteoclasts mediated by TGF-beta. *Nature medicine* **2**, 1132–6. ISSN 1078-8956.

Irawan, V., Sung, T.-C., Higuchi, A. and Ikoma, T. (2018). Collagen Scaffolds in Cartilage Tissue Engineering and Relevant Approaches for Future Development. *Tissue engineering and regenerative medicine* **15**, 673–697. ISSN 2212-5469.

Jacobsen, K. A., Al-Aql, Z. S., Wan, C., Fitch, J. L., Stapleton, S. N., Mason, Z. D., Cole, R. M., Gilbert, S. R., Clemens, T. L., Morgan, E. F., Einhorn, T. A. and Gerstenfeld, L. C. (2008). Bone formation during distraction osteogenesis is dependent on both VEGFR1 and VEGFR2 signaling. *Journal of bone and mineral research : the official journal of the American Society for Bone and Mineral Research* **23**, 596–609. ISSN 1523-4681.

Jane, J. A., Dunford, B. A., Kron, A., Pittman, D. D., Sasaki, T., Li, J. Z., Li, H., Alden, T. D., Dayoub, H., Hankins, G. R., Kallmes, D. F. and Helm, G. A. (2002). Ectopic osteogenesis using adenoviral bone morphogenetic protein (BMP)-4 and BMP-6 gene transfer. *Molecular therapy : the journal of the American Society of Gene Therapy* **6**, 464–70. ISSN 1525-0016.

Jemtland, R., Holden, M., Reppe, S., Olstad, O. K., Reinholt, F. P., Gautvik, V. T., Refvem, H., Frigessi, A., Houston, B. and Gautvik, K. M. (2011). Molecular disease map of bone characterizing the postmenopausal osteoporosis phenotype. *Journal of bone and mineral research : the official journal of the American Society for Bone and Mineral Research* **26**, 1793–801. ISSN 1523-4681.

Kallmes, D. F., Comstock, B. A., Heagerty, P. J., Turner, J. A., Wilson, D. J., Diamond, T. H., Edwards, R., Gray, L. A., Stout, L., Owen, S., Hollingworth, W., Ghdoke, B., Annesley-Williams, D. J., Ralston, S. H. and Jarvik, J. G. (2009). A randomized trial of vertebroplasty for osteoporotic spinal fractures. *The New England journal of medicine* **361**, 569–79. ISSN 1533-4406.

Khosla, S., Atkinson, E. J., Melton, L. J. and Riggs, B. L. (1997). Effects of age and estrogen status on serum parathyroid hormone levels and biochemical markers of bone turnover in women: a population-based study. *The Journal of clinical endocrinology and metabolism* **82**, 1522–7. ISSN 0021-972X.

Kobayashi, Y., Thirukonda, G. J., Nakamura, Y., Koide, M., Yamashita, T., Uehara, S., Kato, H., Udagawa, N. and Takahashi, N. (2015a). Wnt16 regulates osteoclast differentiation in conjunction with Wnt5a. *Biochemical and biophysical research communications* **463**, 1278–83. ISSN 1090-2104.

Kobayashi, Y., Uehara, S., Nobuyuki, U. and Takahashi, N. (2015b). Regulation of bone metabolism by Wnt signals. *Journal of biochemistry* , mvv124ISSN 1756-2651.

Kramer, I., Halleux, C., Keller, H., Pegurri, M., Gooi, J. H., Weber, P. B., Feng, J. Q., Bonewald, L. F. and Kneissel, M. (2010). Osteocyte Wnt/beta-catenin signaling is required for normal bone homeostasis. *Molecular and cellular biology* **30**, 3071–85. ISSN 1098-5549.

Kronenberg, H. M. (2003). Developmental regulation of the growth plate. *Nature* **423**, 332–6. ISSN 0028-0836.

Lee, H. M., Park, S. Y., Lee, S. H., Suh, S. W. and Hong, J. Y. (2012). Comparative analysis of clinical outcomes in patients with osteoporotic vertebral compression fractures (OVCFs): conservative treatment versus balloon kyphoplasty. *The spine journal : official journal of the North American Spine Society* **12**, 998–1005. ISSN 1878-1632.

Lee, K. S., Kim, H. J., Li, Q. L., Chi, X. Z., Ueta, C., Komori, T., Wozney, J. M., Kim, E. G., Choi, J. Y., Ryoo, H. M. and Bae, S. C. (2000). Runx2 is a common target of transforming growth factor beta1 and bone morphogenetic protein 2, and cooperation between Runx2 and

Smad5 induces osteoblast-specific gene expression in the pluripotent mesenchymal precursor cell line C2C12. *Molecular and cellular biology* **20**, 8783–92. ISSN 0270-7306.

Lin, Z., Nica, C., Sculean, A. and Asparuhova, M. B. (2021). Positive Effects of Three-Dimensional Collagen-Based Matrices on the Behavior of Osteoprogenitors. *Frontiers in bioengineering and biotechnology* **9**, 708830. ISSN 2296-4185.

Lissenberg-Thunnissen, S. N., de Gorter, D. J. J., Sier, C. F. M. and Schipper, I. B. (2011). Use and efficacy of bone morphogenetic proteins in fracture healing. *International Orthopaedics* **35**, 1271–1280. ISSN 0341-2695.

Liu, D.-B., Sui, C., Wu, T.-T., Wu, L.-Z., Zhu, Y.-Y. and Ren, Z.-H. (2018a). Association of Bone Morphogenetic Protein (BMP)/Smad Signaling Pathway with Fracture Healing and Osteogenic Ability in Senile Osteoporotic Fracture in Humans and Rats. *Medical science monitor : international medical journal of experimental and clinical research* **24**, 4363–4371. ISSN 1643-3750.

Liu, S., Mou, S., Zhou, C., Guo, L., Zhong, A., Yang, J., Yuan, Q., Wang, J., Sun, J. and Wang, Z. (2018b). Off-the-Shelf Biomimetic Graphene Oxide-Collagen Hybrid Scaffolds Wrapped with Osteoinductive Extracellular Matrix for the Repair of Cranial Defects in Rats. *ACS applied materials & interfaces* **10**, 42948–42958. ISSN 1944-8252.

Liu, W., Huang, J., Chen, F., Xie, D., Wang, L., Ye, C., Zhu, Q., Li, X., Li, X. and Yang, L. (2021). MSC-derived small extracellular vesicles overexpressing miR-20a promoted the osteointegration of porous titanium alloy by enhancing osteogenesis via targeting BAMBI. *Stem cell research & therapy* **12**, 348. ISSN 1757-6512.

MacDonald, B. T., Tamai, K. and He, X. (2009). Wnt/beta-catenin signaling: components, mechanisms, and diseases. *Developmental cell* **17**, 9–26. ISSN 1878-1551.

Matsubara, H., Hogan, D. E., Morgan, E. F., Mortlock, D. P., Einhorn, T. A. and Gerstenfeld, L. C. (2012). Vascular tissues are a primary source of BMP2 expression during bone formation induced by distraction osteogenesis. *Bone* **51**, 168–80. ISSN 1873-2763.

McCarthy, J. and Davis, A. (2016). Diagnosis and Management of Vertebral Compression Fractures. *American family physician* **94**, 44–50. ISSN 1532-0650.

McClung, M. R., Grauer, A., Boonen, S., Bolognese, M. a., Brown, J. P., Diez-Perez, A., Langdahl, B. L., Reginster, J.-Y., Zanchetta, J. R., Wasserman, S. M., Katz, L., Maddox, J., Yang, Y.-C., Libanati, C. and Bone, H. G. (2014). Romosozumab in postmenopausal

women with low bone mineral density. *The New England journal of medicine* **370**, 412–20. ISSN 1533-4406.

McDonald, G. L. K., Wang, M., Hammond, C. L. and Bergen, D. J. M. (2021). Pharmacological Manipulation of Early Zebrafish Skeletal Development Shows an Important Role for Smad9 in Control of Skeletal Progenitor Populations. *Biomolecules* **11**. ISSN 2218-273X.

Mödder, U. I., Clowes, J. A., Hoey, K., Peterson, J. M., McCready, L., Oursler, M. J., Riggs, B. L. and Khosla, S. (2011). Regulation of circulating sclerostin levels by sex steroids in women and in men. *Journal of bone and mineral research : the official journal of the American Society for Bone and Mineral Research* **26**, 27–34. ISSN 1523-4681.

Morikawa, M., Koinuma, D., Miyazono, K. and Heldin, C.-H. (2013). Genome-wide mechanisms of Smad binding. *Oncogene* **32**, 1609–15. ISSN 1476-5594.

Murshed, M., Harmey, D., Millán, J. L., McKee, M. D. and Karsenty, G. (2005). Unique coexpression in osteoblasts of broadly expressed genes accounts for the spatial restriction of ECM mineralization to bone. *Genes & development* **19**, 1093–104. ISSN 0890-9369.

Muschler, G. F., Nakamoto, C. and Griffith, L. G. (2004). Engineering principles of clinical cell-based tissue engineering. *The Journal of bone and joint surgery. American volume* **86-A**, 1541–58. ISSN 0021-9355.

Nakashima, T., Hayashi, M., Fukunaga, T., Kurata, K., Oh-Hora, M., Feng, J. Q., Bonewald, L. F., Kodama, T., Wutz, A., Wagner, E. F., Penninger, J. M. and Takayanagi, H. (2011). Evidence for osteocyte regulation of bone homeostasis through RANKL expression. *Nature medicine* **17**, 1231–4. ISSN 1546-170X.

National Osteoporosis foundation (2021). The BMD.

Neer, R. M., Arnaud, C. D., Zanchetta, J. R., Prince, R., Gaich, G. A., Reginster, J. Y., Hodsman, A. B., Eriksen, E. F., Ish-Shalom, S., Genant, H. K., Wang, O. and Mitlak, B. H. (2001). Effect of parathyroid hormone (1-34) on fractures and bone mineral density in postmenopausal women with osteoporosis. *The New England journal of medicine* **344**, 1434–41. ISSN 0028-4793.

Nguyen, B. N., Hoshino, H., Togawa, D. and Matsuyama, Y. (2018). Cortical Thickness Index of the Proximal Femur: A Radiographic Parameter for Preliminary Assessment of Bone Mineral Density and Osteoporosis Status in the Age 50 Years and Over Population. *Clinics in orthopedic surgery* **10**, 149–156. ISSN 2005-4408.

Novince, C. M., Michalski, M. N., Koh, A. J., Sinder, B. P., Entezami, P., Eber, M. R., Pettway, G. J., Rosol, T. J., Wronski, T. J., Kozloff, K. M. and McCauley, L. K. (2012). Proteoglycan 4: a dynamic regulator of skeletogenesis and parathyroid hormone skeletal anabolism. *Journal of bone and mineral research : the official journal of the American Society for Bone and Mineral Research* **27**, 11–25. ISSN 1523-4681.

Olsen, B. R., Reginato, A. M. and Wang, W. (2000). Bone development. *Annual review of cell and developmental biology* **16**, 191–220. ISSN 1081-0706.

Onichtchouk, D., Chen, Y. G., Dosch, R., Gawantka, V., Delius, H., Massagué, J. and Niehrs, C. (1999). Silencing of TGF-beta signalling by the pseudoreceptor BAMBI. *Nature* **401**, 480–5. ISSN 0028-0836.

Oursler, M. J., Pederson, L., Fitzpatrick, L., Riggs, B. L. and Spelsberg, T. (1994). Human giant cell tumors of the bone (osteoclastomas) are estrogen target cells. *Proceedings of the National Academy of Sciences of the United States of America* **91**, 5227–31. ISSN 0027-8424.

Parfitt, a. M. (2002). Targeted and nontargeted bone remodeling: Relationship to basic multicellular unit origination and progression. *Bone* **30**, 5–7. ISSN 87563282.

Pawaputanon Na Mahasarakham, C., Ezura, Y., Kawasaki, M., Smriti, A., Moriya, S., Yamada, T., Izu, Y., Nifuji, A., Nishimori, K., Izumi, Y. and Noda, M. (2016). BMP-2 Enhances Lgr4 Gene Expression in Osteoblastic Cells. *Journal of cellular physiology* **231**, 887–95. ISSN 1097-4652.

Phimphilai, M., Zhao, Z., Boules, H., Roca, H. and Franceschi, R. T. (2006). BMP signaling is required for RUNX2-dependent induction of the osteoblast phenotype. *Journal of bone and mineral research : the official journal of the American Society for Bone and Mineral Research* **21**, 637–46. ISSN 0884-0431.

Pittenger, M. F., Mackay, A. M., Beck, S. C., Jaiswal, R. K., Douglas, R., Mosca, J. D., Moorman, M. A., Simonetti, D. W., Craig, S. and Marshak, D. R. (1999). Multilineage potential of adult human mesenchymal stem cells. *Science (New York, N.Y.)* **284**, 143–7. ISSN 0036-8075.

Pizette, S. and Niswander, L. (2000). BMPs are required at two steps of limb chondrogenesis: formation of prechondrogenic condensations and their differentiation into chondrocytes. *Developmental biology* **219**, 237–49. ISSN 0012-1606.

Pountos, I., Georgouli, T., Henshaw, K., Bird, H., Jones, E. and Giannoudis, P. V. (2010). The effect of bone morphogenetic protein-2, bone morphogenetic protein-7, parathyroid hormone, and platelet-derived growth factor on the proliferation and osteogenic differentiation of

mesenchymal stem cells derived from osteoporotic bone. *Journal of orthopaedic trauma* **24**, 552–6. ISSN 1531-2291.

Prall, W. C., Haasters, F., Heggebö, J., Polzer, H., Schwarz, C., Gassner, C., Grote, S., Anz, D., Jäger, M., Mutschler, W. and Schieker, M. (2013). Mesenchymal stem cells from osteoporotic patients feature impaired signal transduction but sustained osteoinduction in response to BMP-2 stimulation. *Biochemical and Biophysical Research Communications* **440**, 617–622. ISSN 0006291X.

Provot, S. and Schipani, E. (2005). Molecular mechanisms of endochondral bone development. *Biochemical and biophysical research communications* **328**, 658–65. ISSN 0006-291X.

Puchtler, H., Meloan, S. N. and Terry, M. S. (1969). On the history and mechanism of alizarin and alizarin red S stains for calcium. *The journal of histochemistry and cytochemistry : official journal of the Histochemistry Society* **17**, 110–24. ISSN 0022-1554.

Qin, X., Jiang, Q., Komori, H., Sakane, C., Fukuyama, R., Matsuo, Y., Ito, K., Miyazaki, T. and Komori, T. (2021). Runt-related transcription factor-2 (Runx2) is required for bone matrix protein gene expression in committed osteoblasts in mice. *Journal of bone and mineral research : the official journal of the American Society for Bone and Mineral Research* **36**, 2081–2095. ISSN 1523-4681.

Rahaman, S. H., Jyotsna, V. P., Kandasamy, D., Shreenivas, V., Gupta, N. and Tandon, N. (2018). Bone Health in Patients with Cushing's Syndrome. *Indian journal of endocrinology and metabolism* **22**, 766–769. ISSN 2230-8210.

RESORBA GmbH, M. (2017). KOLLAGEN resorb.

Rizzoli, R., Branco, J., Brandi, M.-L., Boonen, S., Bruyère, O., Cacoub, P., Cooper, C., Diez-Perez, A., Duder, J., Fielding, R. A., Harvey, N. C., Hiligsmann, M., Kanis, J. A., Petermans, J., Ringe, J. D., Tsouderos, Y., Weinman, J. and Reginster, J.-Y. (2014). Management of osteoporosis of the oldest old. *Osteoporosis international : a journal established as result of cooperation between the European Foundation for Osteoporosis and the National Osteoporosis Foundation of the USA* **25**, 2507–29. ISSN 1433-2965.

RKI (2017). 12-Monats-Prävalenz von Osteoporose in Deutschland.

Robling, A. G., Niziolek, P. J., Baldridge, L. A., Condon, K. W., Allen, M. R., Alam, I., Mantila, S. M., Gluhak-Heinrich, J., Bellido, T. M., Harris, S. E. and Turner, C. H. (2008). Mechanical stimulation of bone in vivo reduces osteocyte expression of Sost/sclerostin. *The Journal of biological chemistry* **283**, 5866–75. ISSN 0021-9258.

Roether, J., Bertels, S., Oelschlaeger, C., Bastmeyer, M. and Willenbacher, N. (2018). Microstructure, local viscoelasticity and cell culture suitability of 3D hybrid HA/collagen scaffolds. *PloS one* **13**, e0207397. ISSN 1932-6203.

Roodman, G. D. (1999). Cell biology of the osteoclast. *Experimental Hematology* **27**, 1229–1241. ISSN 0301472X.

Rossouw, J. E., Anderson, G. L., Prentice, R. L., LaCroix, A. Z., Kooperberg, C., Stefanick, M. L., Jackson, R. D., Beresford, S. A. A., Howard, B. V., Johnson, K. C., Kotchen, J. M., Ockene, J. and Writing Group for the Women's Health Initiative Investigators (2002). Risks and benefits of estrogen plus progestin in healthy postmenopausal women: principal results From the Women's Health Initiative randomized controlled trial. *JAMA* **288**, 321–33. ISSN 0098-7484.

Ryu, Y.-M., Hah, Y.-S., Park, B.-W., Kim, D. R., Roh, G. S., Kim, J.-R., Kim, U.-K., Rho, G.-J., Maeng, G.-H. and Byun, J.-H. (2011). Osteogenic differentiation of human periosteal-derived cells in a three-dimensional collagen scaffold. *Molecular biology reports* **38**, 2887–94. ISSN 1573-4978.

Samorezov, J. E., Headley, E. B., Everett, C. R. and Alsberg, E. (2016). Sustained presentation of BMP-2 enhances osteogenic differentiation of human adipose-derived stem cells in gelatin hydrogels. *Journal of biomedical materials research. Part A* **104**, 1387–97. ISSN 1552-4965.

Schaffler, M. B., Cheung, W.-Y., Majeska, R. and Kennedy, O. (2014). Osteocytes: master orchestrators of bone. *Calcified tissue international* **94**, 5–24. ISSN 1432-0827.

Schofer, M. D., Roessler, P. P., Schaefer, J., Theisen, C., Schlimme, S., Heverhagen, J. T., Voelker, M., Dersch, R., Agarwal, S., Fuchs-Winkelmann, S. and Paletta, J. R. J. (2011). Electrospun PLLA nanofiber scaffolds and their use in combination with BMP-2 for reconstruction of bone defects. *PloS one* **6**, e25462. ISSN 1932-6203.

Song, K., Krause, C., Shi, S., Patterson, M., Suto, R., Grgurevic, L., Vukicevic, S., van Dinther, M., Falb, D., ten Dijke, P. and Alaoui-Ismaili, M. H. (2010). Identification of a Key Residue Mediating Bone Morphogenetic Protein (BMP)-6 Resistance to Noggin Inhibition Allows for Engineered BMPs with Superior Agonist Activity. *Journal of Biological Chemistry* **285**, 12169–12180. ISSN 0021-9258.

Takallu, S., Mirzaei, E., Azadi, A., Karimizade, A. and Tavakol, S. (2018). Plate-shape carbonated hydroxyapatite/collagen nanocomposite hydrogel via in situ mineralization of hydrox-

yapatite concurrent with gelation of collagen at pH = 7.4 and 37°C. *Journal of biomedical materials research. Part B, Applied biomaterials* , 1–10ISSN 1552-4981.

Tang, Y., Tang, W., Lin, Y., Long, J., Wang, H., Liu, L. and Tian, W. (2008). Combination of bone tissue engineering and BMP-2 gene transfection promotes bone healing in osteoporotic rats. *Cell Biology International* **32**, 1150–1157. ISSN 10656995.

Tasca, A., Stemig, M., Broege, A., Huang, B., Davydova, J., Zwijsen, A., Umans, L., Jensen, E. D., Gopalakrishnan, R. and Mansky, K. C. (2015). Smad1/5 and Smad4 expression are important for osteoclast differentiation. *Journal of cellular biochemistry* **116**, 1350–60. ISSN 1097-4644.

Tatsumi, S., Ishii, K., Amizuka, N., Li, M., Kobayashi, T., Kohno, K., Ito, M., Takeshita, S. and Ikeda, K. (2007). Targeted ablation of osteocytes induces osteoporosis with defective mechanotransduction. *Cell metabolism* **5**, 464–75. ISSN 1932-7420.

Tella, S. H. and Gallagher, J. C. (2014). Prevention and treatment of postmenopausal osteoporosis. *The Journal of steroid biochemistry and molecular biology* **142**, 155–70. ISSN 1879-1220.

Termaat, M. F., Den Boer, F. C., Bakker, F. C., Patka, P. and Haarman, H. J. T. M. (2005). Bone morphogenetic proteins. Development and clinical efficacy in the treatment of fractures and bone defects. *The Journal of bone and joint surgery. American volume* **87**, 1367–78. ISSN 0021-9355.

Tsukamoto, S., Mizuta, T., Fujimoto, M., Ohte, S., Osawa, K., Miyamoto, A., Yoneyama, K., Murata, E., Machiya, A., Jimi, E., Kokabu, S. and Katagiri, T. (2014). Smad9 is a new type of transcriptional regulator in bone morphogenetic protein signaling. *Scientific reports* **4**, 7596. ISSN 2045-2322.

Tuerlings, M., van Hoolwerff, M., Houtman, E., Suchiman, E. H. E. D., Lakenberg, N., Mei, H., van der Linden, E. H. M. J., Nelissen, R. R. G. H. H., Ramos, Y. Y. F. M., Coutinho de Almeida, R. and Meulenbelt, I. (2021). RNA Sequencing Reveals Interacting Key Determinants of Osteoarthritis Acting in Subchondral Bone and Articular Cartilage: Identification of IL11 and CHADL as Attractive Treatment Targets. *Arthritis & rheumatology (Hoboken, N.J.)* **73**, 789–799. ISSN 2326-5205.

van Hove, R. P., Sierevelt, I. N., van Royen, B. J. and Nolte, P. A. (2015). Titanium-Nitride Coating of Orthopaedic Implants: A Review of the Literature. *BioMed research international* **2015**, 485975. ISSN 2314-6141.

Vanhatupa, S., Ojansivu, M., Autio, R., Juntunen, M. and Miettinen, S. (2015). Bone Morphogenetic Protein-2 Induces Donor-Dependent Osteogenic and Adipogenic Differentiation in Human Adipose Stem Cells. *Stem cells translational medicine* **4**, 1391–402. ISSN 2157-6564.

Velegol, D. and Lanni, F. (2001). Cell traction forces on soft biomaterials. I. Microrheology of type I collagen gels. *Biophysical journal* **81**, 1786–92. ISSN 0006-3495.

Wada, T., Nakashima, T., Hiroshi, N. and Penninger, J. M. (2006). RANKL-RANK signaling in osteoclastogenesis and bone disease. *Trends in molecular medicine* **12**, 17–25. ISSN 1471-4914.

Wagner, D. S. and Mullins, M. C. (2002). Modulation of BMP activity in dorsal-ventral pattern formation by the chordin and ogon antagonists. *Developmental biology* **245**, 109–23. ISSN 0012-1606.

Wang, C., Meng, G., Zhang, L., Xiong, Z. and Liu, J. (2012). Physical properties and biocompatibility of a core-sheath structure composite scaffold for bone tissue engineering in vitro. *Journal of biomedicine & biotechnology* **2012**, 579141. ISSN 1110-7251.

Wang, X., Wei, W., Krzeszinski, J. Y., Wang, Y. and Wan, Y. (2015). A Liver-Bone Endocrine Relay by IGFBP1 Promotes Osteoclastogenesis and Mediates FGF21-Induced Bone Resorption. *Cell metabolism* **22**, 811–24. ISSN 1932-7420.

Waselau, M., Patrikoski, M., Juntunen, M., Kujala, K., Kääriäinen, M., Kuokkanen, H., Sándor, G. K., Vapaavuori, O., Suuronen, R., Mannerström, B., von Rechenberg, B. and Miettinen, S. (2012). Effects of bioactive glass S53P4 or beta-tricalcium phosphate and bone morphogenetic protein-2 and bone morphogenetic protein-7 on osteogenic differentiation of human adipose stem cells. *Journal of tissue engineering* **3**, 2041731412467789. ISSN 2041-7314.

Wozney, J. M., Rosen, V., Celeste, A. J., Mitsock, L. M., Whitters, M. J., Kriz, R. W., Hewick, R. M. and Wang, E. A. (1988). Novel regulators of bone formation: molecular clones and activities. *Science (New York, N.Y.)* **242**, 1528–34. ISSN 0036-8075.

Wozney, J. M. and Seeherman, H. J. (2004). Protein-based tissue engineering in bone and cartilage repair. *Current opinion in biotechnology* **15**, 392–8. ISSN 0958-1669.

Xiong, J., Onal, M., Jilka, R. L., Weinstein, R. S., Manolagas, S. C. and O'Brien, C. A. (2011). Matrix-embedded cells control osteoclast formation. *Nature medicine* **17**, 1235–41. ISSN 1546-170X.

Xiong, J., Piemontese, M., Onal, M., Campbell, J., Goellner, J. J., Dusevich, V., Bonewald, L., Manolagas, S. C. and O'Brien, C. A. (2015). Osteocytes, not Osteoblasts or Lining Cells, are the Main Source of the RANKL Required for Osteoclast Formation in Remodeling Bone. *PloS one* **10**, e0138189. ISSN 1932-6203.

Yi, S., Kim, J. and Lee, S. Y. (2020). GDNF secreted by pre-osteoclasts induces migration of bone marrow mesenchymal stem cells and stimulates osteogenesis. *BMB reports* **53**, 646–651. ISSN 1976-670X.

Zhang, R., Edwards, J. R., Ko, S.-Y., Dong, S., Liu, H., Oyajobi, B. O., Papasian, C., Deng, H.-W. and Zhao, M. (2011). Transcriptional regulation of BMP2 expression by the PTH-CREB signaling pathway in osteoblasts. *PloS one* **6**, e20780. ISSN 1932-6203.

Zuk, P., Chou, Y.-F., Mussano, F., Benhaim, P. and Wu, B. M. (2011). Adipose-derived stem cells and BMP2: part 2. BMP2 may not influence the osteogenic fate of human adipose-derived stem cells. *Connective tissue research* **52**, 119–32. ISSN 1607-8438.

Zweifler, L. E., Koh, A. J., Daignault-Newton, S. and McCauley, L. K. (2021). Anabolic actions of PTH in murine models: two decades of insights. *Journal of bone and mineral research : the official journal of the American Society for Bone and Mineral Research* **36**, 1979–1998. ISSN 1523-4681.

Chapter 10

Appendix

Abbreviations

2D two-dimensional

3D three-dimensional

ALP Alkaline phosphatase

AR Alizarin Red

ATP Adenosine triphosphate

BMD Bone mineral density

BMP Bone morphogenic protein

BMPR BMP receptor

bp base pairs

C-FOS leucine zipper protein FBJ murine osteosarcoma viral oncogene homolog

CSF-1 Colony stimulating factor 1

DAPI 4',6-diamidino-2-phenylindole

dH_2O Distilled Water

DKK1 dickkopf WNT signaling pathway inhibitor 1

DMEM Dulbecco's modified eagle's medium

DMSO Dimethylsulfoxide

DXA Dual-energy X-ray absorptiometry

ECM extracellular matrix

EDTA Ethylenediaminetetraacetic acid

ELISA Enzyme-linked Immunosorbent Assay

FBS Fetal bovine serum

FDA Fluorescein diacetate

GRB-2 growth factor receptor bound protein 2

IGF Insulin-like growth factor

IL Interleukin

IU International units

LDA Life-Dead Assay

Lrp5/6 LDL receptor related protein 5/6

MSC mesenchymal stem cell

NaOH Sodium hydroxide

NFATc1 nuclear factor of activated T-cells 1

NF-kappaB nuclear factor kappa B subunit 1

OD osteogenic differentiation

ODM osteogenic differentiation media

(h)OPC (human) Osteoprogenitor cells

OPG tumor necrosis factor receptor superfamily member 11b (TNFRSF11B; aka. Osteoprotegerin, OPG)

OSX sequence-specific transcription factor 7, aka. Osterix

PBS Phosphate buffered saline

PFA Paraformaldehyd

PI Propidium-iodide

PLLA poly-l-lactic acid

PMMA polymethylmethacrylate

PTH(LH) Parathyroid hormone (like hormone)

PTHR PTH receptor

RANK tumor necrosis factor receptor superfamily member 11a (TNFRSF11A; aka Receptor Activator of NF-$\varkappa$B)

RANKL tumor necrosis factor superfamily member 11 (TNFSF11; aka Receptor Activator of NF-$\varkappa$B Ligand)

rh recombinant human

rpm rounds per minute

RUNX2 runt related transcription factor 2

RT Room temperature

SD Standard deviation

SERM Selective estrogene receptor modulator

(R)-SMAD (receptor-activated) protein similar to the gene products of the Drosophila gene 'mothers against decapentaplegic'

SOST sclerostin

Sp7 sequence-specific transcription factor 7, aka. Osterix

TCF transcription factor 7 like 2

TGF transforming growth factor

TNF tumor necrosis factor

TRAF TNF receptor associated factor

TRAP Tartrate resistant acid phosphatase

WHO World Health Organisation

WNT Wingless-type MMTV integration site

Acknowledgments

Lastly, I want deeply appreciate following persons who contributed in various ways to the realization of this thesis:

Dr. rer. nat. Maximilian Saller, for his patience in supporting me and his expertise in the laboratory.

Prof. Dr. Wolf Christian Prall, for supporting the project and his demanding ideas and annotations.

Dr. Stefan Krebs, for supporting this project by realizing the gene sequenzing.

Team Experimed, for providing me a perfect background environment to complete my thesis focused and without any technical restrictions.

Finally, I also want to thank all other colleagues at the Institute of Developmental Genetics and ExperiMed who I met during the last years.

Last but not least, I want to express my sincere gratitude to my ***family***. Their persistent support during my academic studies and my Doctor thesis has made everything so much easier.

Affidavit

Ich erkläre hiermit an Eides statt,

dass ich die vorliegende Dissertation mit dem Thema:

Evaluation of BMP2-loaded hybrid 3D collagen scaffolds: Proliferation and osteogenic differentiation capacity of human mesenchymal stem cells

selbständig verfasst, mich außer der angegebenen keiner weiteren Hilfsmittel bedient und alle Erkenntnisse, die aus dem Schrifttum ganz oder annähernd übernommen sind, als solche kenntlich gemacht und nach ihrer Herkunft unter Bezeichnung der Fundstelle einzeln nachgewiesen habe.

Ich erkläre des Weiteren, dass die hier vorgelegte Dissertation nicht in gleicher oder in ähnlicher Form bei einer anderen Stelle zur Erlangung eines akademischen Grades eingereicht wurde.

München, den 06.06.2023 Timo Tucholski